INVESTIGATION OF SPOOL-TYPE SOLENOID OPERATED HYDRAULIC DIRECTIONAL CONTROL VALVES

A Thesis submitted to the Council for National Academic Awards for the degree of Master of Philosophy, September 1971.

by

K. G. L. Simpson

Enfield College of Technology

SYNOPSIS

The integrated approach of engineering systems analysis enables one to outline a systematic method of solution of a number of engineering problems.

The investigation of the problem usually starts with the definition of a physical model of the system on the basis of a set of requirements; the system can be some equipment like a valve or a pump. The physical model is normally much too complex to be investigated directly, therefore, through assumptions it is simplified to an abstract model.

From the abstract model, again via assumptions, a mathematical model is derived which combines the separate subsystems (mechanical, hydraulic, etc.,) into an integrated network of ideal network elements. Network topology enables the investigator to obtain a set of independent equations which can then be solved. In parallel with the analytical work tests on the physical model are carried out to compare the accuracy of the analysis and, hence, to make suitable adjustments in the theory.

The knowledge gained from the exercise just described is used with other considerations for the design of a new or improved product.

This is the approach which has been adopted in this thesis to the analysis of a hydraulic, solenoid-actuated, four-port, directional-control valve.

The experimental work was restricted to the operation of the valve with fluid flow through two ports only, further to Fig. 1.1 the hydraulic supply was connected to port 'P' and port 'A' to tank.

This meant that the fluid was passing through a single orifice without flowing into an external load such as a hydraulic motor. This is in accordance with the definition of the system under investigation discussed later.

The complete system was simulated by means of digital and analogue computers, and in addition, programmes have been suggested to make suitable design changes in the valve.

Acknowledgements

I would like to thank Mr. J. Korn, B.Sc.(Eng), M.Phil., C.Eng.,M.I.Mech.E., Senior Lecturer at Enfield College of Technology, for his general supervision and many valuable suggestions; also Mr. J.F. Jackson, A.M.C.S.T.,M.Sc. Technical Director at Pratt Precision Hydraulics Limited for much help and advice.

I would also like to acknowledge the general helpfulness of the Enfield College laboratory technicians, especially Mr. L. Fuller.

My thanks are also due to Dr. J.I. Soliman, M.Sc.(Alex), Ph.D.(London), C.Eng., M.I.Mech.E. Lecturer at Queen Mary College, my third supervisor; to Mr. J.D. Cumbers, B.Sc.(Eng), Lecturer at Enfield College of Technology, for his advice on computing; to the Governors of Enfield College of Technology for the opportunity to carry out this work; and to the Plastic Division of Imperial Chemical Industries Limited for the use of the analogue computing facilities.

CONTENTS

NOTATION

Variables

e	voltage*
i	current*
E	r.m.s. value of voltage
I	r.m.s. value of current
ϕ	flux*
F	magnetomotive force*
v	velocity*
u	maximum velocity
y	displacement*
x	displacement*
z	displacement of spool
f	force*
m	momentum*
θ	angular displacement*
ω	angular velocity
q	flow rate
p	pressure*
t	time
τ	scaled time
d	indicates differentiation
s	Laplace operator

A dot above a variable also indicates differentiation.

Constants

h	height of water*
l	length*
L	length* or inductance
Z	initial compression of springs
r	radius*
D	diameter
R	electrical resistance* or hydraulic resistance*
P	permeance*
μ_o	absolute permeability
μ_r	relative permeability
μ	$=\mu_o\mu_r$
G	conductance*
ϱ	resistivity or density
N	number of turns*
A	area*
S	surface*
M	mass*
g	gravitational acceleration
η	dynamic viscosity
ν	kinematic viscosity
N_R	Reynold's Number
F	viscous friction coefficient

C_v	velocity coefficient
C_c	contraction coefficient
C_D	discharge coefficient ($= C_v C_c$)
Φ_N	function
K	constant*
α	constant*
β	constant*

* suffix will be used where appropriate

Note: Where one symbol can represent more than one variable or constant, the meaning of the symbol will be clear from the text.

INTRODUCTION

In general, a directional control valve is a device which when connected between a hydraulic supply and a hydraulic motor enables the direction of the fluid flow to the motor to be reversed or stopped. Examples of hydraulic systems which use these valves are, industrial presses, earth moving machinery, machine tools etc.

With reference to Fig. 1.1 the valves body is usually made from a rectangular block of cast iron which is mounted to a base plate that allows the hydraulic pipes to be connected. From the pipe connections the fluid is conducted through channels to a centrally bored cylindrical hole in the valve body. Hence the fluid is directed to the ports. The directing of the fluid is achieved by a steel plunger which slides along the centrally bored cylindrical hole. The plunger is shaped like a spool and it is thus known by this name. The spool is centralised by two springs, in this position there will be no fluid flow to the motor. Attached to both ends of the valve body are electrical solenoids. The armature of these solenoids can push the spool, via striker pins, in either direction. The direction depends upon which solenoid is energised. When the spool has been moved in either direction there will be fluid flow to the motor.

In the number of equations English units have been retained and in others S.I. units are used. It is felt that at the time of doing this work English units gave a better "feel" for the problem and would be more meaningful to the possible users of this work.

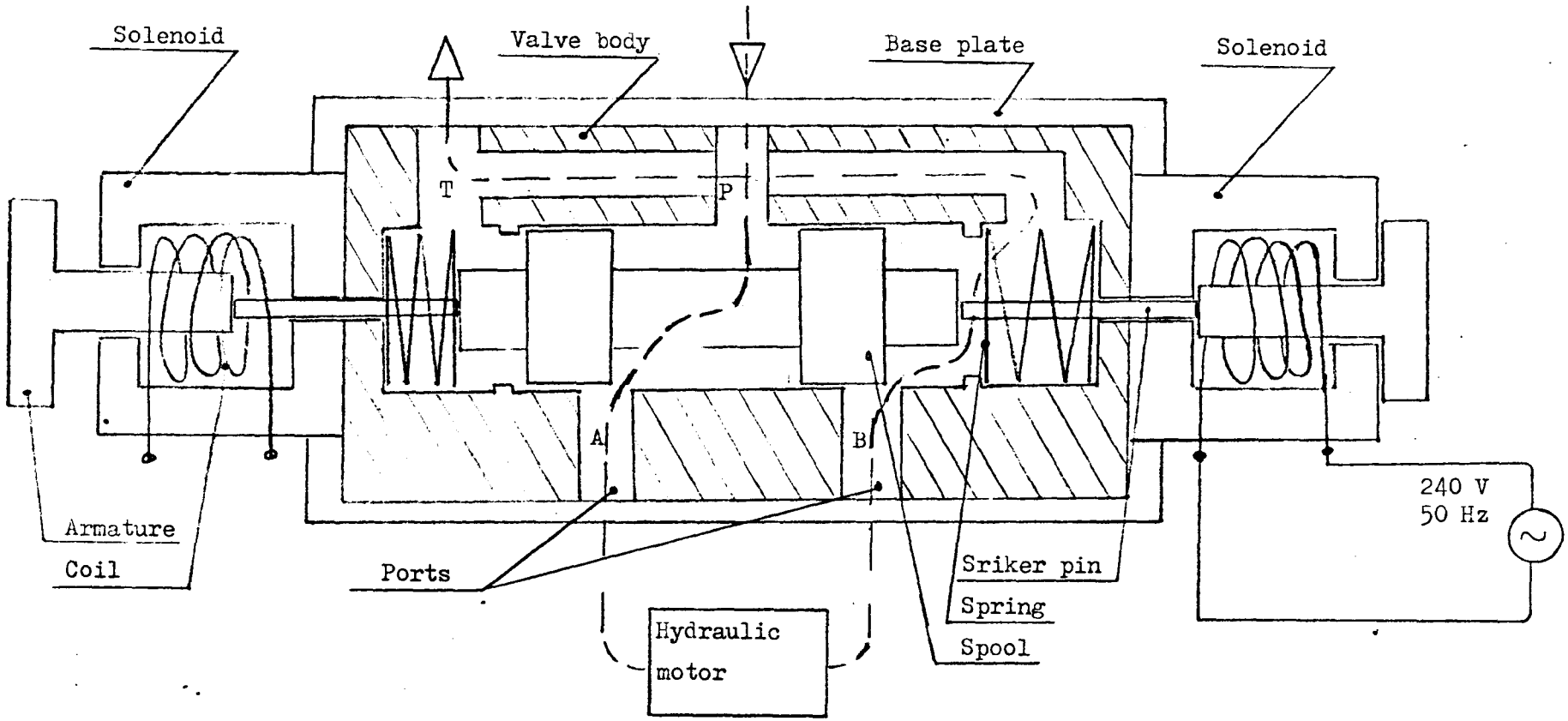

Schematic diagram of directional control valve.

Fig. 1.1

1.1 Statement of the problem

It is thought that there are three main problems concerning these valves.

These are :-

(1) Low force available from solenoid to actuate the spool. The ultimate performance of a particular valve is assessed by the maximum hydraulic power which it can control, this is related to the force available from the solenoid. Hence it appears that the larger the force the higher the controllable power.

(2) There is a tendency towards standardisation of mounting valves. This implies that the overall size of the valve is restricted.

(3) In an increasing number of applications it is desirable to control the solenoid directly from small signal sources (e.g., transducers and solid state devices), This implies that the control current is small.

In addition a further problem, which can be important in certain applications, is the speed of operation of the spool. To effect this, the force available from the solenoid should be large to overcome the resisting force; and the inertia of the moving parts should be small, hence a powerful solenoid and small moving parts are required.

From the foregoing it is concluded that the requirements in design of a solenoid controlled, spool-type, directional control valve are conflicting. To achieve optimum design and performance it is necessary to have a thorough understanding

of the operation, steady state and, dynamic characteristics of the complete system, as defined in Fig. 1.2.

In all previous work the analysis has been concerned with either (a) consideration of the solenoid or (b) the mechanical-hydraulic parts of the valve. It is thus the intention of this investigation to consider the valve system as a whole making use of the systems approach[1,2,3] and in particular to make use of network analysis[4,5].

However, before the complete system, as shown in Fig. 1.2, can be considered it is first necessary to analyse its individual parts. Thus initially, the electrical and hydro-mechanical sub-systems of the valve are considered separately.

The operation of the valve is governed by the motion of the spool. Thus the analysis is basically concerned with the systematic derivation of a set of differential equations effecting this motion. In order to determine the parameters in the equations theoretical and experimental work are to be carried out. Extensive use is made of analogue and digital computing.

1.2 Historical Background

Much work has been done on the analysis and design of servo-valves[6,7,8,9,10,11,12], these normally assume that the spool of the valve is displaced by only a small amount. Very little consideration is given to the devices (solenoid, torque motor) which actuates the spool. There is a scarcity of work which specifically deals with directional control valves.

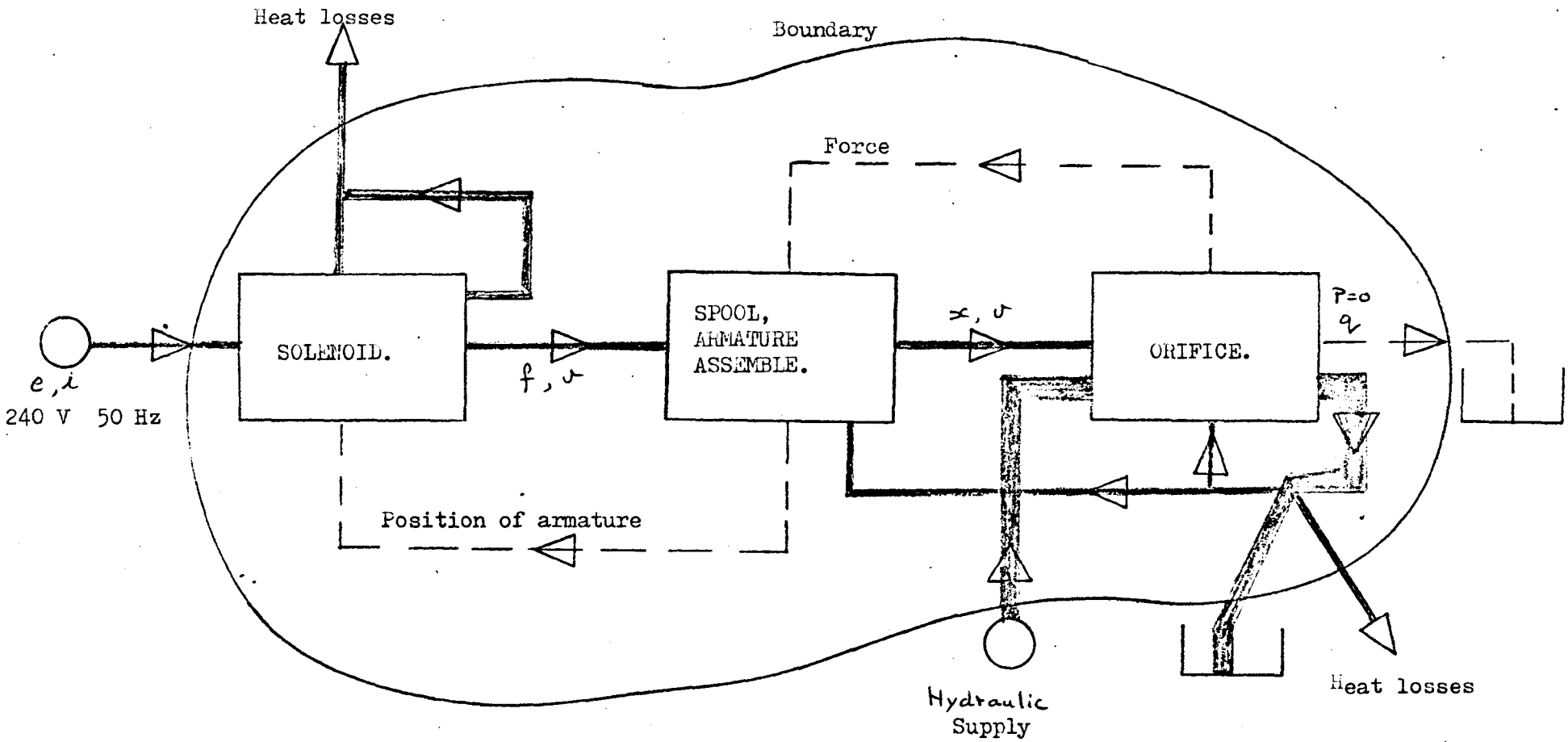

Block diagram of valve system.

Fig. 1.2

Such work that there is consists of detailed investigation of the flow of fluid through the valve[13,14,15] it considers such matters as cavitation in the flow, the angle of the stream of fluid immediately down stream of the orifice, and the type of flow, i.e., turbulant or laminar. The main conclusion that can be drawn from these papers is that the flow characteristics alter as the spool moves across the ports, thus suggesting that there are distinct operating regions. Reference 12 deals with the valves hydromechanical system, and in this paper the operating time of the spool is determined and experimental results are presented which verify the theoretical results. It is of interest to note that the flow characteristics are assumed to be the same throughout the entire spool movement, which is contrary to the conclusion that can be drawn from references[13,14,15]. When considering the operating time of the valve it is equally important to consider the electrical energy stored in the solenoid, as this will cause an additional delay time. It is not thought that the total operating time can be found by simply adding the operating times of the hydromechanical system to that of the solenoid, since there could be interaction between the two systems.

Reference 16 develops analogues between the electrical and hydraulic elements. The reason given for this, quoting from the text is that "Much empirical data is available for specific fluid power design problems, but a systems approach comparable to the electrical science is almost non-existent.

This is a serious handicap to efficient, creative, and analytical synthesis or analysis of hydraulic components and circuits. The essential principles of mechanics, electronics and thermo-dynamics all apply as fluid does its work. This series introduces a powerful new approach in solving dynamic problems in fluid power by using basic analogies. Adapting the techniques of electrical analysis leads to a homogeneous control philosophy which applies to all engineering system". Thus taking this idea one step further, if each element in a system, be it electrical, hydraulic, mechanical, etc., can be represented by its own network and if these networks can be connected together into a complete mixed system, then the powerful methods of network analysis can be used to analyse the behaviour of the system.

A major contribution to the understanding of the hydraulic valve is to be found in the bock by Blackburn, Reethof and Shearer[17]. Similarly the subject of solenoids is well presented in the book by Rotar[18].

For the preparation of this work the above references, along with others mentioned elsewhere in this thesis, have been studied and in addition a post graduate course in Automation Engineering was attended at the City University, details of which are given in the Appendix.

2. Electrical Sub-System

In this chapter the solenoid is considered as a separate system, its network representation is developed and experimental results are presented.

2.1 Theory

The force developed by a solenoid as a function of the relevant quantities is derived from energy considerations. In the resulting equations it is found necessary to consider the permeance, and the rate of change of permeance with respect to displacement of the solenoid's armature.

2.1.1 Development of the abstract model

A solenoid can be termed an electromechanical transducer[2]. The phenomenon that is utilized in a solenoid is that of a mechanical force exerted on a ferromagnetic material tending to align it with, or bring it into the position of, the densest part of the magnetic field (See Fig. 2.1). Provided that the magnetic field is created by a current carrying coil, the process is reversible, i.e., if the ferromagnetic material is moved it will cause a change in flux linking the coil and thus induce a voltage in the coil[18,19,20].

By applying the general principle of conservation of energy to the system the energy flow diagram can be obtained, as in Fig. 2.2

From Fig. 2.2 the energy balance can be written in differential form, thus,

$$dW(elect) = dW(elect.\ loss) + dW(fld.\ stored) + dW(fld.\ loss) + dW(useful\ mech.\ output) + dW(mech.\ loss) \qquad (2.1)$$

Consider each of the terms given in equation 2.1

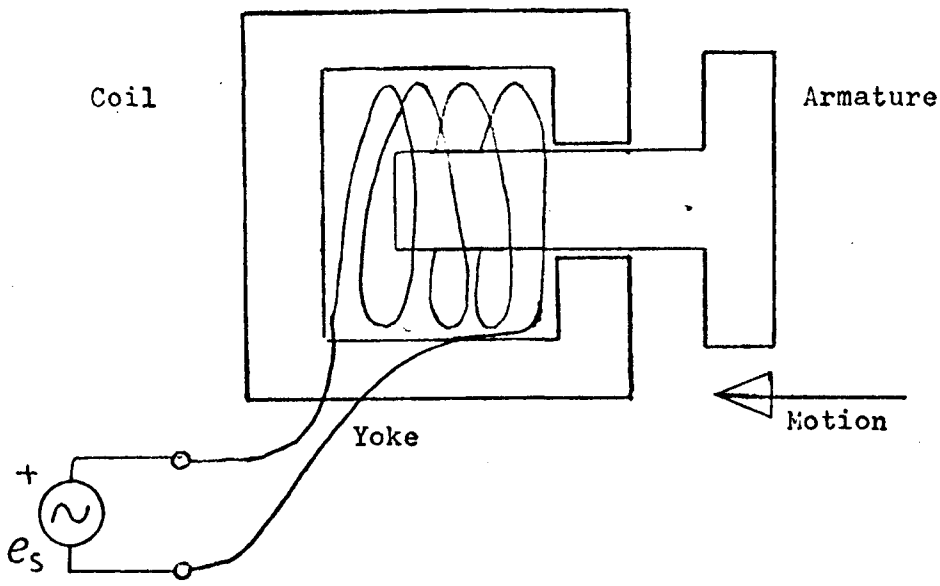

Schematic diagram of the solenoid under consideration.

Fig. 2.1.

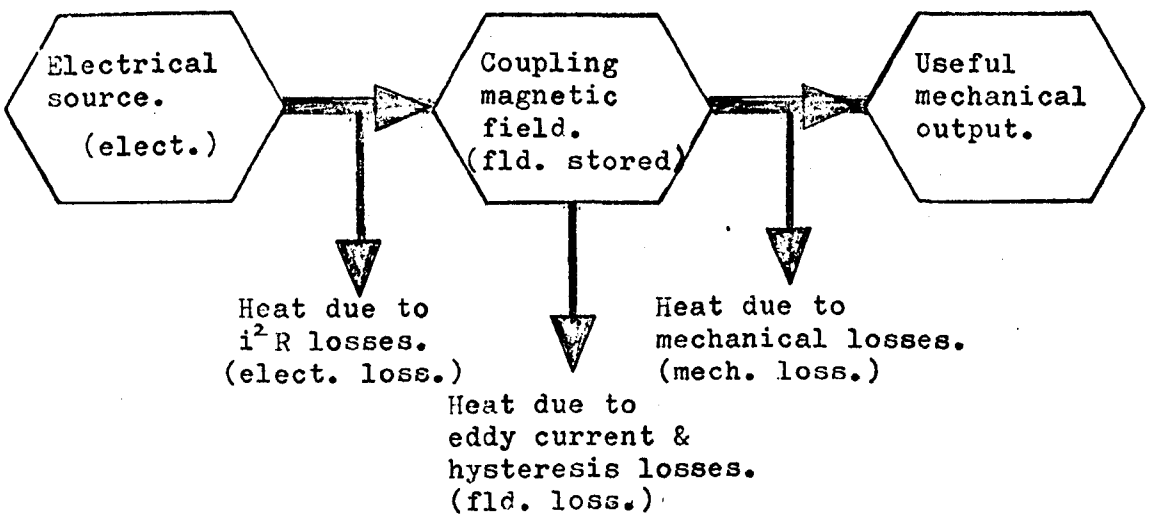

Energy flow diagram for a solenoid.

Fig. 2.2

The dW(elect input) is the energy supplied from some electrical source, which has terminal voltage e_s

$$dW(elect.) = e_s i\, dt \qquad (2.2)$$

The dW(elect. loss) will be due to the resistance of the wire used to wind the coil, let this resistance be R_e,

$$dW(elect.\ loss) = i^2 R_e\, dt \qquad (2.3)$$

The dW(fld. stored) will be the energy necessary to set up the flux in the magnetic circuit and thus will be some function of the flux and the magneto-motive force (m.m.f.) which sets up the flux. The precise relationship will be found from equation 2.1.

$$dW(fld.\ stored) = \Phi_N(\phi, F) \qquad (2.4)$$

The dW(fld. loss) comprises of eddy current and hysteresis, loss. The eddy current loss takes the form of heating in the iron yoke and armature due to circulating currents that are induced by the changing field. Thus this loss will be a function of the frequency of the supply voltage. These currents are reduced by a lamination of the iron paths.

When the flux is changing in a ferromagnetic material it will always lag behind the changing m.m.f., this results in hysteresis loss which is proportional to frequency. This loss

is also dependent on the type of iron, it is minimum when soft iron is used.

The solenoid under consideration operates at 50 Hz and uses soft, laminated iron, therefore these losses will be neglected.

$$dW(\text{fld. loss}) = 0 \tag{2.5}$$

The dW(mech. losses) is the energy necessary to overcome friction losses in the armature. It is intended to consider this loss as part of the system which the solenoid drives and if dW(useful mech.output) is the energy necessary to drive the preceeding system, i.e., spool in this case, then let

$$dW(\text{mech. loss}) + dW(\text{useful mech. output}) = dW(\text{mech. output}) \tag{2.6}$$

Let f be the total force delivered by the armature and dx its incremental movement, then,

$$dW(\text{mech. output}) = f\,dx \tag{2.7}$$

Substituting equation 2.2 to 2.7 in equation 2.1

$$e_s\, i\, dt = i^2 R_e\, dt + dW(\text{fld. stored}) + f\,dx \tag{2.8}$$

rearranging equation 2.8 gives

$$dW(\text{fld. stored}) = (e_s - iR_e)\, i\, dt - f\,dx \tag{2.9}$$

$$\text{Let} \quad (e_s - i R_e) = e \tag{2.10}$$

where e is the induced voltage across the coil and N is the number of turns associated with flux, thus,

$$e = N \frac{d\phi}{dt} \tag{2.11}$$

Therefore substituting equations 2.10 and 2.11 in equation 2.9 gives,

$$dW(\text{fld. stored}) = N i \, d\phi - f \, dx \tag{2.12}$$

If the armature in the system of Fig. 2.1 is held still then dx will be zero and no mechanical work will be done, but a force will still exist acting on the armature,

$$dW(\text{fld. stored}) = N i \, d\phi \tag{2.13}$$

Thus energy stores in field due to change of ϕ from ϕ_1 to ϕ_2 is,

$$W(\text{fld. stored}) = \int_{\phi_1}^{\phi_2} i N \, d\phi \tag{2.14}$$

Now i N is a function of ϕ where[18]

$$i N = \frac{\phi}{P} \tag{2.15}$$

where $i N = F$ or m.m f.

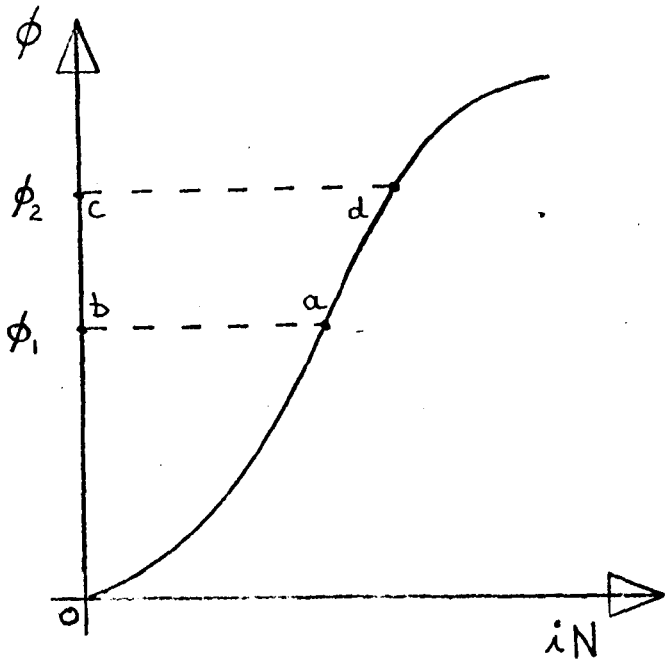

Graph of ϕ against iN for iron.

Fig. 2.3.

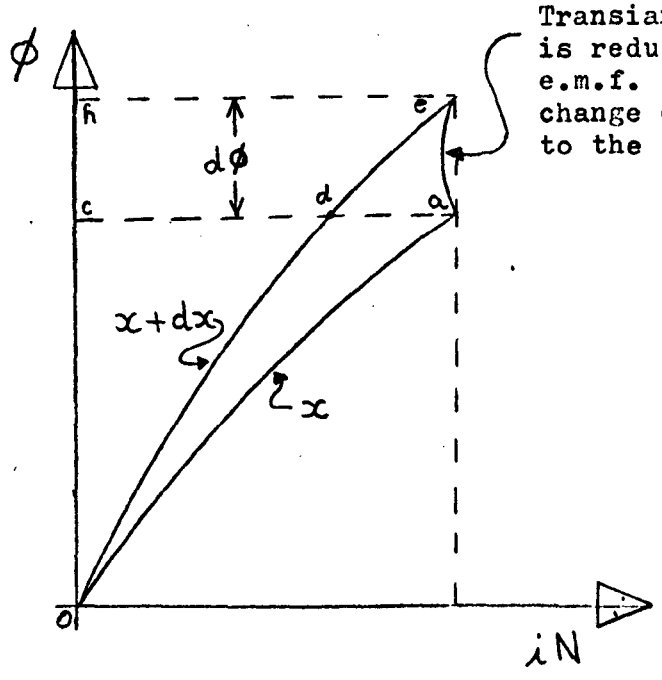

Transiant locus; the m.m.f. is reduced due to an induced e.m.f. caused by the rate of change of flux (which is due to the change in permeance)

Graph of ϕ against iN for a solenoid.

Fig. 2.4.

In air and for a fixed armature displacement P will be a constant but in iron P will depend on the value of ϕ and the slope of the curve in Fig. 2.3 will not be constant.

By considering equation 2.14 it can be seen that the increased energy stored in the field when ϕ increases from ϕ_1 to ϕ_2 is represented by the area a d c b in Fig. 2.3. Substituting equation 2.15 in 2.14 for the case when the field is in air, and letting the flux vary between 0 and ϕ

$$W(\text{fld. stored}) = \int_0^{\phi} \frac{\phi}{P}\, d\phi = \frac{\phi^2}{2P} \qquad (2.16)$$

or by substituting equation 2.15 in 2.16.

$$W(\text{fld. stored}) = \frac{\mathcal{F}\phi}{2} \qquad (2.17)$$

Consider the case when the armature is allowed to move a small distance dx. Let the armature of Fig. 2.1 be held away from the yoke until the current has reached its steady state value and then allowed to move a small distance dx, the resulting flux/m.m.f. curve is shown in Fig. 2.4

Area o a c o = energy extracted from the electrical source and absorbed by the magnetic field.

Area o e h o = energy stored after movement dx.

Thus increase in stored energy is,

$$dW(\text{fld. stored}) = \text{oeho} - \text{oaco}$$

But from equation 2.12 i.e.,

$$dW(\text{fld. stored}) = i N\, d\phi - f\, dx$$

where $iNd\phi$ = area a c h e a

$$oeho - oaco = achea - \int f\,dx$$

$$\text{thus} \quad \int f\,dx = achea - oeho + oaco = oaeo \tag{2.18}$$

o a e o represents the change in stored energy when F is maintained constant and the flux changes by $d\phi$ therefore from equation 2.17.

$$\text{change in stored energy} = -F\,\frac{d\phi}{2} \tag{2.19}$$

(this is a decrease in stored energy)

∴ substituting equation 2.19 in 2.18 yields

$$f = -\frac{F}{2}\,\frac{d\phi}{dx} \tag{2.20}$$

but $\phi = FP$, where P is a function of x.

∴ equation 2.20 becomes

$$f = -\frac{F^2}{2}\,\frac{dP}{dx} \tag{2.21}$$

Having found the relationship for the force developed by the solenoid it is necessary to consider its representation as a network.

If the solenoid's coil has resistance R_e, inductance L, and the applied voltage is e_s, the electric circuit is shown in Fig. 2.5.

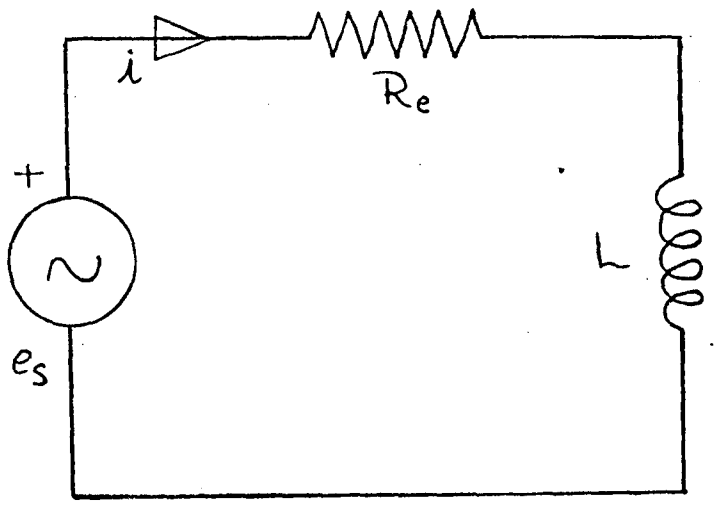

Electric circuit of a solenoid.

Fig. 2.5.

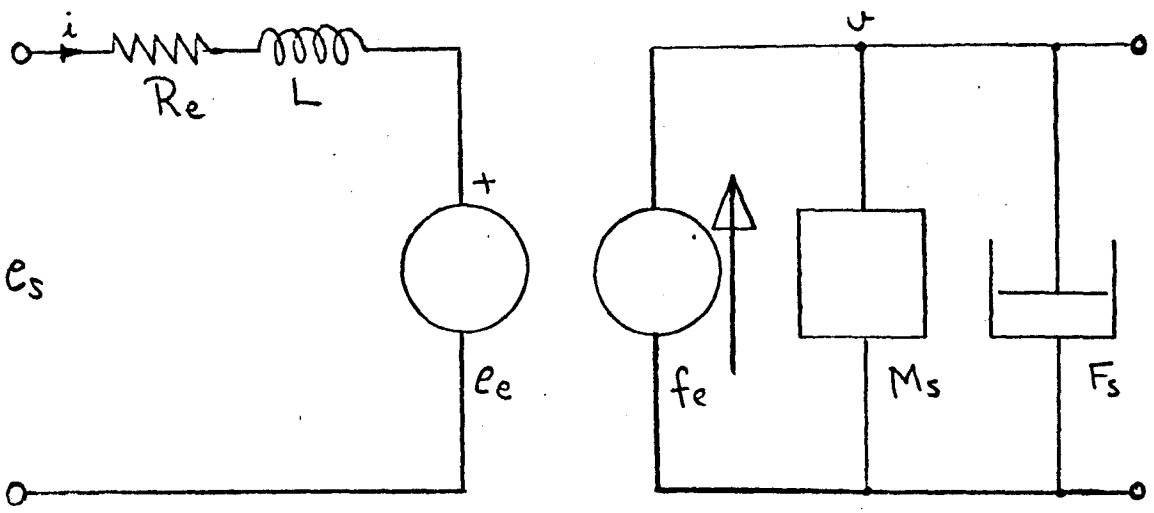

where $$f_e = \frac{F^2}{2}\frac{dP}{dx} = \frac{i^2 N^2}{2}\frac{dP}{dx}$$

$$e_e = i N^2 \frac{dP}{dx} \cdot \frac{dx}{dt}$$

Network of solenoid.

Fig. 2.6.

From this circuit, the mesh equation is,

$$e_s = i R_e + \frac{d(Li)}{dt} \tag{2.22}$$

Now since e_s is a sinusoidally varying voltage, i will be time dependent. The self-inductance L is defined as the ratio of flux linkage to current

$$L = \frac{N\phi}{i} = N^2 P \tag{2.23}$$

P depends on x which in turn is time dependent, therefore equation 2.22 becomes,

$$e_s = i R_e + L \frac{di}{dt} + i \frac{dL}{dt} \tag{2.24}$$

and substituting for equation 2.23,

$$e_s = i R_e + N^2 P \frac{di}{dt} + i N^2 \frac{dP}{dt} \tag{2.25}$$

$$\text{or } e_s = i R_e + N^2 P \frac{di}{dt} + i N^2 \frac{dP}{dx} \frac{dx}{dt} \tag{2.26}$$

Equation 2.25 is modified to give 2.26 because it is more convenient to calculate dP/dx than dP/dt.

If the mass of the solenoid armature is represented by M_s and its viscous friction coefficient is F_s then by considering equation 2.21 and 2.26 the network in Fig. 2.6 representing the solenoid can be constructed.

In any numerical work it is necessary to find P and dP/dx. Usually[19,20,21] only the main flux paths are considered and fringing and leakage are neglected. However, to obtain reasonably accurate results it is necessary to consider these flux paths. A comparison of results showing the validity of this statement is given under section 2.4.

The permeance is given by[20]

$$P = \frac{\mu_0 \mu_r \text{ area}}{\text{length}} \qquad (2.27)$$

To estimate the permeance of a flux path for a given geometrical configuration the mean length of that path and its average cross-sectional area must be determined. This has been done in reference 18 and these results are used in this work.

Consider the cross-section of the solenoid as shown in Fig. 2.7.

To find the total permeance of the flux paths initially, the following assumptions will be made.

(1) the permeance of the air path will always be much greater than that of the iron path.

(2) the effect of the shading rings is small when there is any significant air gap.

The effect of these assumptions are investigated in 2.1.3 and 2.4. Let each air path be represented by a resistor of conductance G_1, G_2 .... etc., where G_1 is equivalent to P_1 and similarly for others. Therefore the electrical analogue[21] of the magnetic circuit shown in Fig. 2.7 is given in Fig. 2.8.

The numbering of conductances corresponds to flux paths in Fig. 2.7.

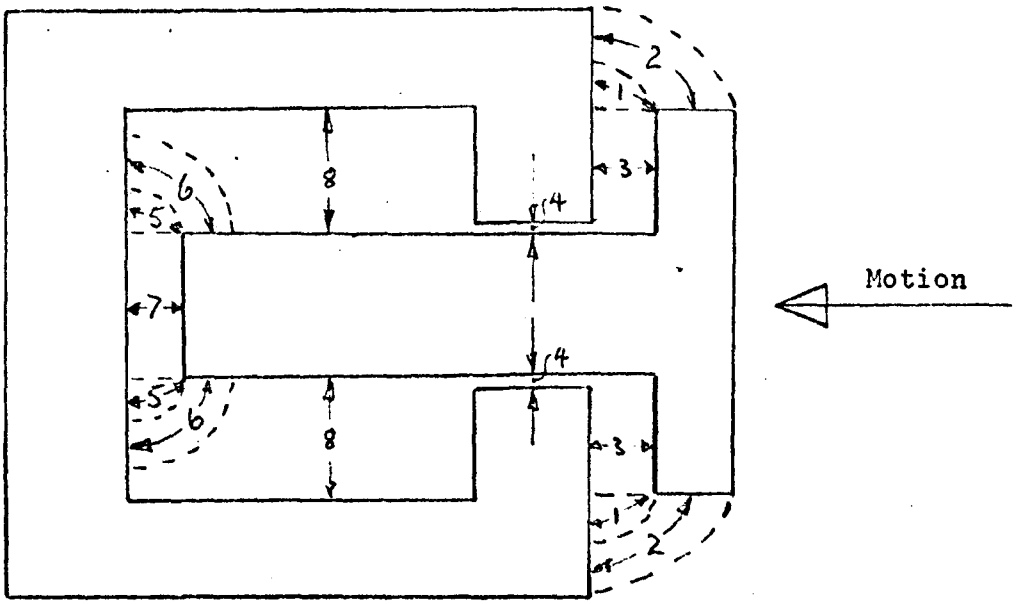

Flux paths in a solenoid.

Fig. 2.7.

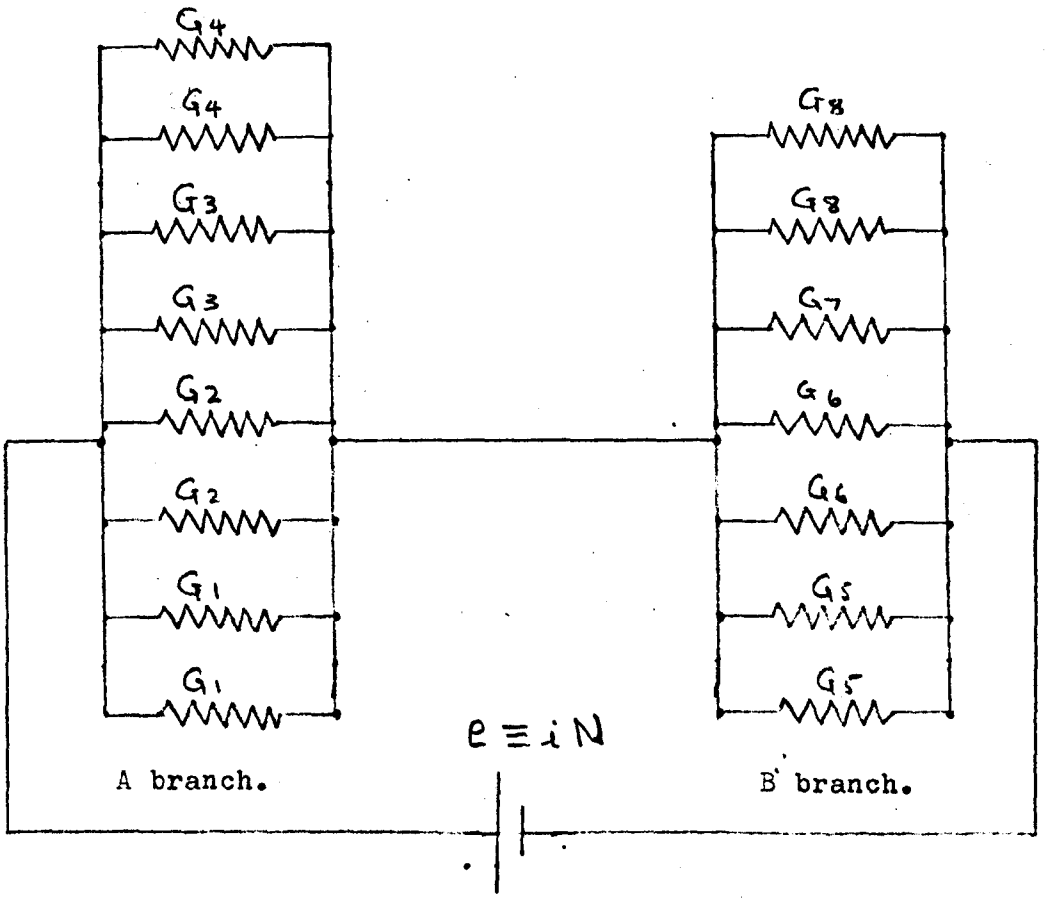

Electrical analogue of flux paths.

Fig. 2.8.

Considering Fig. 2.8.

Conductance of branch A and B

$$G_A = 2G_4 + 2G_3 + 2G_2 + 2G_1 \tag{2.28}$$

$$G_B = 2G_5 + 2G_6 + 2G_8 + G_7 \tag{2.29}$$

Now total conductance of circuit is,

$$G_T = \frac{G_A G_B}{G_A + G_B} \tag{2.30}$$

Combining equation 2.28 and 2.29 with 2.30 gives,

$$G_T = \frac{(2G_4 + 2G_3 + 2G_2 + 2G_1)(2G_5 + 2G_6 + 2G_8 + G_7)}{2G_1 + 2G_2 + 2G_3 + 2G_4 + 2G_5 + 2G_6 + G_7 + 2G_8} \tag{2.31}$$

Replacing G's for P's in equation 2.31.

$$P_T = \frac{(2P_1 + 2P_2 + 2P_3 + 2P_4)(2P_5 + 2P_6 + 2P_8 + P_7)}{2P_1 + 2P_2 + 2P_3 + 2P_4 + 2P_5 + 2P_6 + 2P_8 + P_7} \tag{2.32}$$

From equation 2.27 the values of P_1 to P_8 are determined using the solenoid's dimensions, for the different configurations shown in Fig. 2.7, see Figs. 2.9 to 2.13.

2.1.2 Application of theory to particular solenoids

The directional control, valve under consideration[22] uses solenoids type 18-7202[23], the valve manufacturers are considering the use of other types of solenoids[24]. It is, therefore, intended to apply the theory developed in section 2.1.1 to both solenoids.

These formula from reference 18,

For paths 1 and 5.

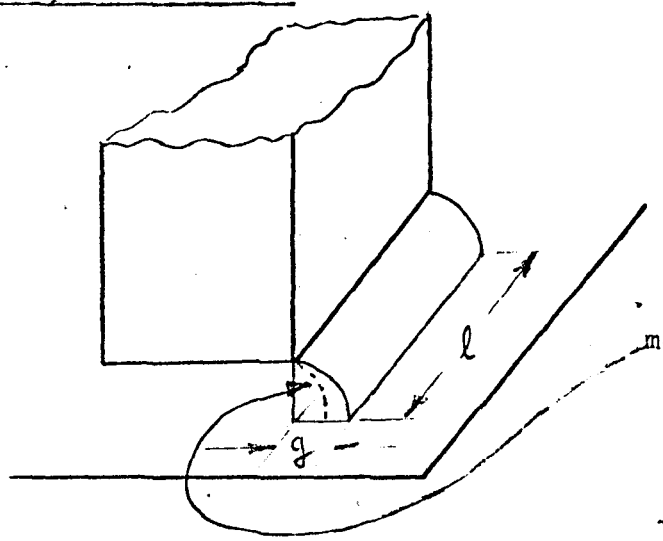

Fig. 2.9.

$$P_{1,5} = 0.52\mu_0 l \qquad (2.33)$$

since $\mu_r = 1$ for air.

For paths 2 and 6.

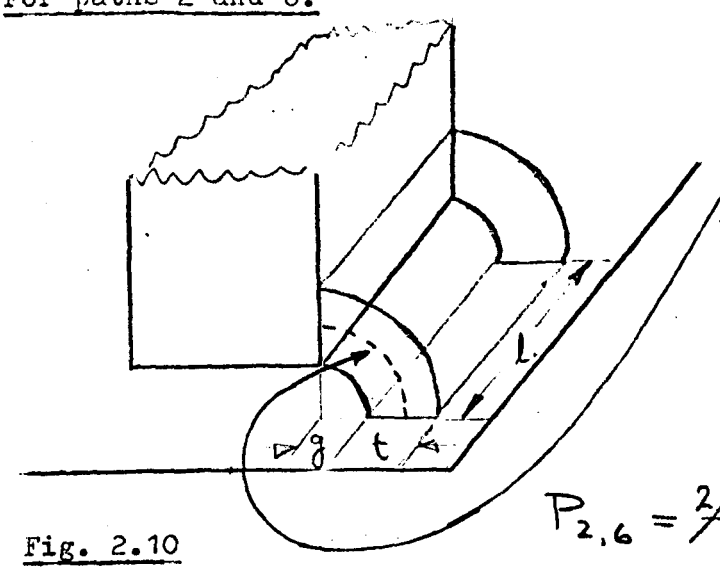

Fig. 2.10

$$P_{2,6} = \frac{1.28\mu_0 l}{1+2g/t} \qquad (2.34)$$

or when $g < 1.5t$

$$P_{2,6} = \frac{2\mu_0 l}{\pi} \log_e\left(1+\frac{t}{g}\right) \qquad (2.35)$$

For path 4.

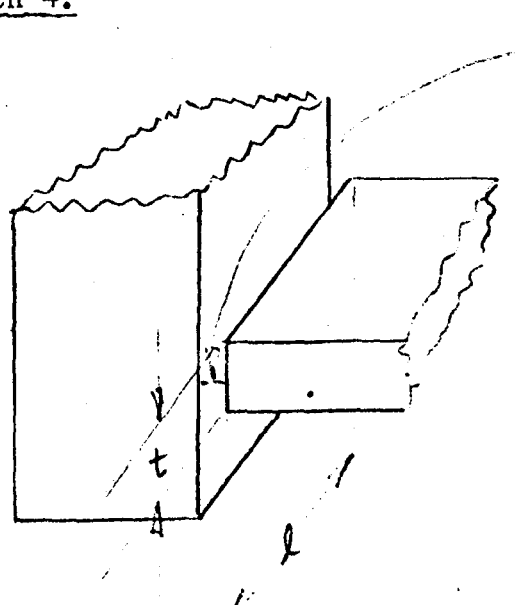

Fig. 2.11

$$P_4 = \frac{\mu_0 l t}{g} \qquad (2.36)$$

For path 3, and 7.

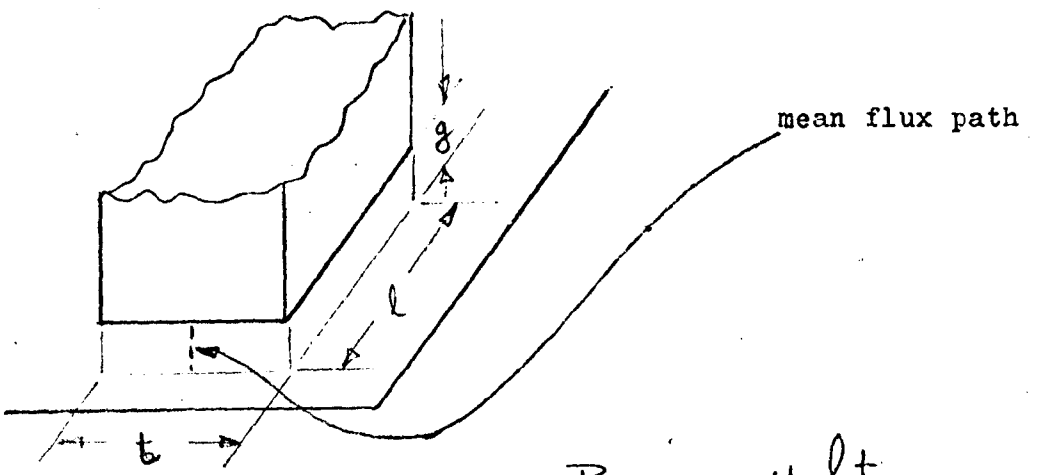

Fig. 2.12

$$P_{3,7} = \frac{\mu_0 l t}{g} \qquad (2.37)$$

For path 8.

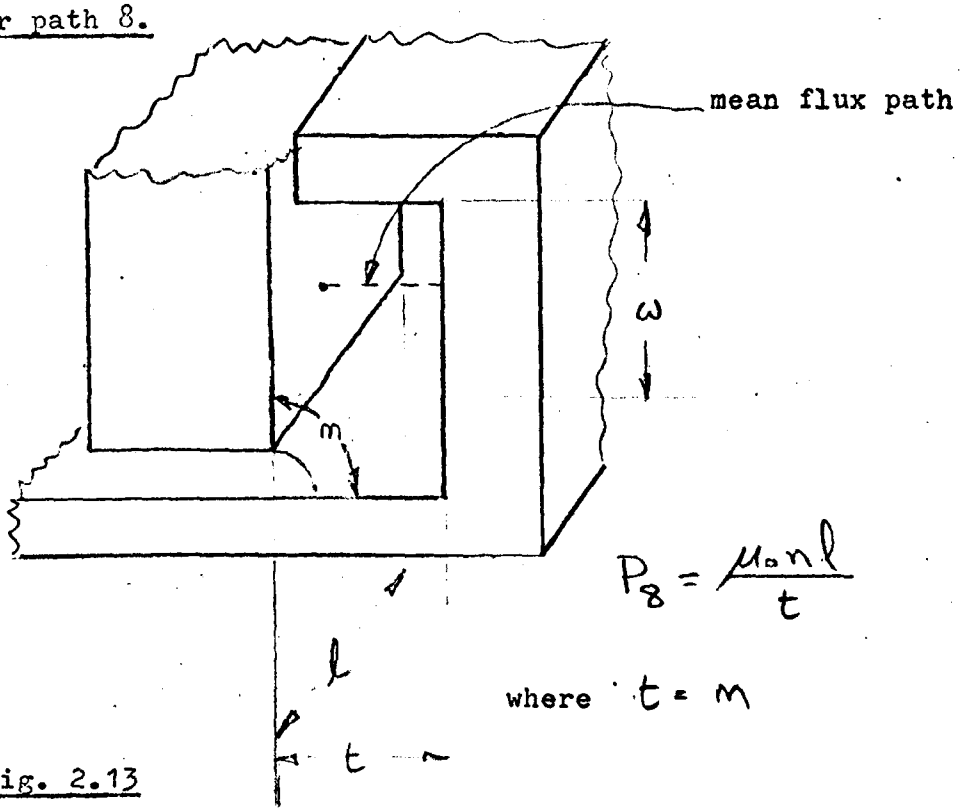

$$P_8 = \frac{\mu_0 n l}{t} \qquad (2.38)$$

where $t = m$

Fig. 2.13

However, due to the distribution of the coil in the space $t\omega$, Fig. 2.13, equation 2.38 becomes[18],

$$P_8 = \frac{\mu_0 l n^2}{2 \omega t} \qquad (2.39)$$

The physical dimensions of solenoid type 18-7202 are given in Fig. 2.14.

From considering Fig. 2.7 to 2.14 and equations 2.33 to 2.39 the total permeance of the flux paths can be determined. Thus substituting the resulting equations into equations 2.28 and 2.29, gives,

$$P_A' = 2\left[10.275 + 0.775 \log_e\left(1 + \frac{0.27}{x}\right) + \frac{0.457}{x}\right] 2.54 \mu_0 10^{-2} \quad (2.40)$$

$$P_B' = 2\left[1.515 + 0.775 \log_e\left(\frac{0.242}{x + 0.006}\right) + \frac{0.61}{2(x + 0.006)}\right] 2.54 \mu_0 10^{-2} \quad (2.41)$$

$$P_A' + P_B' = 2\left[11.79 + \frac{0.457}{x} + \frac{0.305}{x + 0.006} + 0.775 \log_e\left(1 + \frac{0.27}{x}\right) + 0.775 \log_e\left(\frac{0.242}{x + 0.006}\right)\right] 2.54 \mu_0 10^{-2} \quad (2.42)$$

Let $P_A' = 2 P_A 2.54 \mu_0 10^{-2}$ and $P_B' = 2 P_B 2.54 \mu_0 10^{-2}$

Therefore from equation 2.30

$$P_T = 5.08 \mu_0 10^{-2} \frac{P_A P_B}{P_A + P_B} \quad (H) \quad (2.43)$$

Thus the numerical value of P_T for any particular value of x can be found by substituting equations 2.40, 2.41 and 2.42 into equation 2.43 where x has the units of inches. Equation 2.43 is calculated by means of digital computer and the resulting curve is generated on analogue computer as explained in 2.2

It is also required to find the function dP_T/dx, differentiating equation 2.43

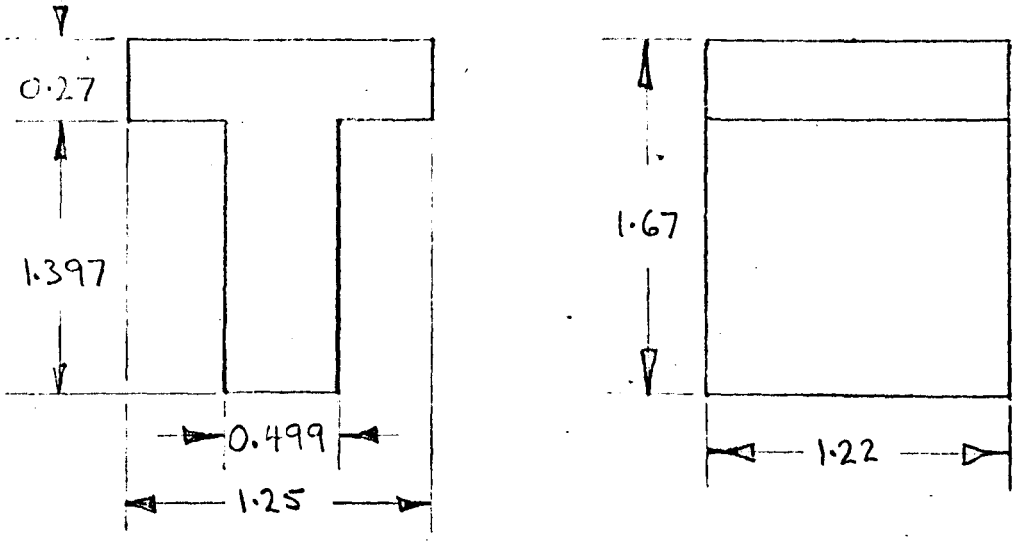

(a) Armature

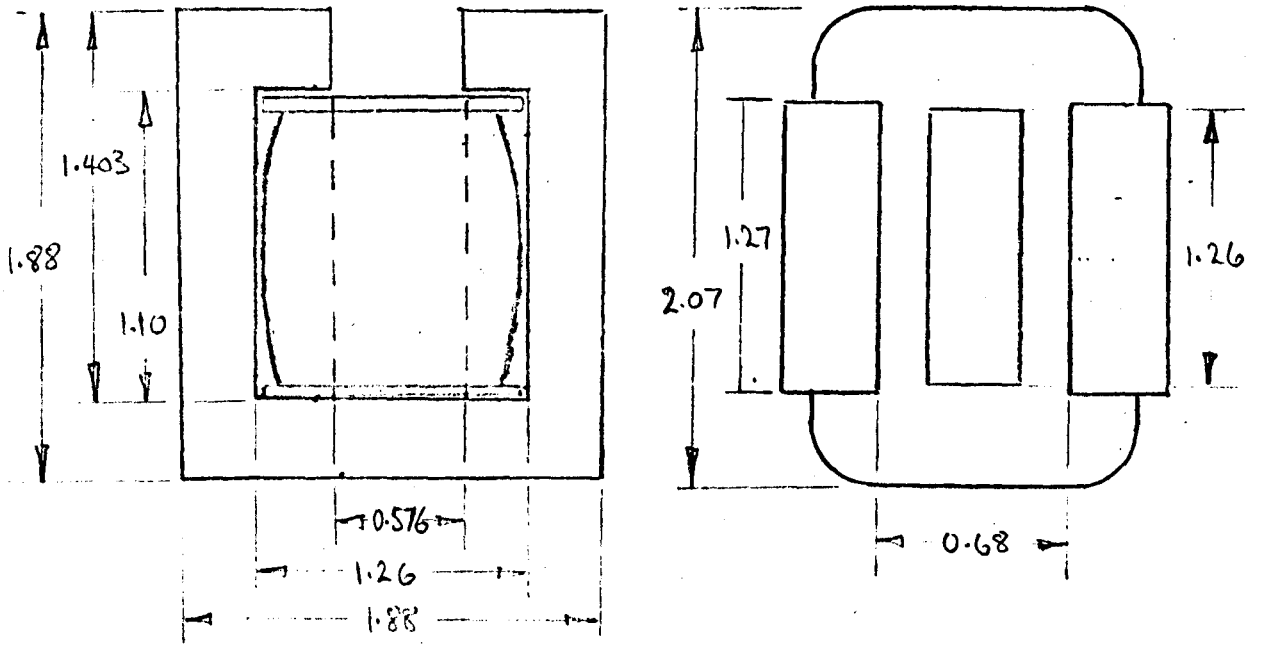

(b) Yoke and coil

All dimensions in inches.

Solenoid type 18-7202 dimensions.

Fig. 2.14.

$$\frac{dP_T}{dx} = 2\mu_0 \left[\frac{P_A}{(P_A+P_B)} \frac{dP_B}{dx} + \frac{P_B}{(P_A+P_B)} \frac{dP_A}{dx} - \frac{P_A P_B}{(P_A+P_B)^2} \frac{d(P_A+P_B)}{dx} \right] \quad (2.44)$$

where $$\frac{dP_B}{dx} = +3.2(x+0.006) - \frac{0.305}{(x+0.006)^2} \quad (2.45)$$

$$\frac{dP_A}{dx} = -\frac{0.207}{x^2+0.27x} - \frac{0.457}{x^2} \quad (2.46)$$

$$\frac{d(P_A+P_B)}{dx} = -\frac{0.457}{x^2} - \frac{0.305}{(x+0.006)^2} - \frac{0.207}{x^2+0.27x} + 3.2(x+0.006) \quad (2.47)$$

Thus the substitution of equations 2.45, 2.46 and 2.47 into equation 2.44 will give the function of dP_T/dx in terms of **x**. This is also found numerically by computing.

For the particular solenoid under test R_e was measured as 62 Ω and N given by the manufacturer as 1605. Thus equation 2.21 numerically.

$$f_e = \frac{i^2 1605^2}{2} \frac{dP_T}{dx}$$

in which i can be substituted from equation 2.26.

Considering the case when the armature is held open at a fixed position and a sinusoidally varying input is applied

$$\therefore \quad \frac{dx}{dt} = 0$$

and $$I = \frac{E^2}{\left(R_e^2 + (\omega N - P_T)^2\right)^{1/2}} \quad (2.48)$$

Substituting equation 2.48 in the force equation 2.21 gives:

$$f_e = \frac{(EN)^2}{2\left(R_e^2 + (\omega N^2 P_T)^2\right)} \frac{dP_T}{dx} \qquad (2.49)$$

Magnet Schultz Solenoid

This solenoid is of very similar design to the Expert solenoid and thus the same procedure is adopted. Fig. 2.15 shows the physical dimensions of the solenoid.

The solenoid will have the same flux paths, thus from considering Fig. 2.7 to 2.13 and 2.15 and equations 2.28, 2.29 and 2.33 to 2.39 the total permeance of the flux paths can be found.

$$P'_{SA} = 2\left[7.77 + 0.764 \log_e\left(1 + \frac{0.292}{x}\right) + \frac{0.376}{x}\right] 2.54 \mu_0 10^{-2} \qquad (2.50)$$

$$P'_{SB} = 2\left[1.097 + 0.764 \log_e\left(\frac{0.312}{x + 0.006}\right) + \frac{0.331}{x}\right] 2.54 \mu_0 10^{-2} \qquad (2.51)$$

$$(P'_{SA} + P'_{SB}) = 2\left[8.87 + 0.764 \log_e\left(1 + \frac{0.292}{x}\right) + 0.764 \log_e\left(\frac{0.312}{x + 0.006}\right) + \frac{0.376}{x} + \frac{0.331}{x + 0.006}\right] 2.54 \mu_0 10^{-2} \qquad (2.52)$$

As before $P'_{SA} = 5.08 P_{SA} \mu_0 10^{-2}$ etc.

$$\therefore P_{ST} = 5.08 \mu_0 10^{-2} \frac{P_{SA} P_{SB}}{P_{SA} + P_{SB}} \quad (H) \qquad (2.53)$$

$$\text{and } \frac{dP_{ST}}{dx} = 2\mu_0 \left[\frac{P_{SA}}{(P_{SA} + P_{SB})} \frac{dP_{SB}}{dx} + \frac{P_{SB}}{(P_{SA} + P_{SB})} \frac{dP_{SA}}{dx} - \frac{P_{SA} P_{SB}}{(P_{SA} + P_{SB})^2} \frac{d(P_{SA} + P_{SB})}{dx}\right] \qquad (2.54)$$

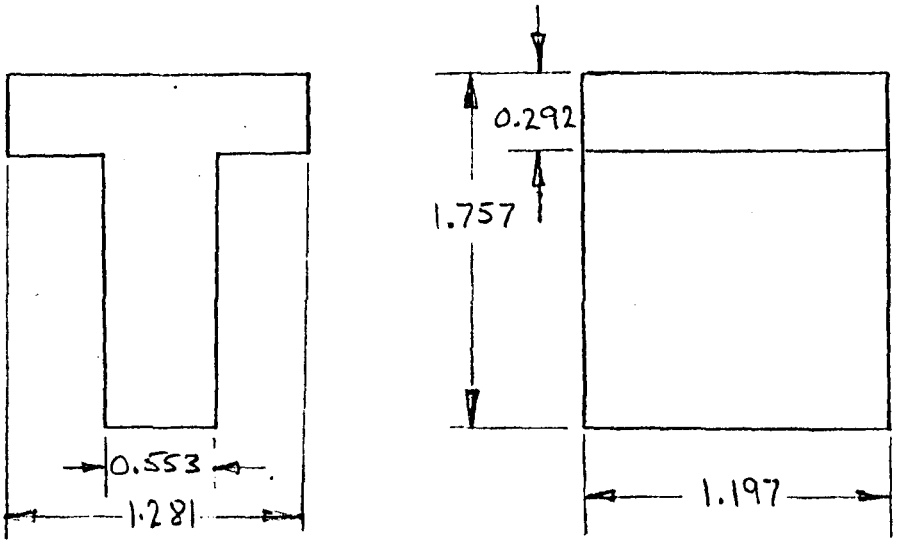

(a) Armature

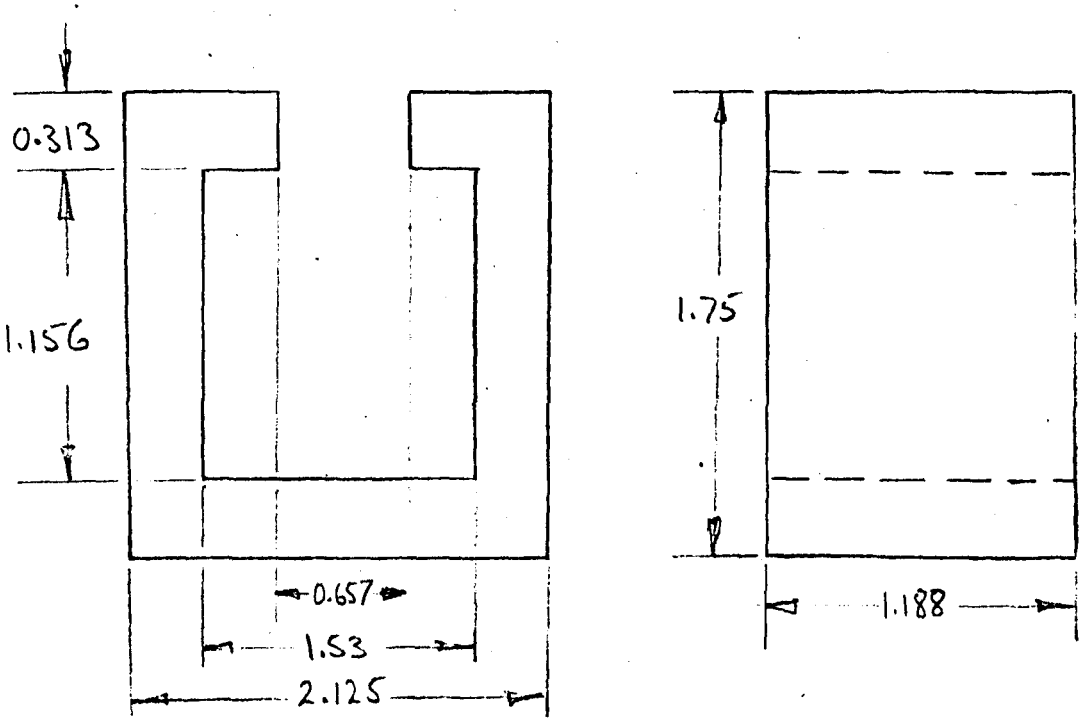

(b) Yoke and coil

All dimensions in inches.

Magnet Schultz solenoid.

Fig. 2.15.

where $$\frac{dP_{SB}}{dx} = 2.45(x+0.006) - \frac{0.331}{(x+0.006)^2} \quad (2.55)$$

$$\frac{dP_{SA}}{dx} = -\frac{0.223}{x^2+0.292x} - \frac{0.376}{x^2} \quad (2.56)$$

$$\frac{d(P_{SA}+P_{SB})}{dx} = \frac{dP_{SA}}{dx} + \frac{dP_{SB}}{dx} \quad (2.57)$$

From manufacturers literature number of turns is 1652 and resistance is 53.5 Ω

2.1.3 Effect of shading rings

Since a sinusoidally varying voltage is applied to the terminals of the solenoid the force generated will be proportional to sine square (equation 2.21). This means that the force becomes zero twice in one cycle causing vibrations in the valve system.

With reference to Fig. 2.16 single turns of copper wire lying at right angles to the main flux path are inserted which set up a secondary flux in the solenoid at 90° out of phase with the main flux i.e., when the main flux goes to zero the secondary flux is at its maximum. This prevents the force generated by the armature from going completely to zero, therefore the vibrations of the armature will be reduced. The turns of copper wire are termed shading rings and in the solenoids under consideration there are two such shading rings.

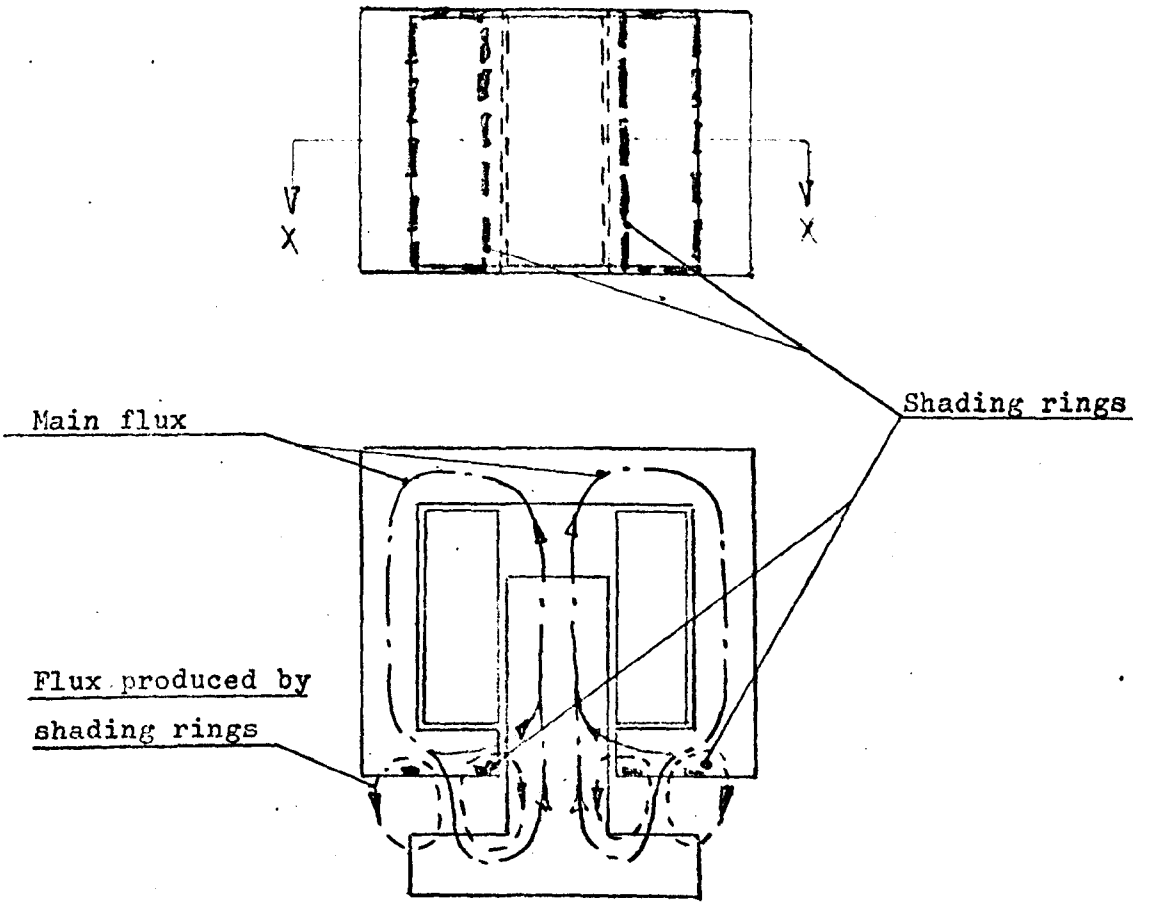

Cross-sectional view through XX

View of solenoid showing position of shading rings

Fig. 2.16

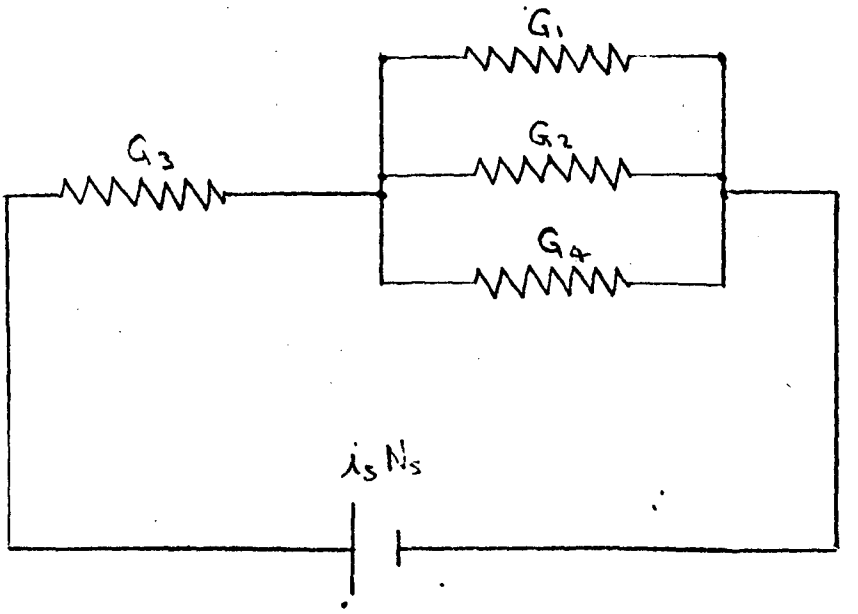

Flux paths of shading rings

Fig. 2.17

It is now intended to calculate the additional force acting on the armature due to the shading rings.

From equation 2.21

$$f = - \frac{i_s N_s}{2} \frac{dP_s}{dx} \qquad (2.58)$$

where i_s is the current circulating in the shading rings, P_s is the permeance of the flux path produced by the shading rings and N_s is the number of turns.

Consider i_s :-

$$i_s = \frac{e_s}{R_s} \qquad (2.59)$$

where R_s is the resistance of the shading rings and can be calculated from the knowledge of their dimensions and material.

$$R_s = \frac{\rho l}{A} \qquad (2.60)$$

where ρ is the resistivity of the material, l is the length of shading rings and A is the cross-sectional area.

e_s the induced voltage,

$$e_s = - N_s \frac{d(\phi_s)}{dt} \qquad (2.61)$$

ϕ_s is that portion of the main flux cutting the shading rings which passes through path 3 indicated in Figs. 2.7 and 2.16. Thus it is necessary to find this portion.

Referring to Fig. 2.8 let iN' be the magneto-motive force across branch A then,

$$\phi_s = i N' P_3 \tag{2.62}$$

$$\text{and } i N' = \phi_T \left[\frac{1}{2P_3 + 2P_4 + 2P_2 + 2P_1} \right] \tag{2.63}$$

where $\phi_T = i N P_T$

where P_T is the total permeance, i is the current in main coil.

Substituting

$$\phi_s = i N \left(\frac{P_T P_3}{2P_3 + 2P_4 + 2P_2 + 2P_1} \right) = i N \left(\frac{P_T P_3}{P_A'} \right) \tag{2.64}$$

Substituting equation 2.64 for 2.61 and then into 2.59 results

$$i_s = - \frac{N_s}{R_s} \frac{d\left(i N P_T P_3 / P_A'\right)}{dt}$$

differentiating

$$i_s = - \left[\frac{N N_s P_3 P_T}{R_s P_A'} \frac{di}{dt} + \frac{N_s N i}{R_s} \frac{d(P_3 P_T / P_A')}{dx} \frac{dx}{dt} \right] \tag{2.65}$$

Referring to Fig. 2.7 and 2.16 it is assumed that the flux generated by the shading rings will have a path passing through P_1, P_2, P_3 and P_4. The electrical analogue of these flux paths is given in Fig. 2.17.

From Fig. 2.17

$$P_s = \frac{(P_1 + P_2 + P_4) P_3}{P_1 + P_2 + P_3 + P_4} \tag{2.66}$$

Substituting equation 2.66 and 2.65 into equation 2.58, noting that for the particular case under consideration $N_s = 1$,

$$f_s = \frac{-1}{2}\left[\frac{NP_3P_T}{R_sP_A'}\frac{di}{dt} + \frac{Ni}{R_s}\frac{d(P_3P_T/P_A')}{dx}\frac{dx}{dt}\right]^2 \frac{d}{dx}\left(\frac{(P_1+P_2+P_4)P_3}{P_1+P_2+P_3+P_4}\right) \quad (2.67)$$

There are two identical coils placed symmetrically on either side of the armature therefore the total force will be $2\,f_s$.

Application to solenoid type 18-7202

Calculation of R_s

Length of copper coil = 0.071 m

Cross-sectional area of copper coil = $1.2\ 10^{-6}\ m^2$

resistivity at 20°C = $1.75\ 10^{-8}\ \Omega\ m$

Therefore from equation 2.60

$$R_s = 10^{-3}\ \Omega$$

Calculation of the permeances

P_3 is given by equation 2.37

P_T is given by equation 2.43

P_A' is given by equation 2.40

From equation 2.40

$$\frac{P_A'}{2} = P_1 + P_2 + P_3 + P_4$$

and from equation 2.37, 2.36, 2.35 and 2.33 equation 2.66 becomes

$$P_s = \frac{\left[10.275\mu_o + 0.775\mu_o \log_e\left(1+\frac{0.27}{x}\right)\right] 2\mu_o 0.457 (2.54\,10^{-2})^2}{P'_A x} \qquad (2.68)$$

differentiating,

$$\frac{dP_s}{dx} = \frac{5.08\,10^{-2}\left[\frac{\mu_o^2 4.7}{x^2} - \frac{\mu_o^2 0.355}{x^2}\log_e\left(1+\frac{0.27}{x}\right) - \frac{\mu_o^2 0.096}{x^3+0.27x^2}\right]}{P'_A} - \frac{\left[\frac{\mu_o^2 4.7}{x} + \frac{\mu_o^2 0.355}{x}\log_e\left(1+\frac{0.27}{x}\right)\right]\left[-\frac{0.207}{x^2+0.27x} - \frac{0.457}{x^2}\right](5.08\,10^{-2})^2}{(P'_A)^2} \qquad (2.69)$$

Thus the force equation 2.67 can be solved. Equations 2.69 and 2.67 have been solved numerically by analogue and digital computers.

Since the flux set up by the shading rings is 90° out of phase with the main flux, were this flux of comparable value to the main flux it would reduce substantially the current in the main coil and thus reduce the main flux. It was subsequently found from theoretical and experimental work that this condition only occurred when the armature was virtually in the fully closed position. Therefore, this effect on the transient behaviour of the solenoid can be neglected.

2.2 Computing

A Honeywell 200 digital computer at Enfield College of Technology was used for the calculations of,

(a) values of permeance

(b) values of rate of change of permeance with respect to displacement

(c) the average force generated for solenoid type 18-7202.

All these calculations were computed for discrete values of armature displacement. The computer language used for programming was Fortran IV[25,26].

Since the force produced by armature of the solenoid is time varying, even when the armature is stationary, the solenoid was simulated on an analogue computer for

(a) when the armature was held at a fixed displacement. For this case the potentiometers were set at given values of permeance obtained from calculations by the digital computer.

(b) when the armature was allowed to move. For this case the graph of permeance as a function of displacement and rate of change of permeance with respect to displacement was obtained from the digital computer and set by function generators in the analogue computer.

Since condition (b) is only of interest when the armature of the solenoid is pushing some object it is not considered here but under Chapter 4.

For solving (a) a Pace TR 48 analogue computer, available at Enfield College of Technology, was used.

2.2.1 Digital Computing

Calculation of (a) permeance (b) rate of change of permeance with respect to displacement and (c) the average force generated for solenoid type 18-7202. These three factors are computed on one programme where;

(a) to compute the permeance it is necessary to solve equation 2.43.

$$\left.\begin{aligned} P_A &= 10.275 + 0.775 \log_e\left(1 + \frac{0.27}{x}\right) + \frac{0.457}{x} \\ P_B &= 1.515 + 0.775 \log_e\left(\frac{0.242}{x+0.006}\right) + \frac{0.305}{x+0.006} \\ P_T &= 0.638\, 10^{-7} \cdot \frac{P_A P_B}{P_A + P_B} \end{aligned}\right\} \quad (2.70)$$

Where in the programme, P_A, P_B, and P_T are designated as A, B and P respectively

(b) to compute dP_T/dx it is necessary to solve equation 2.44

$$\left.\begin{aligned} \frac{dP_B}{dx} &= 0.32(x+0.006) - \frac{0.305}{(x+0.006)^2} \\ \frac{dP_A}{dx} &= -\frac{0.207}{x^2+0.27x} - \frac{0.457}{x^2} \\ \frac{d(P_A+P_B)}{dx} &= \frac{dP_B}{dx} + \frac{dP_A}{dx} \\ \frac{dP_T}{dx} &= 0.251\, 10^{-5}\left[\frac{P_A\, dP_B/dx + P_B\, dP_A/dx}{(P_A+P_B)} - \frac{P_A P_B\, d(P_A+P_B)/dx}{(P_A+P_B)^2}\right] \end{aligned}\right\} \quad (2.71)$$

Where in the programme $\frac{dP_A}{dx}$, $\frac{dP_B}{dx}$, $\frac{d(P_A+P_B)}{dx}$ and $\frac{dP_T}{dx}$ are designated as E, D, F and G respectively.

(c) to compute the average force it is necessary to solve equation 2.49

$$f_e = \frac{(EN)^2\, dP_T/dx}{2\left(R_c^2 + \cdot(\omega N^2 P_T)^2\right)}$$

Where dP_T/dx and P_T have been found before and $R_e = 62\ \Omega$

$N = 1605$ and $\omega = 2\ \pi\ 50$ rad/s.

The applied voltage considered for this case is 240 V., therefore equation 2.49 becomes,

$$f_e = \frac{0.745\ 10^{11}\ dP_T/dx}{\left[3850 + (0.81\ 10^9\ P_T)^2\right]} \qquad (2.72)$$

in the programme f_e is designated as A5.

Thus a programme can now be written for solving equation 2.70, 2.71 and 2.72 for various values of x from 0.01 in. to 0.26 in. (0.25 in. is the working stroke of the solenoid). This programme is shown in Fig. 2.18 and the results are plotted in Fig. 2.19 and 2.20.

If the resulting values of P_T are substituted into equation 2.48 then the theoretical values of current can be calculated. These results are presented in graphical form in Fig. 2.19, Graph B.

In addition to the final results information is computed and printed out in the programme (i.e., A1, A2, A3 and A4), these are intermediate calculations for checking the computation.

Regarding the Magnet-Schultz solenoid, the same computations are carried out as for the solenoid type 18-7202. Thus the same form of programme is used and the notation is identical with that of the previous programme.

The equations programmed are equations 2.53, 2.54 and 2.49 with the appropriate numerical values. This programme is given in Fig. 2.21 and the results in Figs. 2.19 and 2.20.

```
                                                    FORTRAN  D  SYSTEM TAPE
*JOBID,F12

            JOB NAME  *NONAM

FORTRAN     200       SOURCE LISTING AND DIAGNOSTICS

       C        K.SIMPSON STAFF
001              X=0.01
002     13       A=10.275+0.775*ALOG(1.0+0.27/X)+0.457/X
003              B=1.515+0.775*ALOG(0.242/(X+0.006))+0.305/(X+0.006)
004              C=A+B
005              P=0.638*(10.0**(-7))*A*B/C
006              E=3.2*(X+0.006)-0.305/(X+0.006)**2
007              D=-0.207/(X*X+0.27*X)-0.457/(X*X)
010              F=E+D
011              G=0.251*(10.0**(-5))*(A*E/C+B*D/C-A*B*F/(C*C))
012              A1=0.745E11*G
013              A2=(0.81E9*P)**2
014              A3=3850.0+A2
015              A4=A1/A3
016              A5=0.745E11*G/(3850.0+(0.81E9*P)**2)
017              WRITE(3,11)X,P,G,A1,A2,A3,A4,A5
020     11       FORMAT(4(2X,E18.12)/10X,4(2X,E18.12))
021              X=X+0.01
022              IF(X.GT.0.26)GO TO 12
023              GO TO 13
024     12       STOP
025              END
```

Programme for solenoid type 18-7202

Fig. 2.18

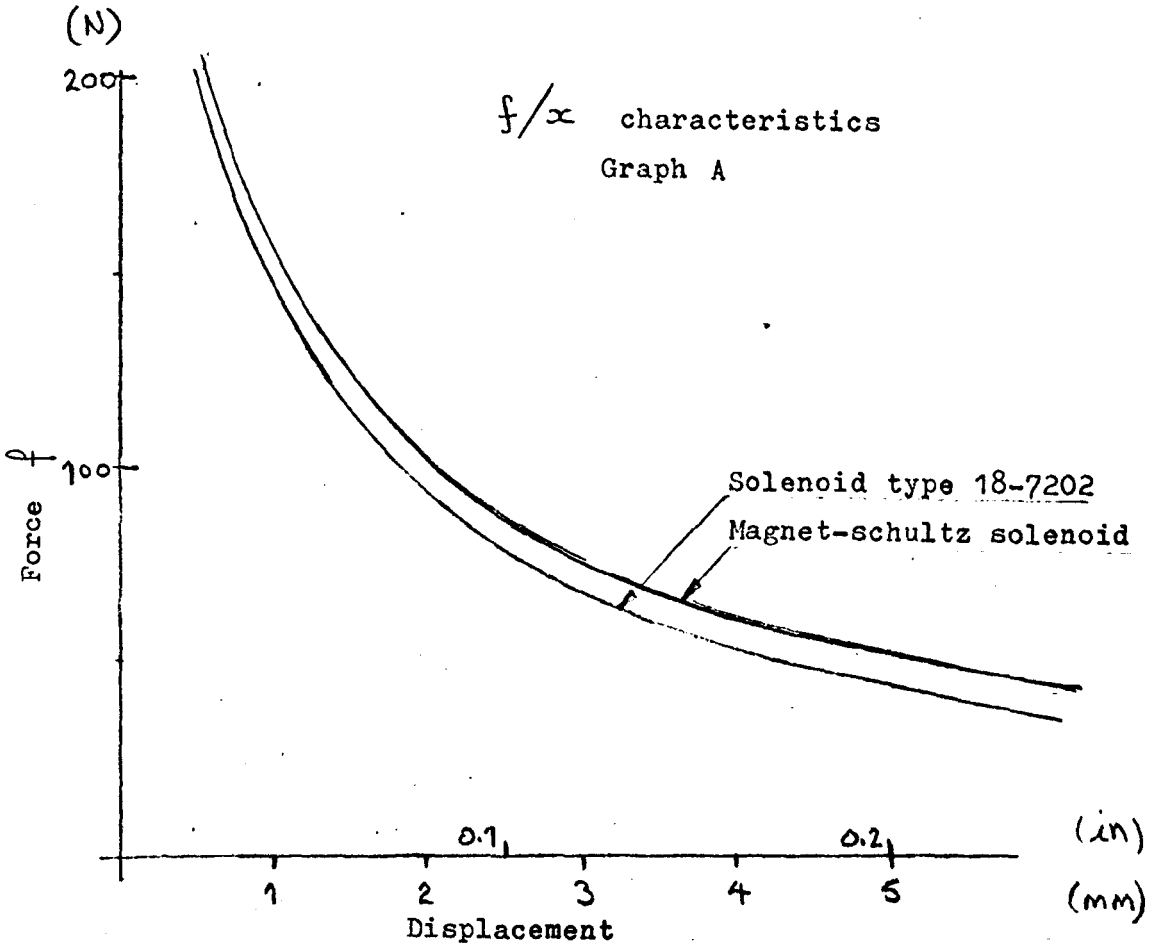

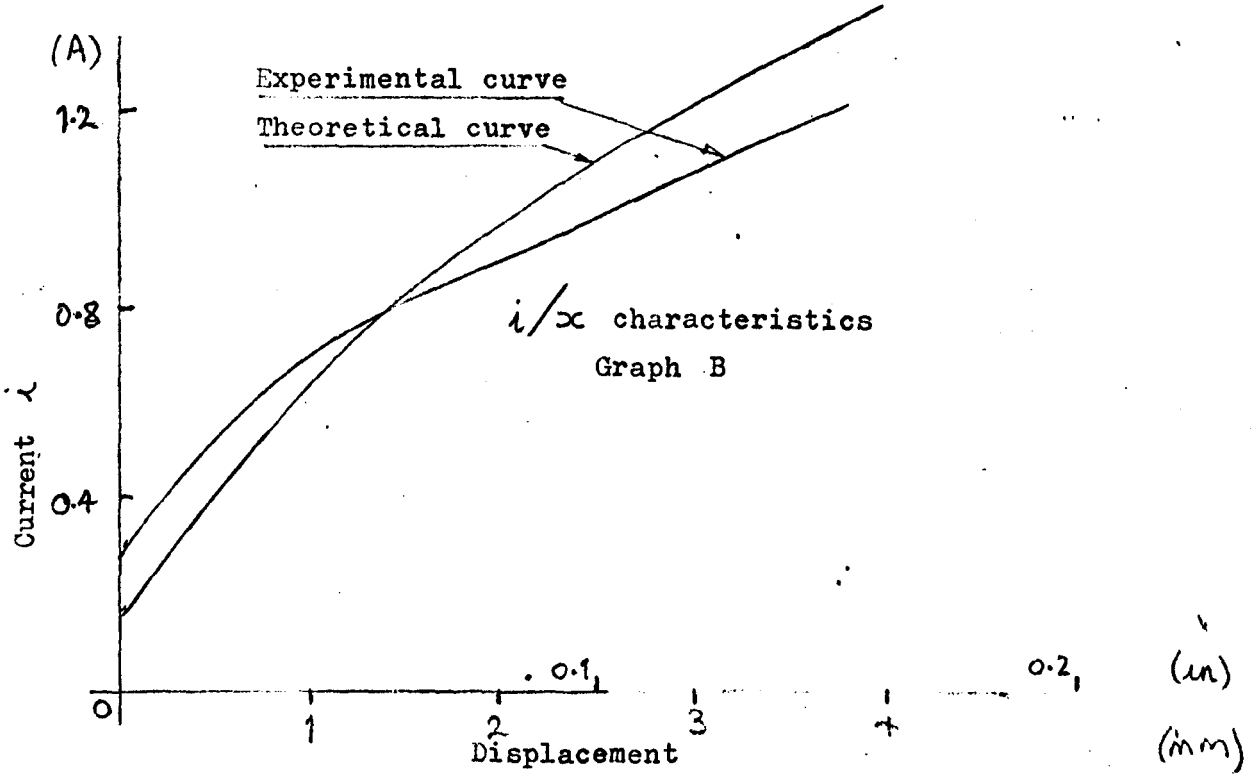

Digital computer results

Fig. 2.19

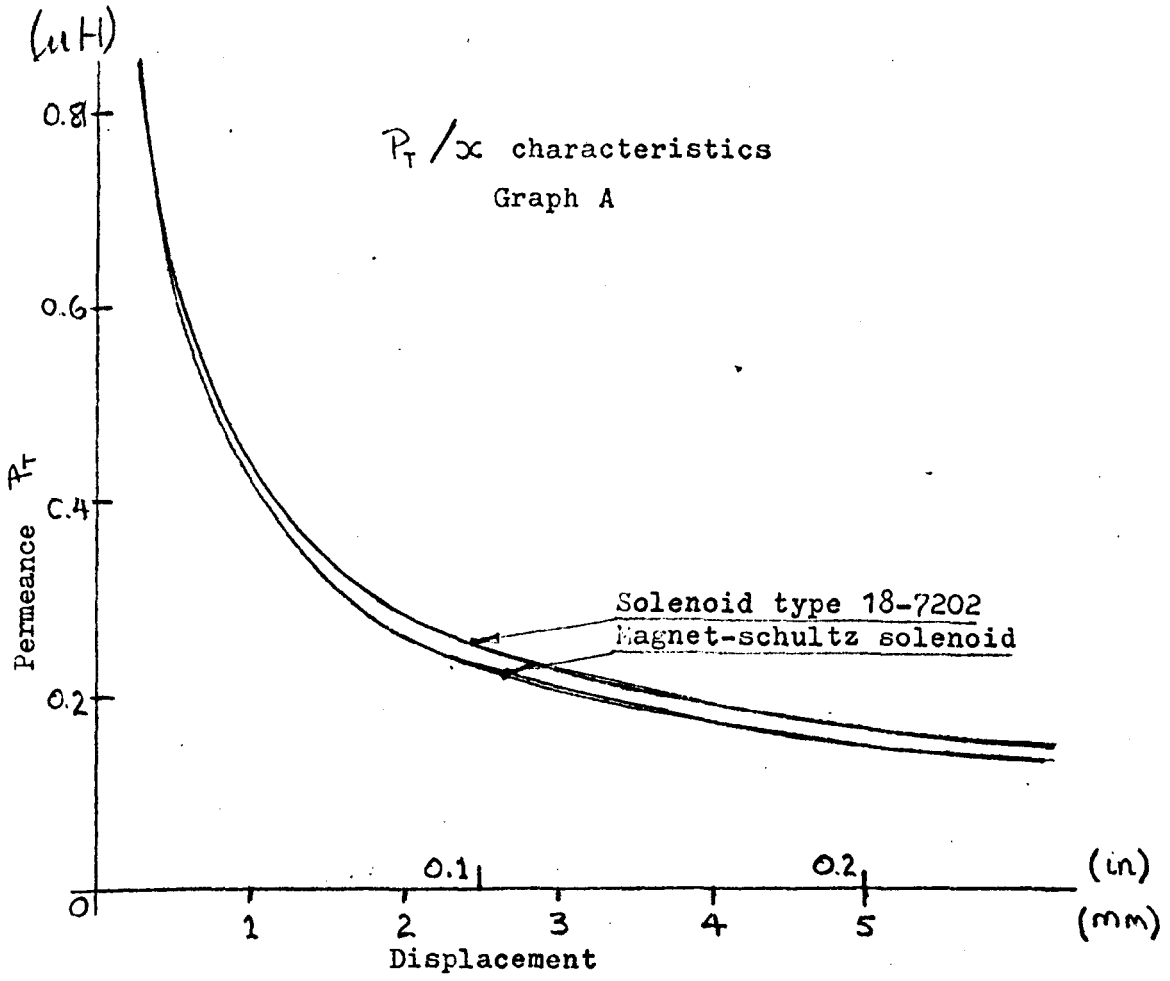

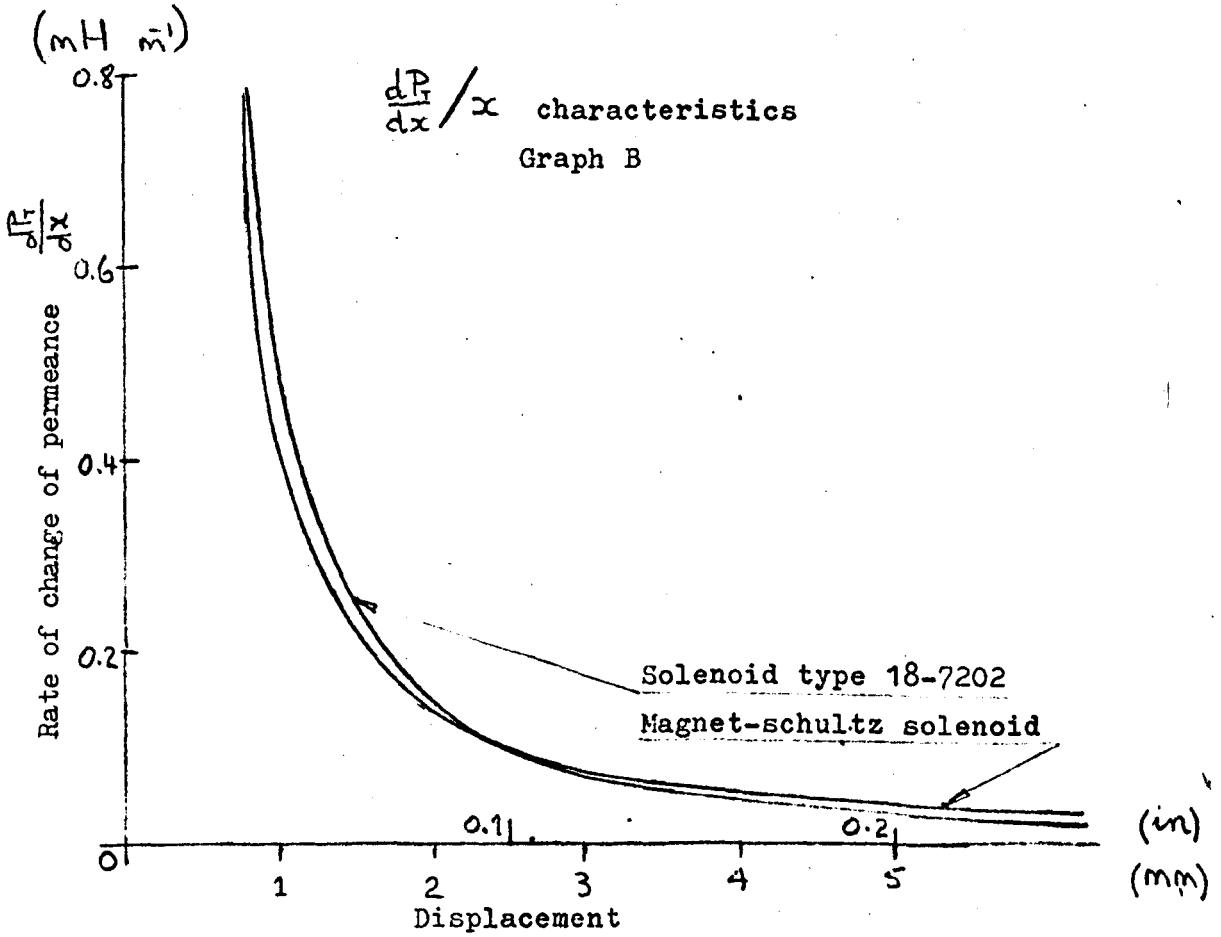

Digital computer results

Fig. 2.20

```
                                        FORTRAN  D  SYSTEM TAPE  REVISION NUMBER
*JOBID,F12

            JOB NAME  *NONAM

FORTRAN     200       SOURCE LISTING AND DIAGNOSTICS                PROGRAM: NON

      C       K.SIMPSON STAFF
001            WRITE(3,23)
002     23     FORMAT(4X,15HDISPLACEMENT IN;,3X,13HPERMENANCE H;,8X,21HDELTA PERME
              1NANCE H/M;,3X,8HFORCE N;)
003            X=0.01
004     13     A=7.77+0.764*ALOG(1.0+0.292/X)+0.376/X
005            B=1.097+0.764*ALOG(0.312/(X+0.006))+0.331/(X+0.006)
006            C=A+B
007            P=0.638*(10.0**(-7))*A*B/C
010            E=2.45*(X+0.006)-0.331/(X+0.006)**2
011            D=-0.223/(X*X+X*0.292)-0.376/(X*X)
012            F=E+D
013            G=0.251*(10.0**(-5))*(A*E/C+B*D/C-A*B*F/(C*C))
014            A5=0.788E11*G/(2850.0+(0.86E9*P)**2)
015            WRITE(3,11)X,P,G,A5
016     11     FORMAT(4(2X,E18.12))
017            X=X+0.01
020            IF(X.GT.0.26)GO TO 12
021            GO TO 13
022     12     STOP
023            END
```

Magnet-schultz solenoid programme

Fig. 2.21

Calculations of the effects of the shading rings alone.

These calculations are similar to those previously carried out and the equations to be evaluated are 2.68, 2.69 and 2.67 multiplied by factor 2 since there are two shading rings.

It should be noted that those equations only apply to the solenoid type 18-7202 and the force calculated is the average force due to the shading rings. The programme for these results is in Fig. 2.22 and the results are in Fig. 2.23.

2.2.2 Analogue Computing

Analogue computer circuit for condition (a):-
The equations to be programmed[26,27] are, 2.26 and the sum of equations 2.21 and 2.67 (noting that for this case $\frac{dx}{dt} = 0$)
From equation 2.26,

$$e_s = i R_e + N^2 P_T \frac{di}{dt}$$

rearranging

$$\frac{di}{dt} = \frac{e_s}{N^2 P_T} - \frac{R_e}{N^2 P_T} i \qquad (2.73)$$

The total force due to both shading rings and main coil is :-

$$f = -\frac{(iN)^2}{2} \frac{dP_T}{dx} - \left[\frac{N P_3 P_T}{R_s P'_A} \frac{di}{dt}\right]^2 \frac{dP_s}{dx} \qquad (2.74)$$

```
                                        FORTRAN  D  SYSTEM TAPE  REVISION NUMBER
*JOBID,F12

          JOB NAME  *NONAM

FORTRAN     200       SOURCE LISTING AND DIAGNOSTICS                  PROGRAM: SHA

       TITLESHADING RINGS
      C       K.SIMPSON STAFF
001           REAL N
002           WRITE(3,23)
003     23    FORMAT(9X,1HX,18X,2HPU,17X,2HPT,18X,2HPX/18X,1HC,17X,3HDPX,18X,1HF
             1)
004           X=0.001
005     13    PU=(0.457/X+10.28+0.775*ALOG(1.0+0.27/X))*63.8*(10.0**(-9))
006           A=10.275+0.775*ALOG(1.0+0.27/X)+0.457/X
007           B=1.515+0.775*ALOG(0.242/(X+0.006))+0.305/(X+0.006)
010           CC=A+B
011           PT=0.638E-7*A*B/CC
012           PX=(10.275+0.775*ALOG(1.+0.27/X))*(0.457/X)*2.*(0.319E-7)**2/PU
013           E=240.0
014           N=1605.0
015           RS=0.1E-2
016           P3=0.1455E-7/X
017           C=(N*P3*PT/(RS*PU))**2
020           R=62.0
021           DPX=-((4.7/(X*X)+(0.355*ALOG(1.+0.27/X))/(X*X)+0.096/(X**3+0.27*X*
             1X))/A+((4.7/X+(0.355*ALOG(1.+0.27/X))/X)*(-0.207/(X*X+0.27*X)-0.45
             27/(X*X))/A*A))*0.1256E-9
022           F=C*DPX*(E/(PT*N*N)-E*R/(N*N*PT*(R*R+(314.2*N*N*PT)**2)**0.5))**2
023           WRITE(3,11)X,PU,PT,PX,C,DPX,F
024     11    FORMAT(4(2X,E18.12)/10X,3(2X,E18.12))
025           X=X+0.001
026           IF(X.GT.0.03)GO TO 12
027           GO TO 13
030     12    STOP
031           END
```

Shading rings digital programme

Fig. 2.22

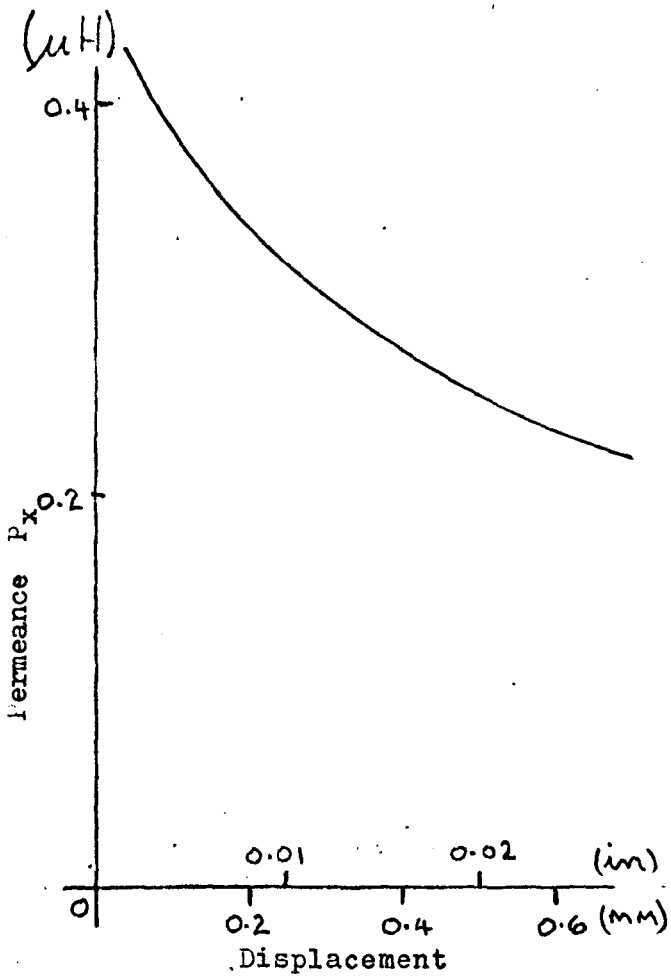

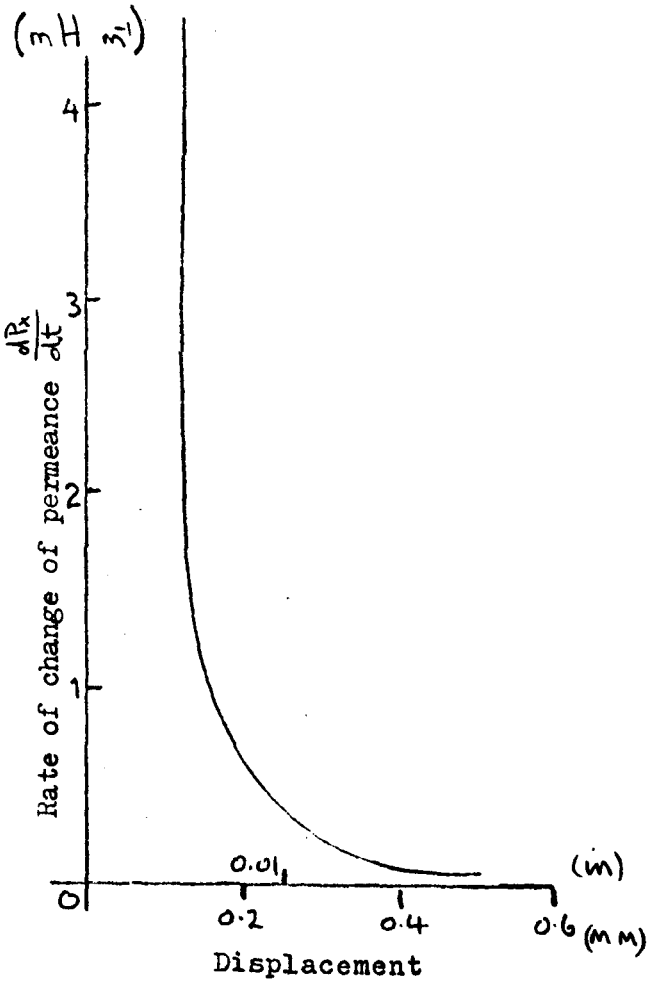

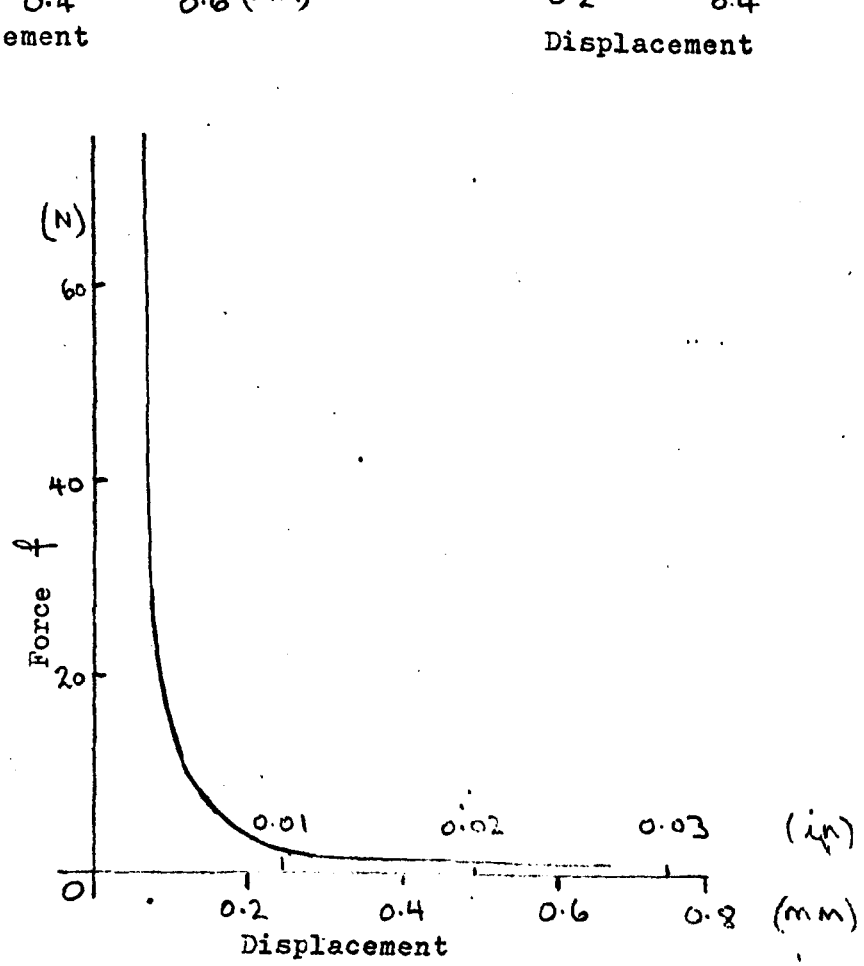

Digital computer results for shading rings.

Fig. 2.23

The parameters of equations 2.73 and 2.74 are found for any particular displacement from the digital computer results. Thus for a particular displacement the equations can be amplitude and time scaled. As an example consider a displacement of 0.02 in. From the numerical results (not included) corresponding to Figs. 2.20 and 2.23

$$P_T = 0.67 \ 10^{-6} \ (H)$$

$$\frac{dP_s}{dx} = 0.42 \ 10^{-4} \ (H \ m^{-1})$$

$$\left(\frac{N P_3 P_T}{R_s P_A'}\right) = 0.121 \ (H \ \Omega^{-1})$$

$$\frac{dP_T}{dx} = 0.82 \ 10^{-3} \ (H \ m^{-1})$$

Therefore equations 2.73 and 2.74 become

$$f = -\left[1060 \, i^2 + 0.504 \ 10^{-5} \left(\frac{di}{dt}\right)^2\right] \qquad (2.75)$$

$$\frac{di}{dt} = \frac{e}{1.67} - 36 \, i \qquad (2.76)$$

Scaling the variables ,

$$f_{max.} = 200 \, N$$

$$i_{max.} = 1 \, A$$

$$e_{max.} = 500 \, v$$

$$t = \tau / 1000$$

Thus equations 2.75 and 2.76 become,

$$\left(\frac{f}{200}\right) = -\left(\frac{i}{1}\right)^2 2.12 - 0.001\left[\frac{d(i/1)}{d\tau}\right]^2 \qquad (2.77)$$

$$\frac{d(i/1)}{d\tau} = \left(\frac{e}{500}\right)0.29 - 0.036\left(\frac{i}{1}\right) \qquad (2.78)$$

To enable an analogue computer circuit diagram to be drawn it is useful to first draw a signal flow graph[28] representing the equations as in Fig. 2.24a. The analogue computer circuit diagram and potentiometer settings are given in Fig. 2.24b. This technique of obtaining the analogue computer circuit diagram is used throughout this work, however, other signal flow graphs used have not been reproduced in this thesis.

Consideration of the input voltage

$$e = E_{max.} \sin \omega t$$

taking the Laplace transform

$$e_{(s)} = \frac{E_{max.}\ \omega}{s^2 + \omega^2}$$

or $$s^2 e_{(s)} + e_{(s)}\omega^2 - E_{max.}\omega = 0 \qquad (2.79)$$

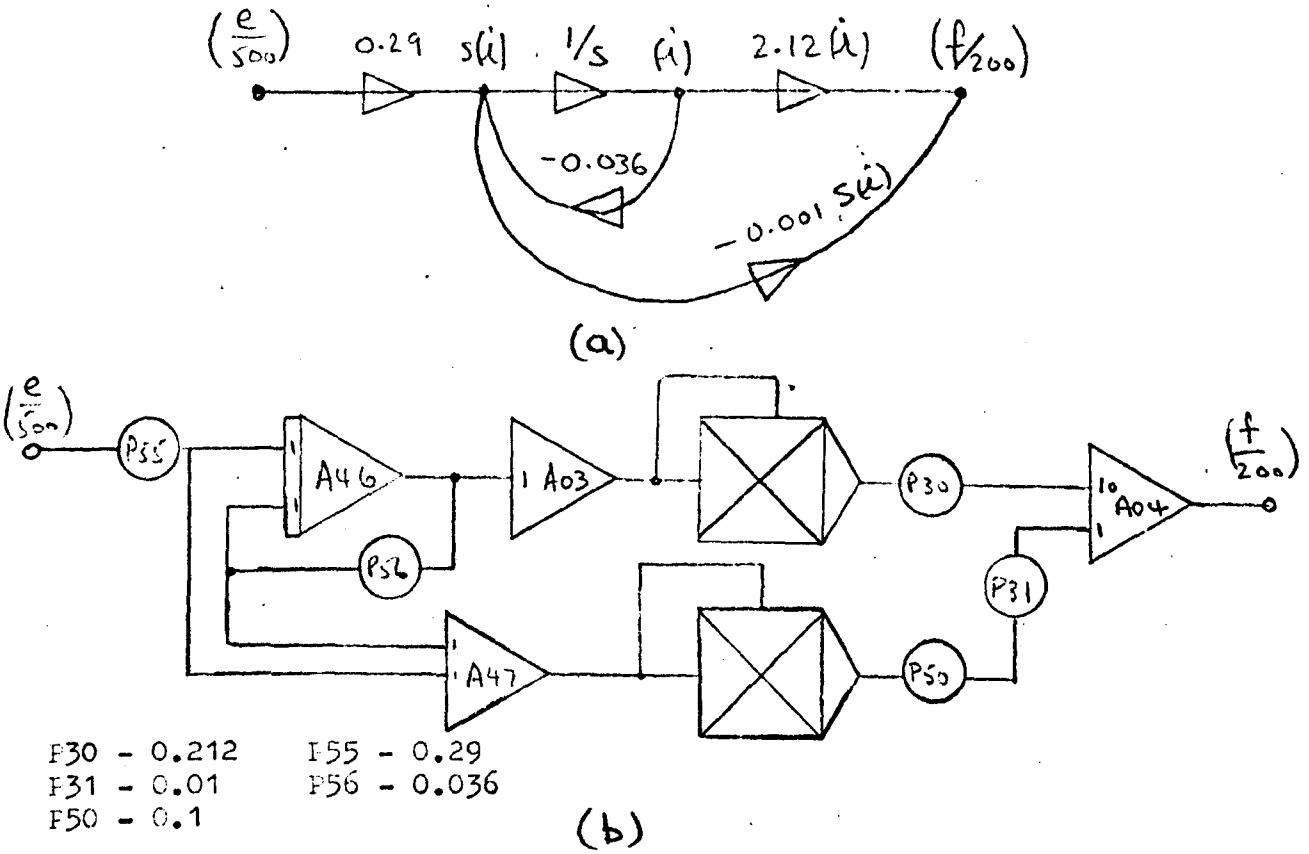

Analogue computer circuit diagram for a solenoid at fixed displacements

Fig. 2.24

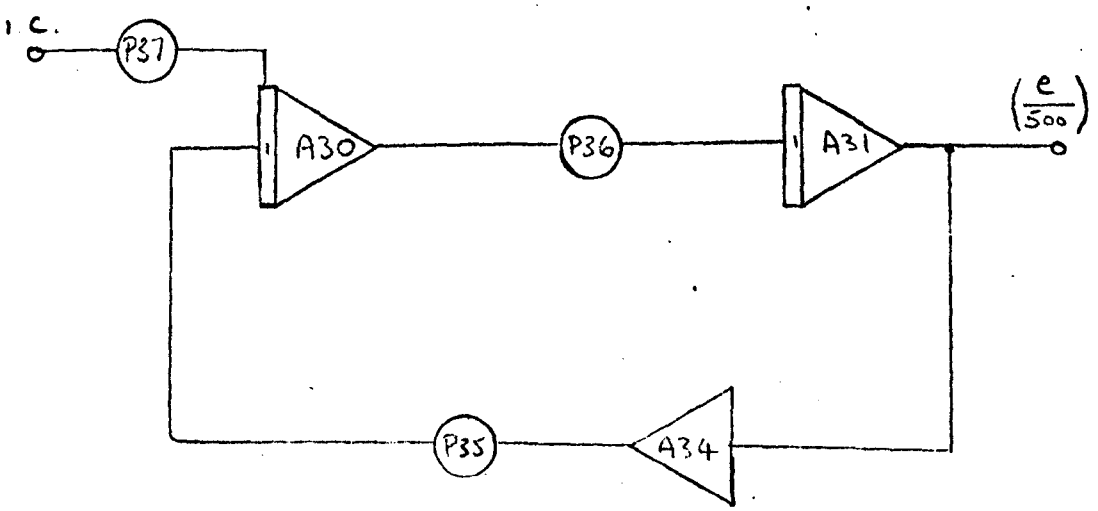

P36, P35 (ω) - 0.314
P37 (e_{max}) -0.68

Sinewave generation.

Fig. 2.25

Consider

$$\frac{d^2e}{dt^2} + \omega^2 e = 0 \qquad (2.80)$$

Taking the Laplace Transform of equation 2.80 gives,

$$s^2 e_{(s)} - \left(\frac{de}{dt}\right)_{(0)} - s e_{(0)} + \omega^2 e_{(s)} = 0 \qquad (2.81)$$

By comparing equations 2.79 and 2.81

$$s e_{(0)} = 0 \qquad \text{and} \quad \left(\frac{de}{dt}\right)_{(0)} = E_{max.}\,\omega$$

Equation 2.80 is simulated to generate sinusoidally varying functions of angular frequency ω in Fig. 2.25.

With the aid of the two circuit diagrams (Figs. 2.24b and 2.25) the force generated by the solenoid, as a function of time, can be determined. These results are given in Fig. 2.26.

2.3 Experimental Work

Tests carried out on solenoid type 18-7202 consisted of holding the armature at a given displacement and noting either the average or the instantaneous value of the force when the input terminals of the solenoid were connected to the 240 V 50Hz mains. The average force tests were also performed by Pratt Hydraulics Limited on both the solenoid type 18-7202 and the Magnet Schultz solenoid. Since the results for the

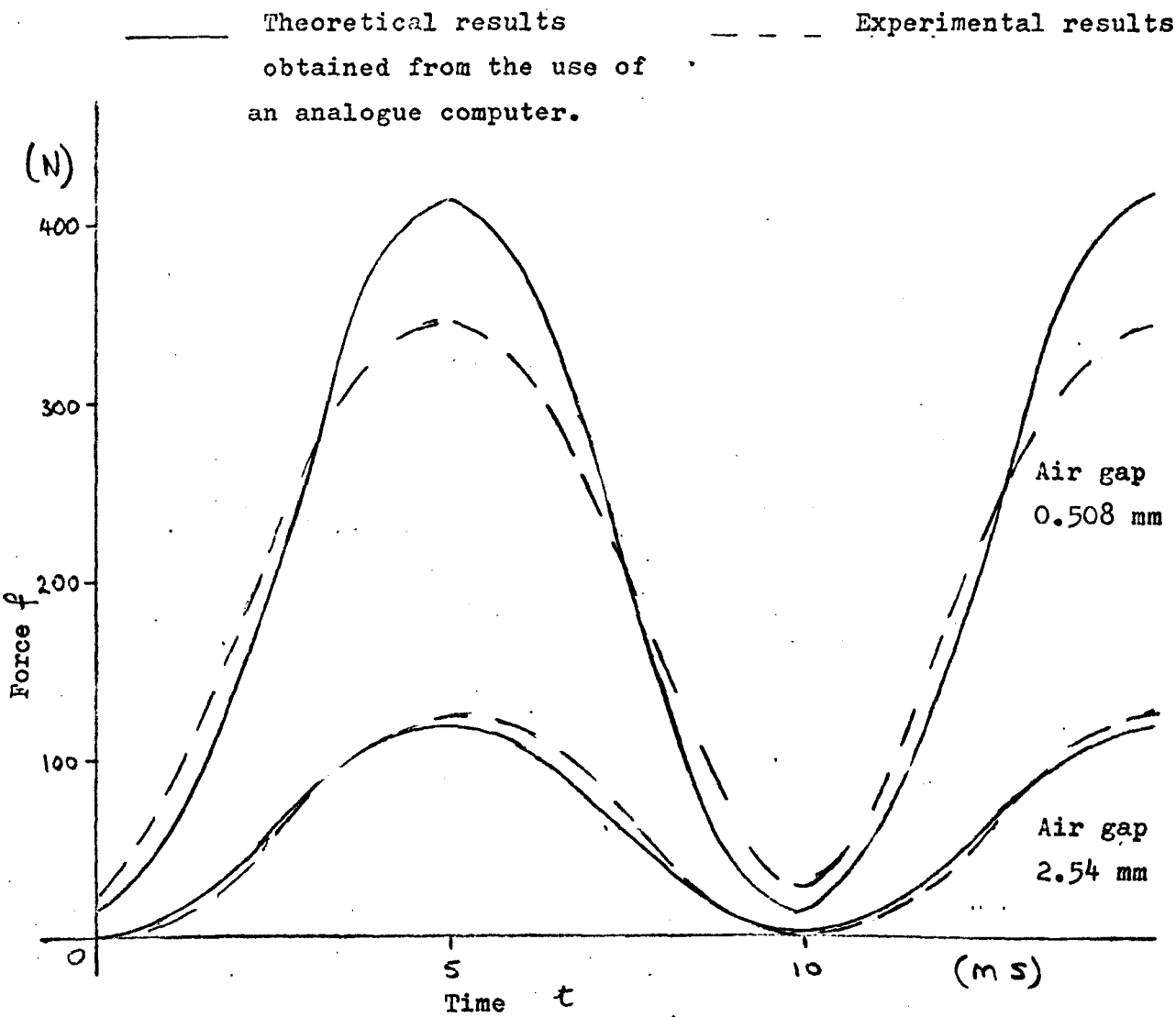

Graph of solenoid generated force against time.

Fig. 2.26

solenoid type 18-7202 were in agreement with those found at Enfield (see graph in Fig. 2.29) their results for the Magnet Schultz solenoid are used for comparison purposes in this thesis.

2.3.1 Description of apparatus

The purpose of this apparatus was to measure the force generated by the armature for fixed displacements. Thus the device for measuring force should have very little relative movement between its sensing head and body when the force is applied.

The equipment used was a load transducer[29], and to measure the displacement of the armature an inductive-type, displacement transducer[30]. The equipment was mounted on a vice, the solenoid being fixed to one jaw and the force transducer to the other jaw, as in Fig. 2.27. Attached to the sensing head of the load transducer was a short rod which displaced the armature of the solenoid when the vice jaws were moved, as arranged in Fig. 2.28.

To measure the average force generated by the solenoid the output of the load transducer was connected via an amplifier to a moving coil d.c. voltmeter. The current taken by the solenoid was also monitored by means of an a.c. moving coil instrument. To monitor force as a function of time the output of the load transducer was connected to an oscilloscope[31] which had facilities for recording the trace onto a chart.

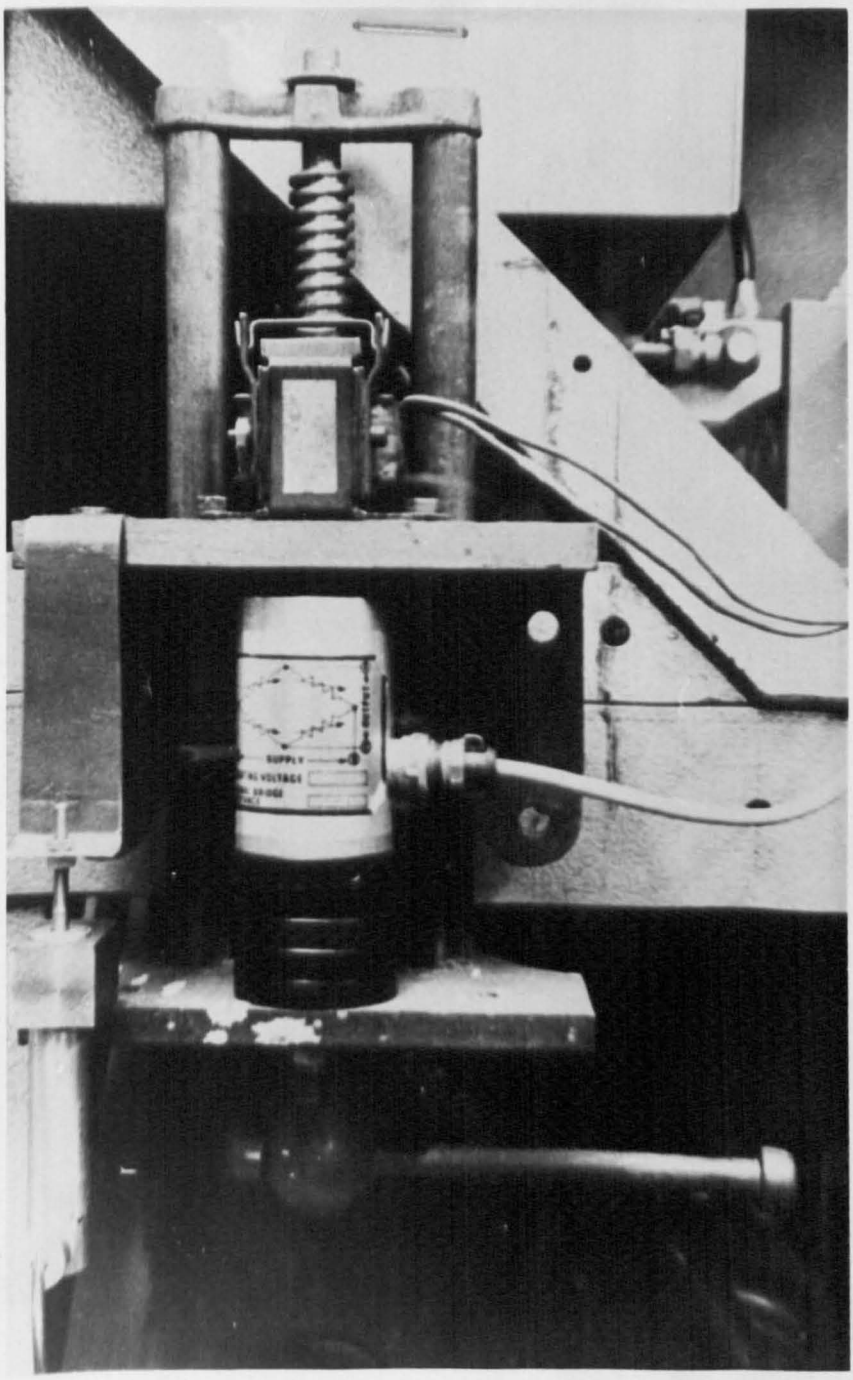

Photograph of apparatus

Fig. 2.27

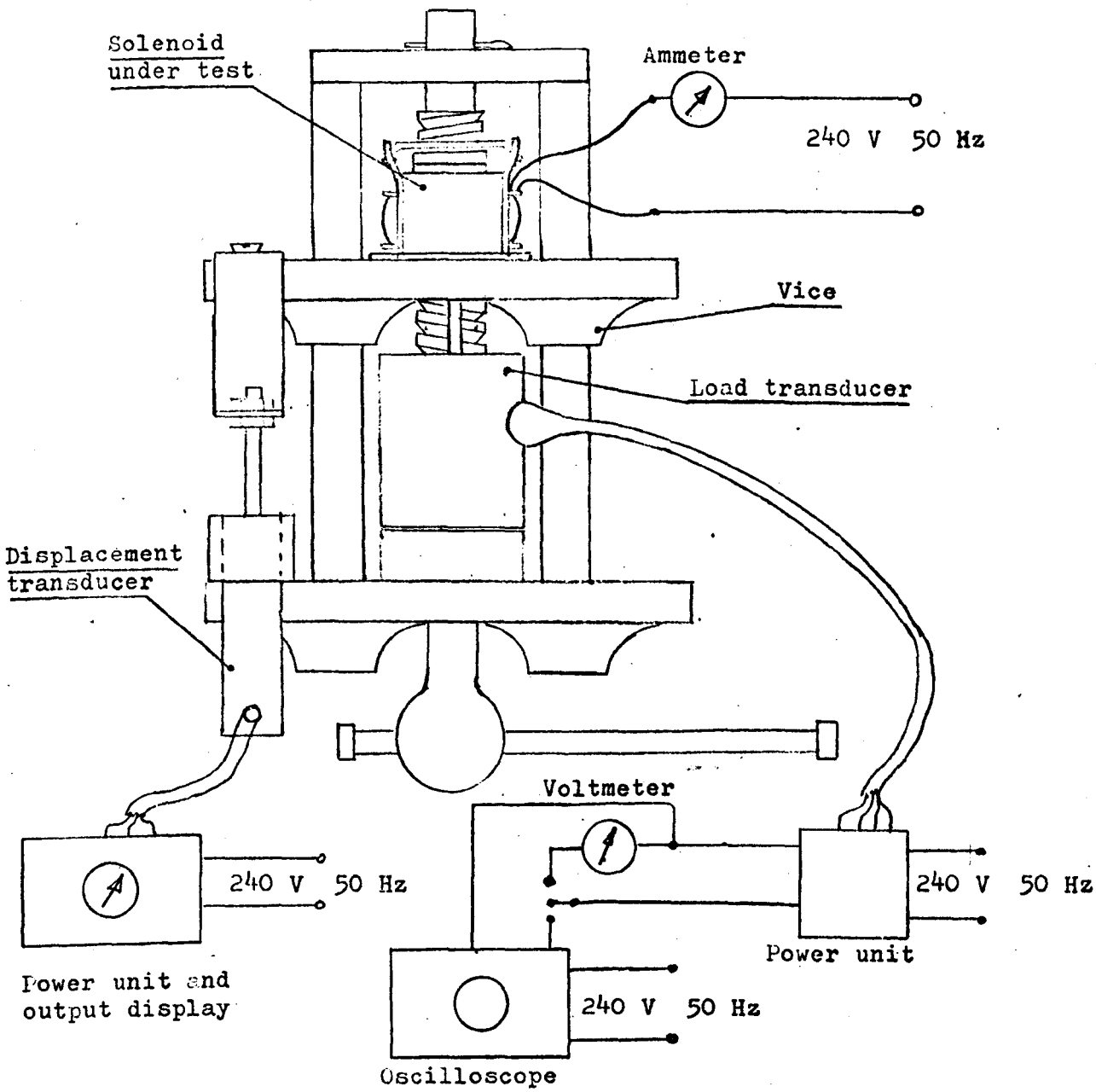

Schematic diagram of apparatus for testing solenoids.

Fig. 2.28

The load transducer was a tensile/compressive type with a range of 0 N to 222 N and overall accuracy of 1.5%. The power supply for this load transducer was obtained from a "strain gauge power supply and signal conditioning unit".(32) The "signal conditioning" part of the unit consisted of a d.c. amplifier to amplify the load transducer's output signal from the order of millivolts to volts. The displacement transducer had a range of 0 mm to 12 mm and with its read out equipment(33) its resolution was 0.01 mm.

2.3.2 Experimental Results

Results of average force against displacement for the solenoid type 18-7202 obtained at Enfield College and also by Pratt Hydraulics Limited are shown in Fig. 2.29.

Fig. 2.30 gives the experimental and theoretical (average force)/displacement characteristics for solenoid type 18-7202 and Magnet-Schultz Solenoid.

The (average current)/displacement curves for the solenoid type 18-7202 is shown in Fig. 2.19, Graph B.

Curves of force as a function of time for fixed displacements are shown in Fig. 2.19, Graph A.

2.4 Conclusions

Further to Fig. 2.7 if only the main flux paths P_3 and P_7 are considered then the total permeance of the air path will be

$$P_T = \frac{2P_3P_7}{2P_3 + P_7} \quad . \qquad (2.82)$$

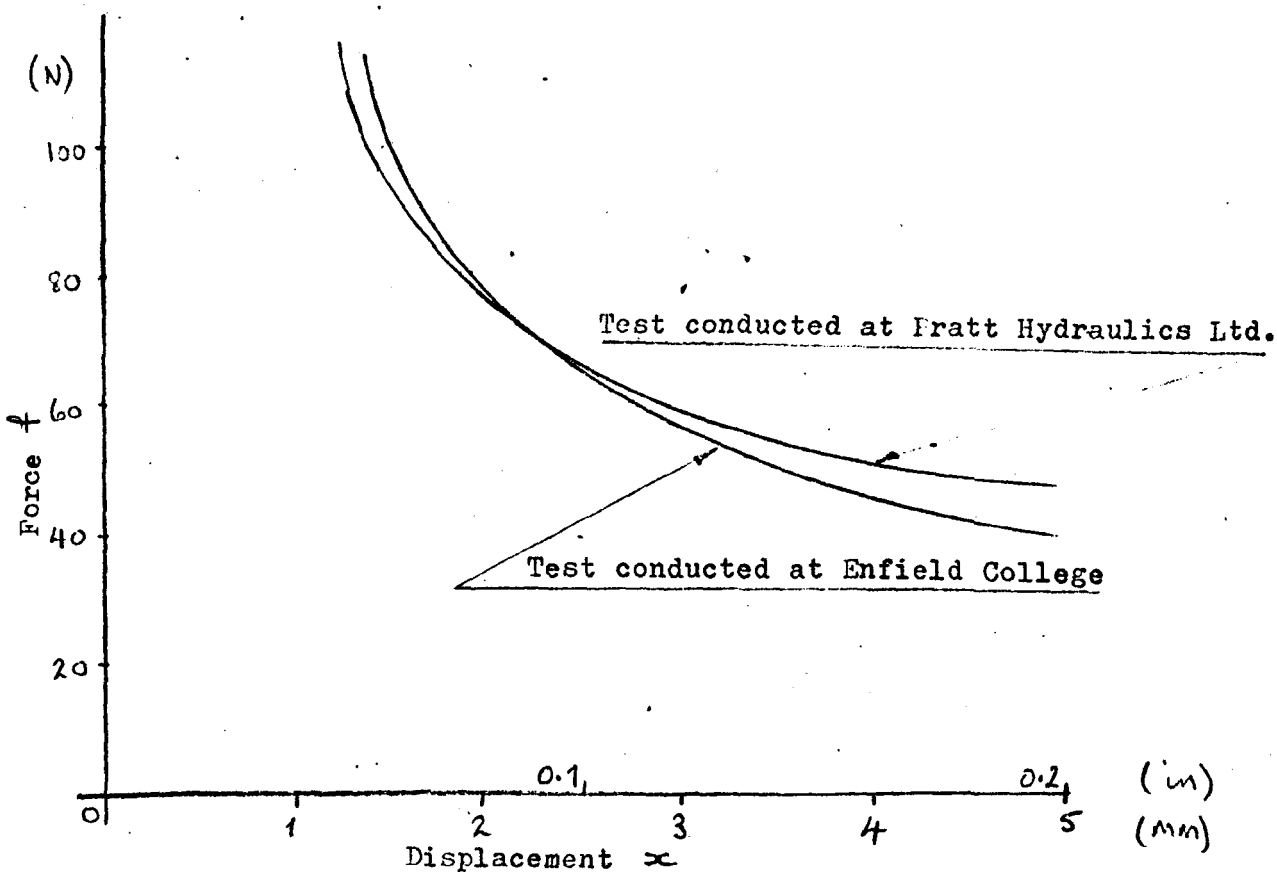

Tests on solenoid type 18-7202

Fig. 2.29

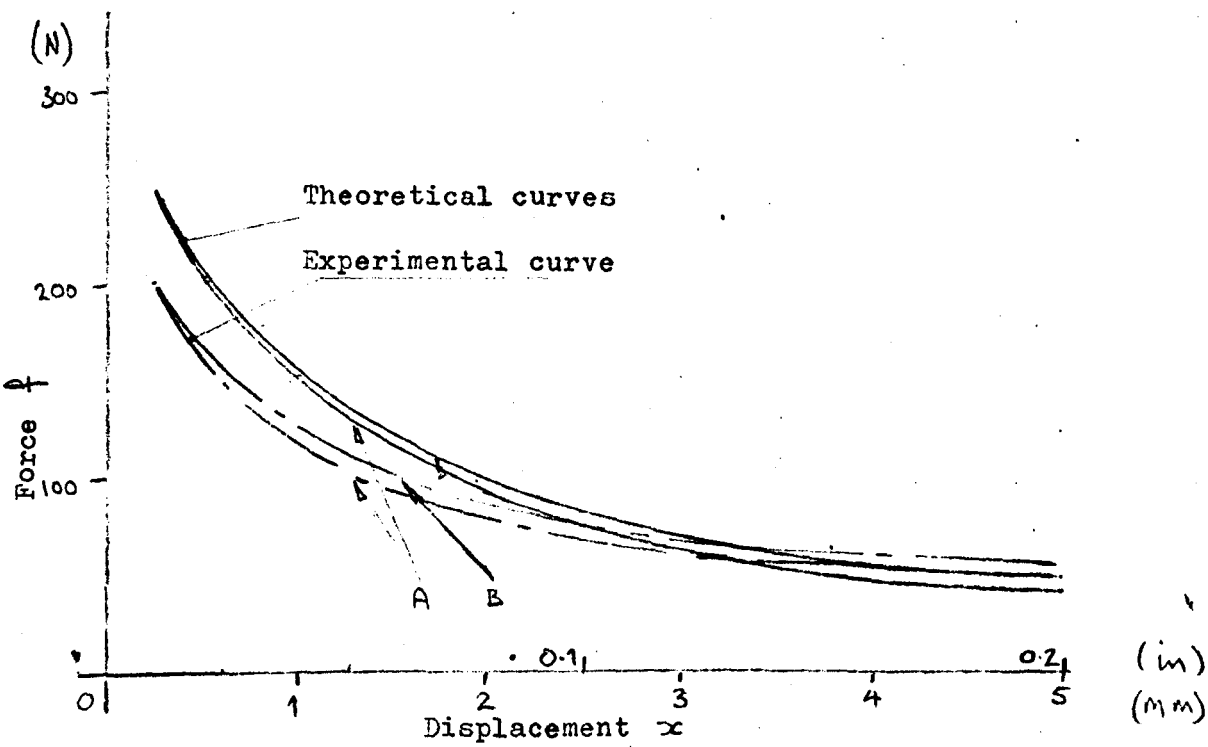

f/x curves for solenoid type 18-7202 (A) and Magnet-schulz (B)

Fig. 2.30

Substituting this equation into equation 2.49 the curve in Fig. 2.31 can be plotted. In Fig. 2.31 the experimental curve is also given and by comparing these two results it is clear that the leakage and fringing fluxes must be considered.

From consideration of the B/H curve, supplied by the manufacturers for the iron used in the solenoid, the permeance of the iron path was estimated and it was found that it did not become comparable with that of the air path until the main air gap was below 0.01 in. Also, if the results obtained for the shading rings in Fig. 2.23 are considered it will be observed that these have negligible effect when the air gap is greater than 0.01 in. When the width of the air gap becomes 0.01 in. or less, the valve can be considered fully open and the force generated by the solenoid is very large, therefore the effective operating range of the solenoid is greater than 0.01 in. it is in fact from 0.01 in. to 0.125 in. Because of this the effect of the permeance of the iron path and shading rings can be neglected. This simplification results in the network representation of the solenoid as shown in Fig. 2.6.

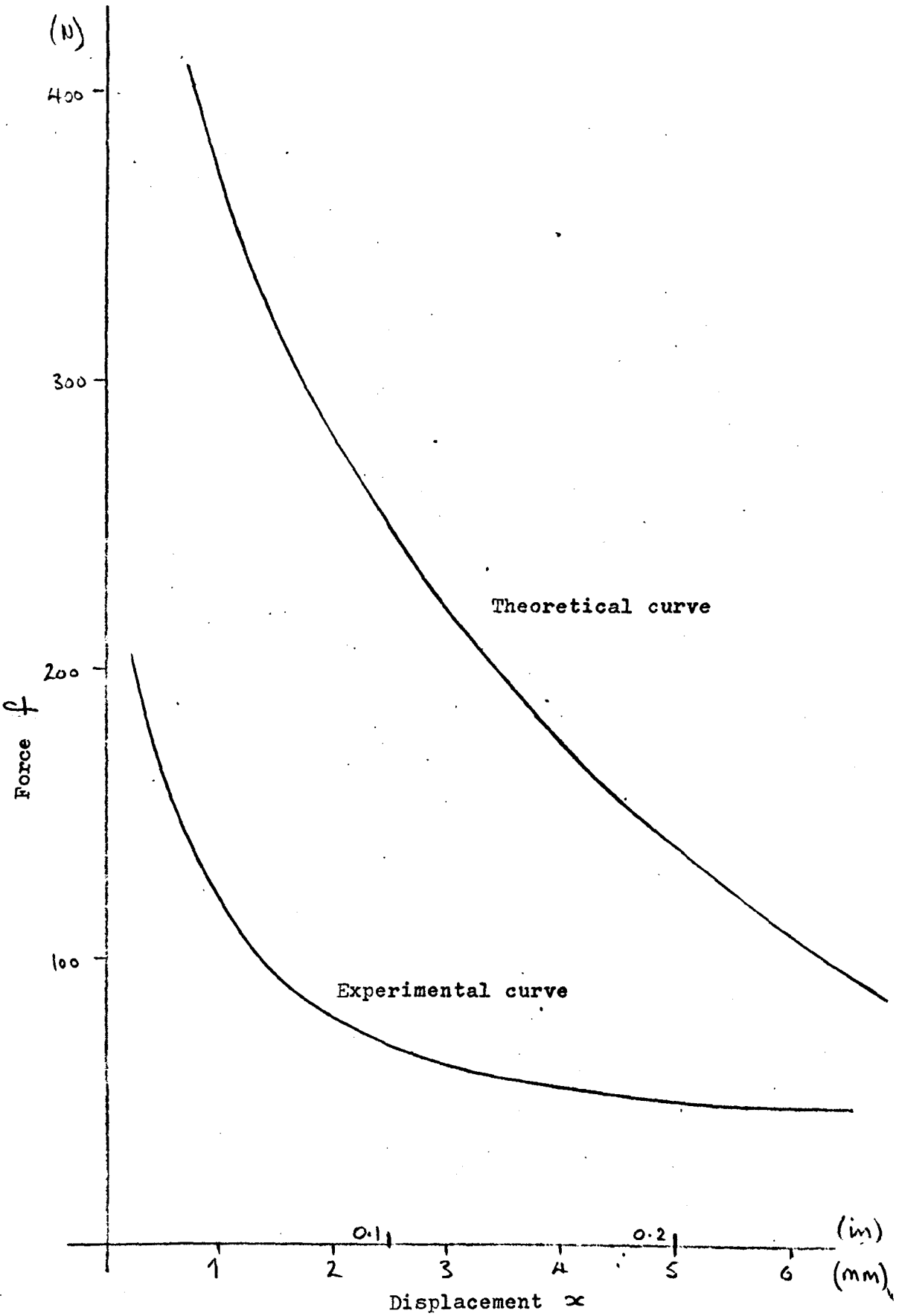

f/x theoretical curve, calculated assuming no fringing or leakage flux paths, and experimental curve

Fig. 2.31

3. Mechanical and Hydraulic Sub-systems

The basic purpose of this chapter is to evaluate all the forces which will act against the force generated by the solenoid. These forces can be divided into two, viz. mechanical and hydraulic, and initially will be considered separately. To gain a greater understanding of the operation of the overall system, the network representation of mechanical and hydraulic sub-systems are found. Experimental results are presented to enable some of the required constants to be found and to support certain parts of the theory.

3.1 Theory

The relevant theory is derived to represent both mechanical hydraulic sub-systems as networks.

3.1.1 Development of abstract model for the mechanical sub-system

A mechanical system can be considered to contain three elements viz. mass spring and friction.[34] These will now be discussed in relation to the valve system.

With reference to Fig. 3.1 the mass of the moving parts M consist of those of the spool, the two solenoid armatures and the striker pins.

When the spool is in the centre position both springs are slightly compressed. Let this compression be Z and if z is the displacement of the spool taken from the central position, then the spring force,

$$f_1 = K(Z + z) \qquad (3.1)$$

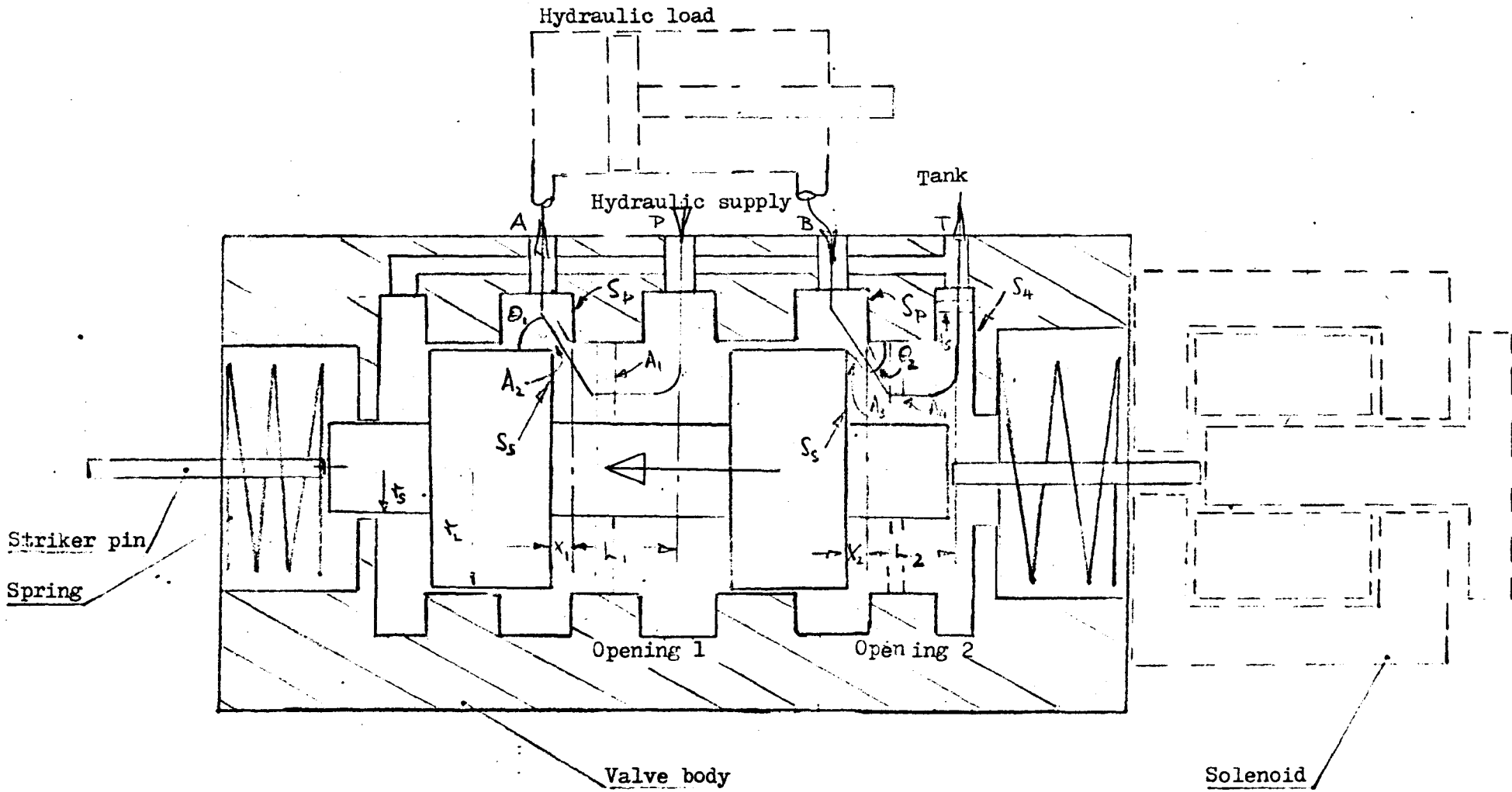

Schematic diagram of a spool type directional control valve

Fig. 3.1

where K is the spring constant assuming the springs to be linear.

There are two main sources of friction in the valve.

(i) friction between the spool and valve body, and

(ii) friction between the striker pin and the '0' ring in the seal.

Consider (i)

It is assumed that the area of the contact remains constant, there is a thin film of oil between the two surfaces thus the friction will be viscous[35] and iso-thermal operation is considered

$$f_2 = -\eta \frac{A v}{h} = F v \qquad (3.2)$$

where

A - area of contact

h - clearance between the two surfaces

Consider (ii)

In this case the friction will appear in two parts viz. break-out and running. The break-out friction is operative when the striker pin first starts to move and its value depends on the length of time the metal and rubber surfaces have been in contact because the materials interact altering the value of the coefficient of friction[35]. The running friction exists when there is movement between the '0' ring and the striker pin. Since the surface finish of the striker pin has a low R.M.S. value and the diameter of the '0' ring is small, the effect of this friction is neglected.

If f is the applied force the equation of equilibrium is

$$f = M\frac{dv}{dt} + K(Z+z) + Fv \qquad (3.3)$$

From equation 3.3 the network representing the mechanical system is shown in Fig. 3.2.

3.1.2 Development of abstract model for the hydraulic sub-system

Further to Fig. 3.1 let the spool move in the direction shown, a gap will open between port A and P and similarly between port B and T, which allows fluid to flow between the respective ports. These gaps between the valve body and the spool at ports A and B can be considered as orifices which have an area equal to the circumference of the spool at surface S_s times the axial length between this spool surface S_s and the port surface S_p.

The force acting on the spool due to the flow of fluid is obtained from consideration of the conservation of momentum. The following assumptions are made.

(i) the fluid is nonviscous and incompressible

(ii) the perimeter of the orifice is large compared with its axial length so that the flow can be considered two dimensional.

(iii) the leakage between spool and valve body is neglected.

The momentum theorem states that the net force acting on a fluid within a stated volume is equal to the rate of change

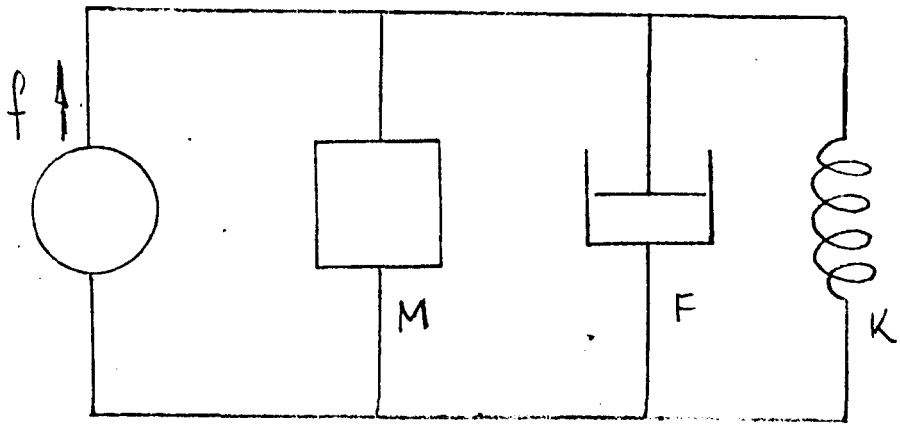

Mechanical network

Fig. 3.2

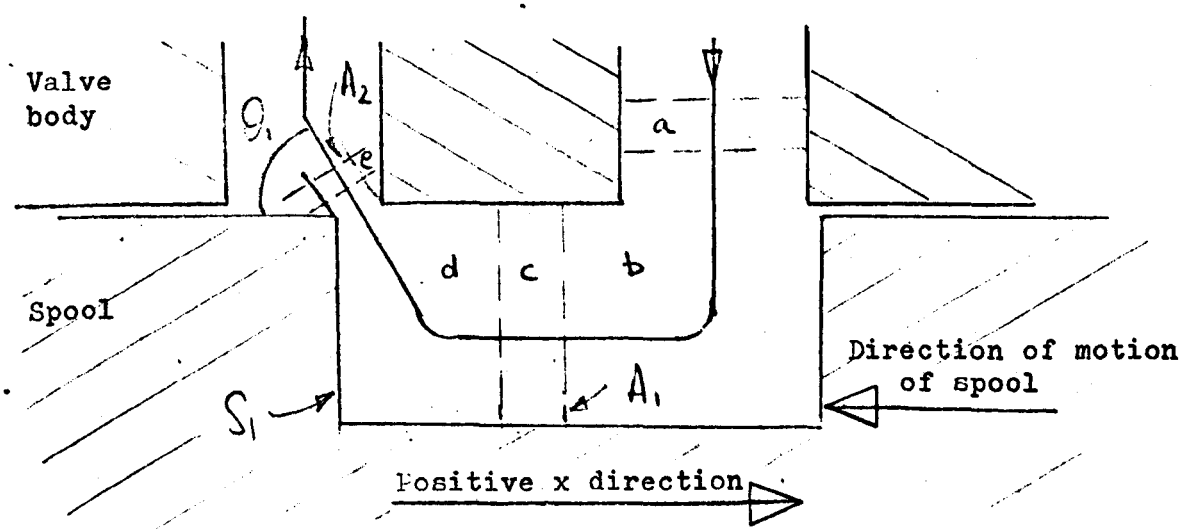

Opening 1

Fig. 3.3

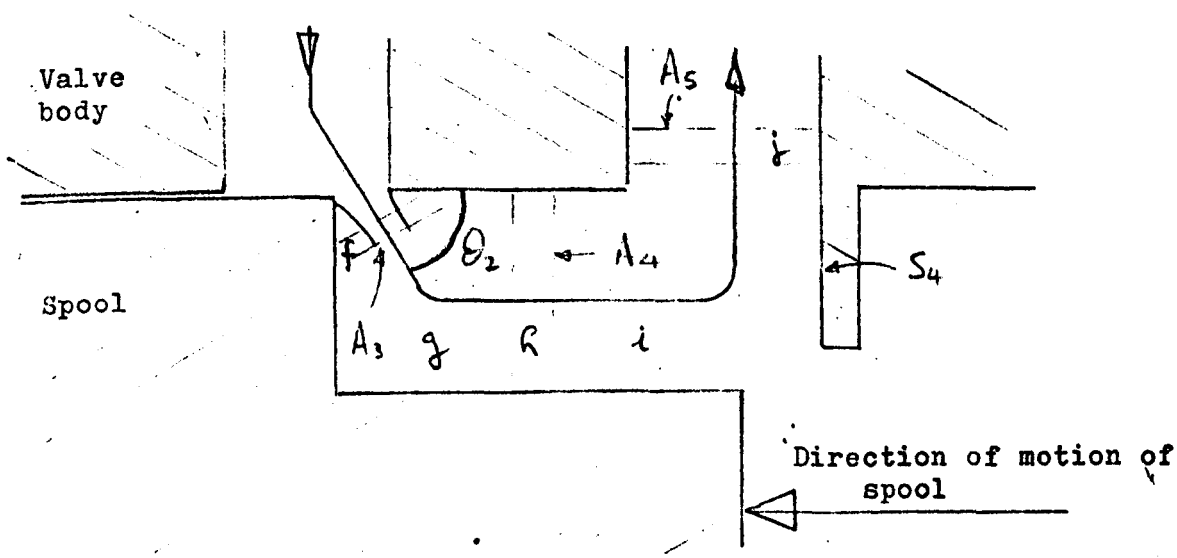

Opening 2

Fig. 3.4

of momentum of the fluid inside this volume plus the rate of change of momentum due to the net rate of flow of fluid leaving the stated volume.

Newton's second law states that the rate of change of momentum of a system of fixed identity is equal to the net force acting on it.

The application of these two statements will now be considered. Fig. 3.3 shows part of Opening 1 redrawn from Fig. 3.1. Considering the fluid in volume 'a' and 'b' flowing into volume 'b' and 'c' in time dt and letting m_{ax} be the momentum of fluid in volume 'a' in the 'X' direction and similarly for m_{bx} and m_{cx}.

The total momentum at (t = o)

$$m_{1x} = m_{ax} + m_{bx}$$

and the total momentum at (t = dt)

$$m_{2x} = m_{bx} + m_{cx}$$

From the momentum theorem, the rate of change of momentum in time dt which is the force in the x direction exerted on the fluid

$$\left(-f_{x11}\right) = \frac{m_{2x} - m_{1x}}{dt} = \frac{m_{bx} + m_{cx} - m_{ax} - m_{bx}}{dt}$$

$$= \frac{m_{cx} - m_{ax}}{dt} \qquad (3.4)$$

where in general m = mass. velocity

$$= \frac{\rho q^2}{A} dt \qquad (3.5)$$

$$\left.\begin{aligned} \therefore\ m_{cx} &= -\frac{\rho q^2}{A_1}\,dt \\ \text{and}\quad m_{ax} &= 0 \end{aligned}\right\} \qquad (3.6)$$

Substituting equations 3.6 in 3.4 gives,

$$(-f_{x11}) = -\frac{\rho q^2}{A_1} \qquad (3.7)$$

Similarly by considering volumes e, d and c, in Fig. 3.3

$$(-f_{x12}) = \frac{m_{ex} - m_{cx}}{dt}$$

$$= -\frac{q^2 \rho \cos\theta_1}{A_2} + \frac{q^2 \rho}{A_1} \qquad (3.8)$$

Therefore the net force on the fluid in Opening 1 is the sum of equations 3.7 and 3.8.

$$(-f_{x11}) + (-f_{x12}) = -\frac{q^2 \rho \cos\theta_1}{A_2} \qquad (3.9)$$

and the force on the spool $= -\left[(-f_{x11}) + (-f_{x12})\right]$

$$= f_{x1}$$

$$\therefore\ f_{x1} = \frac{q^2 \rho \cos\theta_1}{A_2} \qquad (3.10)$$

It can be noted that this force is opposing the motion and thus will try to close the valve.

Re-drawing Opening 2 in Fig. 3.1 gives Fig. 3.4.

Using the same notation and approach as for Opening 1 yields;

Considering volumes f, g and h;

$$(-f_{x13}) = \frac{m_{xh} - m_{xf}}{dt} = \frac{q^2 \rho}{A_4} - \frac{q^2 \rho \cos\theta_2}{A_3} \quad (3.11)$$

Considering volumes h, i and j;

$$(-f_{x14}) = \frac{m_{ix} - m_{hx}}{dt} = 0 - \frac{\rho q^2}{A_4} \quad (3.12)$$

From equations 3.11 and 3.12 the total force acting on the fluid in Opening 2 is,

$$(-f_{x2}) = + \frac{q^2 \rho}{A_4} - \frac{q^2 \rho \cos\theta_2}{A_3} - \frac{\rho q^2}{A_4} \quad (3.13)$$

It should be noted that force f_{x14} acts on the surface S_4 which is not part of the spool and thus will have no effect. Provided the force f_{x13} is negative, in equation 3.11, it will act on the spool thus the total force due to fluid flow in Opening 2 is,

$$f_{x2} = -\left[\frac{q^2 \rho}{A_4} - \frac{q^2 \rho \cos\theta_2}{A_3}\right] \quad (3.14)$$

Equations 3.10 and 3.14 give the force acting on the spool due to steady state fluid flow.

Considering Newton's 2nd law it is possible to obtain the force acting on the spool due to the time rate of change of momentum of fluid in a space with fixed boundaries. Further to Fig. 3.1, for each opening there is a volume of fluid between spool and the valve's body. Since the direction of fluid flow is altered within this volume, which causes eddy currents, only a portion of this volume contains fluid capable of being accelerated in the x-direction, this volume, for Opening 1, is $(L_1 + x_1/2\ )A_1$, where $(L_1 + x_1/2\ )$ is the distance between the mid-position of the inlet port and the mid-position of the outlet port, thus,

$$\text{Force} = \text{mass.acceleration} \tag{3.15}$$

Therefore for Opening 1,

$$(-f_{x15}) = -\left(L_1 + \frac{x_1}{2}\right)\rho\frac{dq}{dt} \tag{3.16}$$

and for Opening 2,

$$(-f_{x16}) = \left(L_2 + \frac{x_2}{2}\right)\rho\frac{dq}{dt} \tag{3.17}$$

Thus the force acting on the spool due to these forces

$$f_{x3} = -\left[(-f_{x15}) + (-f_{x16})\right] = \left(L_1 + \frac{x_1}{2} - L_2 - \frac{x_2}{2}\right)\rho\frac{dq}{dt} \tag{3.18}$$

Thus equations 3.10, 3.14 and 3.18 give the forces acting on the spool due to fluid flow.

These force equations govern the effect the hydraulic system has on the mechanical system. It is now necessary to consider the internal operation of the hydraulic system, which is basically a controlled orifice and for simplicity this orifice will be represented by a circular hole. From consideration of the operation of an orifice it is thought that there are three cases:

i) orifice discharging to atmosphere,

ii) orifice discharging onto a plate which can be stationary or can move,

iii) orifice discharging into a pipe in which the pressure is higher than atmospheric.

(i) Orifice discharging to atmosphere.

If v_1 is assumed negligible compared with v_2 and $p_2 = 0$, applying Bernoulli's equation[36,37,38,39,40] to the orifice in Fig. 3.5.

$$q = C_v C_c A_o \sqrt{\frac{2p_1}{\rho}} \qquad (3.19)$$

Since the aim of this analysis is to attempt to represent the valve system as an integrated network, equation 3.19 can be translated to network form by assuming it represents ideal orifice (i.e., $c_v = 1$, which is an ideal flow source) in series with a restrictor. If there is an intermediate pressure p_3 the network representation will be as shown in Fig. 3.6.

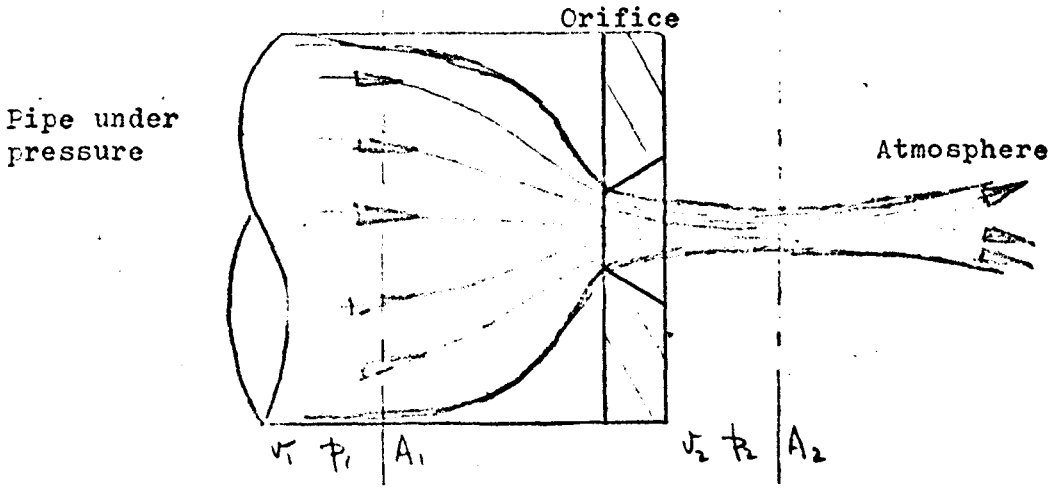

Orifice discharging to atmosphere

Fig. 3.5

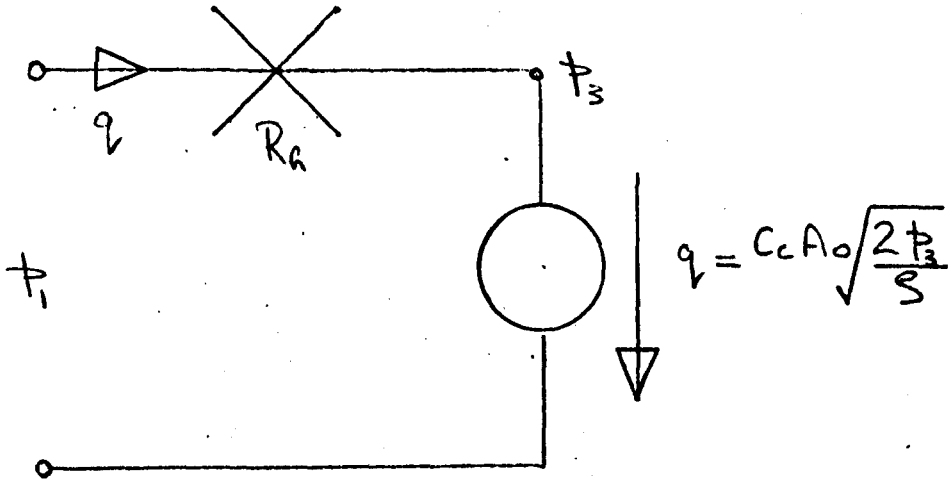

Network representation of an orifice discharging to atmosphere

Fig. 3.6

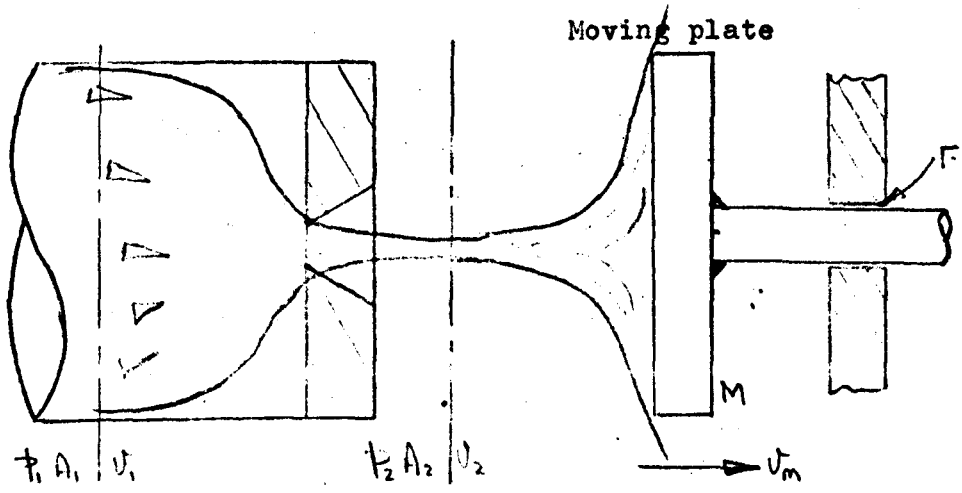

Orifice discharging onto a moving plate

Fig. 3.7

From Fig. 3.6 the network equations are,

$$q = C_c A_o \sqrt{\frac{2p_3}{\rho}} \tag{3.20}$$

$$R_h = \frac{p_1 - p_3}{q^2} \tag{3.21}$$

by equating equations 3.19 and 3.20 the relationship between p_1 and p_3 is obtained

$$C_v^2 p_1 = p_3 \tag{3.22}$$

Substituting equations 3.22 and 3.19 into 3.21 R_h is obtained

$$R_h = \frac{\rho(1 - C_v^2)}{2(C_v C_c A_o)^2} \tag{3.23}$$

(ii) Orifice discharging onto a moving plate.

Essentially the hydraulic system in this case is as above (see Fig. 3.7) therefore the network representation will be the same except that there will be an additional mechanical network. It is thus necessary to find the value of the force acting on the plate. Considering the momentum equation[40].

$$f_o = \rho A_2 v_2 (v_2 - v_m) \tag{3.24}$$

re-writing in terms of flow rate

$$f_o = \rho q^2 \left(\frac{1}{A_o C_c} - \frac{v_m}{q} \right) \qquad (3.25)$$

and by substitution of equation 3.19 the force is determined in terms of the input pressure,

$$f_o = \rho C_c C_v A_o \sqrt{\frac{2p_1}{\rho}} \left(C_v \sqrt{\frac{2p_1}{\rho}} - v_m \right) \qquad (3.26)$$

and for the case when v_m is zero equation 3.25 and 3.26 become

$$f_o = \rho \frac{q^2}{A_o C_c} \qquad (3.27)$$

$$\text{or } f_o = C_v^2 C_c A_o 2p_1 \qquad (3.28)$$

Thus the network representation in this case is as in Fig. 3.8 where f_o can be obtained from equations 3.25 or 3.26 or 3.27 or 3.28; p_3 from equations 3.20 or 3.22; and R_h from equation 3.23

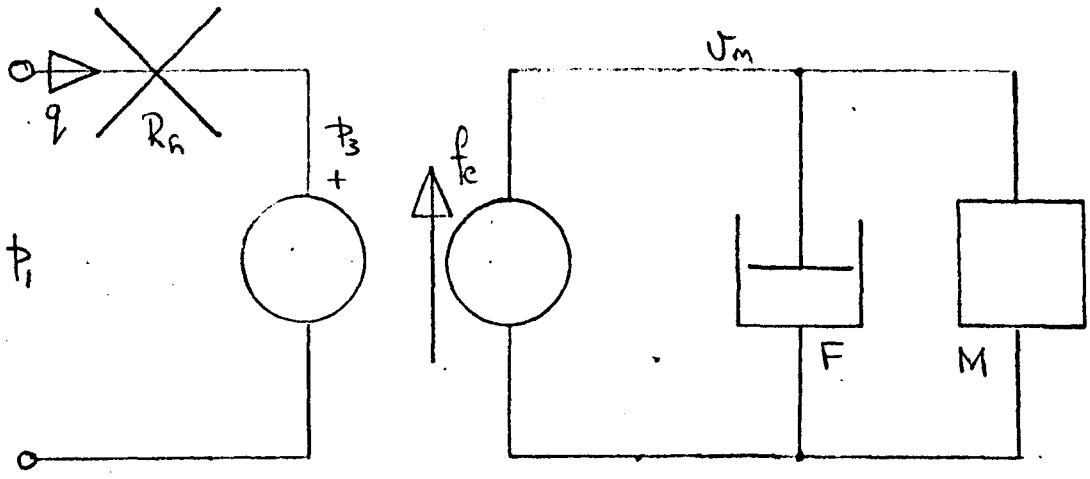

Network representation of an orifice with moving plate

Fig. 3.8

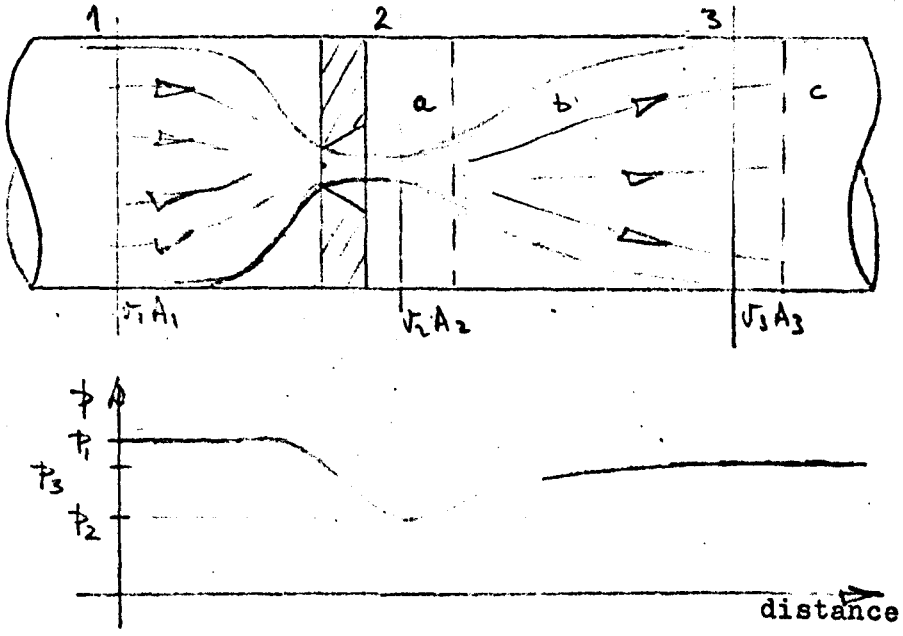

Orifice discharging into a pipe

Fig. 3.9

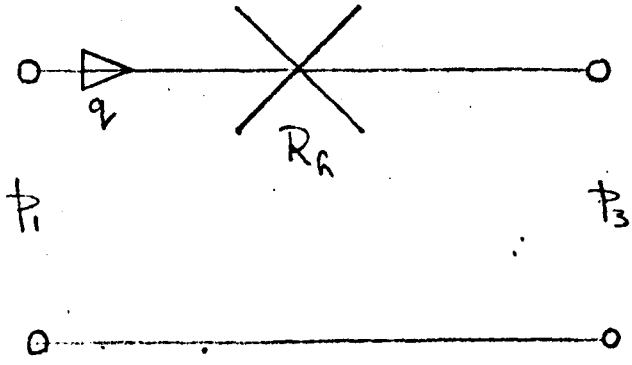

Network representation of an orifice discharging into a pipe

Fig. 3.10

(iii) Orifice discharging into a pipe in which the pressure is higher than atmosphere.

Applying Bernoulli's equation between section 1 and 2, in Fig. 3.9

$$\frac{v_1^2}{2} + \frac{p_1}{\rho} = \frac{v_{1t}^2}{2} + \frac{p_2}{\rho} \qquad (3.29)$$

where v_1 and p_1 are the input variables and v_{2t} and p_2 the resultant theoretical output variables.

From continuity equation

$$A_1 v_1 = A_2 v_{2t} \qquad (3.30)$$

where A_2 = Ao Cc, the smallest area of fluid flow; and $v_{2t} = \frac{v_2}{C_v}$ where v_2 is the actual velocity. Therefore noting these facts and substituting equation 3.30 in 3.29,

$$\frac{p_1 - p_2}{\rho} = \frac{v_1^2}{2}\left[\left(\frac{A_1}{A_o C_c C_v}\right)^2 - 1\right] \qquad (3.31)$$

Considering the momentum equation (in the steady state) between sections 2 and 3.

Thrust on fluid[40] in section 2 - 3 is,

$$F = A_3(p_2 - p_3) \qquad (3.32)$$

Let the fluid which is in volumes a and b at t = 0 flow into volumes b and c in time dt therefore

rate of change of momentum = $\frac{d(m_b + m_c - m_b - m_a)}{dt}$

$$= \frac{d(m_c - m_a)}{dt} \qquad (3.33)$$

in general $m = \frac{\rho q^2}{A} dt$ (3.34)

Substituting equation 3.34 into 3.33 and equating the resultant with equation 3.32

$$A_3(P_2 - P_3) = \rho q^2 \left(\frac{1}{A_3} - \frac{1}{A_2}\right) \qquad (3.35)$$

$$\therefore \frac{P_2 - P_3}{\rho} = q^2 \left(\frac{1}{A_3^2} - \frac{1}{A_2 A_3}\right) \qquad (3.36)$$

Adding equations 3.31 and 3.36

$$\frac{P_1 - P_3}{\rho} = q^2 \left[\frac{1}{A_3^2} - \frac{1}{A_3 A_0 C_c} + \frac{1}{2(A_0 C_c C_v)^2} - \frac{1}{2A_1^2}\right] \qquad (3.37)$$

If the diameter of the upstream pipe is the same as the down stream pipe, then $A_1 = A_3$, utilizing this fact and rearranging equation 3.37 to give q,

$$q = \frac{C_c C_v A_0}{\sqrt{\left[1 + \left(\frac{C_v C_c A_0}{A_1}\right)^2 \left(1 - \frac{2A_1}{C_c A_0}\right)\right]}} \sqrt{\frac{2(P_1 - P_3)}{\rho}} \qquad (3.38)$$

Thus equation 3.38 represents an hydraulic resistive loss and has a network representation as in Fig. 3.10.

From Fig. 3.10

$$R_L = \frac{\rho\left[1 + \left(\frac{C_v C_c A_0}{A_1}\right)^2\left(1 - \frac{2A_1}{C_c A_0}\right)\right]}{2\left(C_v C_c A_0\right)^2} \qquad (3.39)$$

Consideration of velocity distribution:

In the previous derivation use has been made of the relationship,

$$v = \frac{q}{A}$$

this formular assumes that there is uniform velocity distribution over the flow's cross-section. It is now intended to consider this statement.

The velocity distribution of the fluid particles in a pipe mainly depends on whether the flow is turbulent or laminar. The determination of whether the fluid is in turbulent or laminar motion can be determined by consideration of Reynold's Number (36,38) where, the Reynold's Number

$$N_R = \frac{v 4 r \rho}{\mu} \qquad (3.40)$$

v - average velocity of flow

r - hydraulic radius $\left(= \frac{\text{area of flow}}{\text{wetted parimeter}}\right)$

If the flow is turbulent then very little error is made if the velocity is assumed to be uniform over the cross-section of the pipe. However, if the flow is fully developed laminar then the velocity distribution over the cross-section will be that of a parabola[38,36], when the flow is laminar, Bernoulli's equation becomes

$$\frac{P_1}{\rho} + \alpha_1 \frac{v_1^2}{2} = \frac{P_2}{\rho} + \alpha_2 \frac{v_2^2}{2} \qquad (3.41)$$

$$\text{where } \alpha_1 = \frac{1}{A v_1^3} \int_A v_1^3 \, dA \qquad (3.42)$$

v - average velocity of flow

similarly for α_2.

Since for fully developed laminar flow the velocity distribution across the cross-section of the pipe is a parabola, equation 3.42 becomes,

$$\alpha = \left(\frac{u}{v}\right)^3 \int_0^{r_0} \left[1 - \left(\frac{r}{r_0}\right)^2\right] \frac{2r}{r_0^2} \, dr = 2$$

where u - maximum velocity.

When the flow is laminar, the momentum equation becomes[38,36]

$$A(P_1 - P_2) = \rho q v (\beta_2 v_2 - \beta_1 v_1) \qquad (3.43)$$

$$\text{where } \beta_1 = \frac{1}{A_1 v_1^2} \int_{A_1} v_1^2 \, dA \qquad (3.44)$$

and for fully developed laminar flow,

$$\beta_1 = \left(\frac{u}{v_1}\right)^2 \int_0^{r_0} \left[1 - \left(\frac{r}{r_0}\right)^2\right]^2 \frac{2\pi r\,dr}{\pi r_0^2} = \frac{4}{3}$$

Similarly for β_2.

In general if the fluid is in a state of laminar motion these correction factors have to be applied. However, consider the case when the fluid is flowing from a large container through a small orifice and the final flow down stream of the orifice is laminar. It is found[40] that when a fluid enters an orifice from a tank its velocity distribution is uniform and it has to flow a distance L down stream of the orifice before fully developed laminar flow occurs, where,

$$L = D\ 0.0575\ N_R \qquad (3.45)$$

where D - inside diameter of pipe.

Thus if the Bernoulli's equation or the momentum equation is applied for the region of flow immediately down stream of the orifice it is thought that these correction factors should not be applied.

For the case of fluid flowing out of a tank through an orifice it is assumed that the velocity of the fluid just before the orifice is negligible with that velocity just after the orifice. When considering the orifice in the valve this assumption is also made and by also noting the valves dimensions, it is concluded that a uniform velocity distribution can be assumed for the cases under consideration.

The valve was tested with the pressure being supplied to the P port of the valve and the A port outlet being exhausted to tank. Thus only Opening 1 was used in the valve. The orifice operation for this case is considered to be case (ii) (i.e., orifice discharging onto a plate), the plate being effectively the spool. However v_m was considered to be negligible compared to the fluid velocity and therefore the orifice operation reverts back to case (i).

3.1.3 Application of Theory to V.D.S.34 Directional Control Valve

It is intended to apply the theory to valve VDS 34 manufactured by Pratt Hydraulics Limited and to a circular, sharp-edged orifice. Experimental results will be presented for an orifice when discharging to atmosphere and when discharging into a pipe with pressure greater than atmospheric. Consider valve VDS 34:

The value of the force as in equation 3.10 and 3.14 will be greatest when there is maximum pressure drop across the valve. This condition occurs when the valve is discharging to tank, the relevant relationships from 3.1.1 and 3.1.2 will now be worked out numerically.

The mass of the moving parts

spool	-	0.0454 kg
striker pin	-	0.00335 kg
solenoid armature	-	0.1555 kg

Therefore the total mass of moving parts

$$= 0.0454 + 2\,(0.00335) + 2\,(0.1555)$$

$$= 0.363 \text{ kg}$$

The total mass of the springs is 0.0059 kg. This represents a distributed mass and is assumed to be negligible compared to the mass of the other moving parts. The mass of the oil contained in the volume enclosed by the spool and the valve's body is considered to be negligible (this was calculated to be 0.0023 kg).

The viscous friction coefficient is evaluated by considering the parameters in equation 3.2.

Kinematic viscosity of Tellus 27[41] oil at 35°C = $0.35\ 10^{-4}\ m^2\ s^{-1}$ and its density is 858 kg m^{-3}.

Hence dynamic viscosity = $\rho\nu = 0.03002 \text{ kg } s^{-1}$

The clearance between spool and valve body = $6.35\ 10^{-6}$ m

A, area of surfaces in contact = $2.79\ 10^{-4}\ m^2$.

Hence the viscous friction coefficient is,

$$F = \frac{\mu A}{h} = 1.32 \text{ N s m}^{-1}$$

The springs:

The initial compression in equation 3.1 was found to be $0.198\ 10^{-2}$ m and the stiffness K = 10900 N m^{-1}.

Considering equations 3.10, 3.14 and 3.18 the following constants are required:

Further to Fig. 3.1, A_2 is the cross-sectional area of the fluid stream immediately down stream of the orifice in the valve,

$A_2 = C_o$ (Area of orifice)

and, area of orifice $= x \pi D$

where D - diameter of the spool $1.585\ 10^{-2}$ m

x - amount of spool opening

Also $A_2 = A_3$

and $A_2 = \propto 4.99\ 10^{-2}\ m^2$

A_4 and A_1 are the cross-sectional area of the fluid stream between the spool and valve body,

$A_4 = \pi (r_1^2 - r_s^2)$

$A_4, A_1 = 1.2\ 10^{-4}\ m^2$

$L_1 = 0.715\ 10^{-2}$ m

$L_2 = 0.791\ 10^{-2}$ m

From experimental data in table 3.1

$$\frac{C_c \cos\theta}{C_c} = 0.57 \quad \text{and} \quad C_c C_v = 0.60$$

Substituting these values into equation 3.10, 3.14, 3.18 and 3.19

equation 3.10 becomes,

$$f_{x1} = \frac{q^2\ 10460}{x} \tag{3.46}$$

equation 3.14 becomes

$$f_{x2} = q^2 \left[\frac{6.72\ 10^3}{x} - 7.15\ 10^{-6}\right] \tag{3.47}$$

Since x can vary between 0 and $0.163\ 10^{-2}$ m when the valve orifice is fully open f_{x2} varies between infinity and $q^2(-\ 3.02\ 10^6)$.

Thus the overall value of this force changes from positive to negative, the change over point being when $x = 0.94\ 10^{-3}$ m. For values of x below $0.94\ 10^{-3}$ m the force is positive and therefore acts on surface S4, which is not part of the spool. Thus this force term can only be considered for values of x greater than $0.94\ 10^{-3}$ m (0.037 in.),

equation 3.18 becomes,

$$f_{x3} = \left(0.715\ 10^{-2} + \frac{x_1}{2} - 0.791\ 10^{-2} - \frac{x_2}{2}\right) 858 \frac{dq}{dt} \qquad (3.48)$$

Now $x_1 \approx x_2$

and since $L_1 - L_2 \gg \frac{x_1}{2} - \frac{x_2}{2}$ equation 3.48 becomes,

$$f_{x3} = -\ 0.654 \frac{dq}{dt} \qquad (3.49)$$

However, if only one opening is used, say Opening 1, equation 3.48 becomes

$$f_{x3} = 6.13 \frac{dq}{dt} \qquad (3.50)$$

equation 3.19 becomes

$$q = 1.49\ 10^{-3} \times p_1^{1/2} \qquad (3.51)$$

where $x = (z - 1.88\ 10^{-3})$

$1.88\ 10^{-3}$ m being the distance the spool has to travel before the orifice starts to open, and z is the movement of the spool from the centre position.

These equations are sufficient to describe the motion of the spool when only one of the two Openings of the valve is operating. Combining equations 3.3, 3.10, 3.14 and 3.18 gives the equation of motion of the spool.

$$0.208 \frac{d}{dt}\left(\frac{dz}{dt}\right) = f_e - 1.32\frac{dz}{dt} - 10900\,y - \frac{10460}{x}q^2 - 6.13\frac{dp}{dt} \qquad (3.52)$$

$$q = 1.49\ 10^{-3}\, x (p_1)^{1/2} \qquad (3.53)$$

$$x = (z - 1.88\ 10^{-3}) \qquad (3.54)$$

$$y = (z + 1.98\ 10^{-3}) \qquad (3.55)$$

Should the hydraulic network elements in Fig. 3.6 and 3.10 be required, which might well be the case of the analysis of a complete hydraulic system, then it is necessary to solve numerically equation 3.23 or 3.39. To solve these equations C_v and C_c, are required separately. For the above condition, i.e., valve discharging to tank, only $\frac{\cos\theta}{C_c}$ and

C_D (where $C_D = C_v C_c$) were found by considering equations 3.10 and 3.19. However, to solve all three constants separately, i.e., Cv, Cc and cos θ three equations are necessary. The third equation can be found by considering the case when the valve is discharging to tank via some restriction. Thus equation 3.38 can be used as this third equation.

It was considered useful to carry out experimental work regarding equation 3.38 by conducting tests on simple orifices in addition to tests on the orifice in the valve. These tests and results are given in the next section.

3.2 Experimental Work

Tests have been carried out on the VDS 34 valve to determine the necessary constants. When testing the simple orifice the fluid was water.

3.2.1 Description of apparatus

Test on VDS 34 valve:

With reference to Fig. 3.11 and 3.12 the valve without its two solenoids was mounted on a stand. The striker pins were rigidly fixed to the spool and one of them was also connected to a displacement transducer[30] and the other, via a load transducer[29], to a device which enabled the spool to be moved and held at any position. The hydraulic supply was connected to the valve and the input and output pressures were monitored by strain gauge pressure transducers[42]. The volume flow rate was measured by a turbine flow meter[43] and

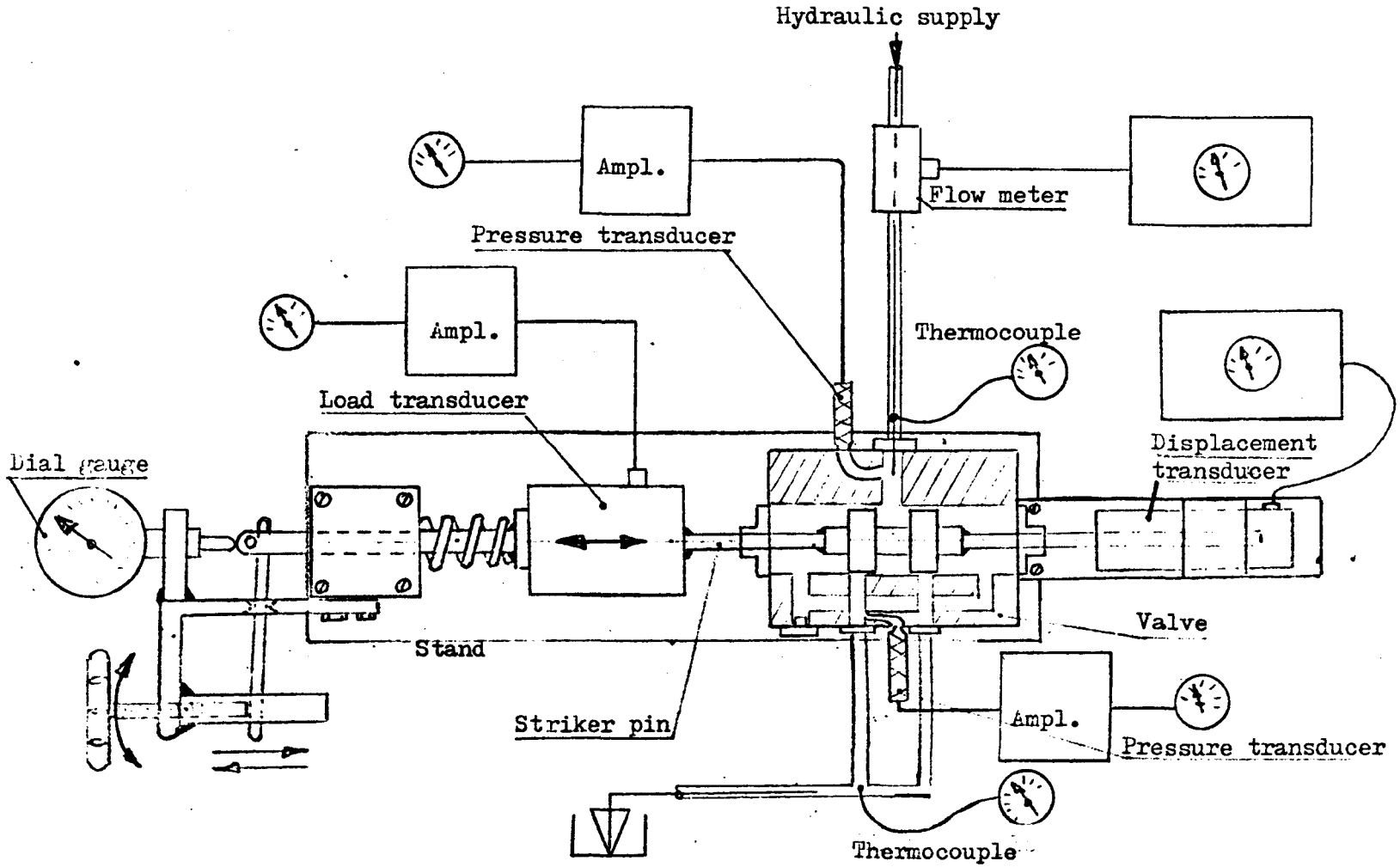

Schematic diagram of apparatus

Fig. 3.II

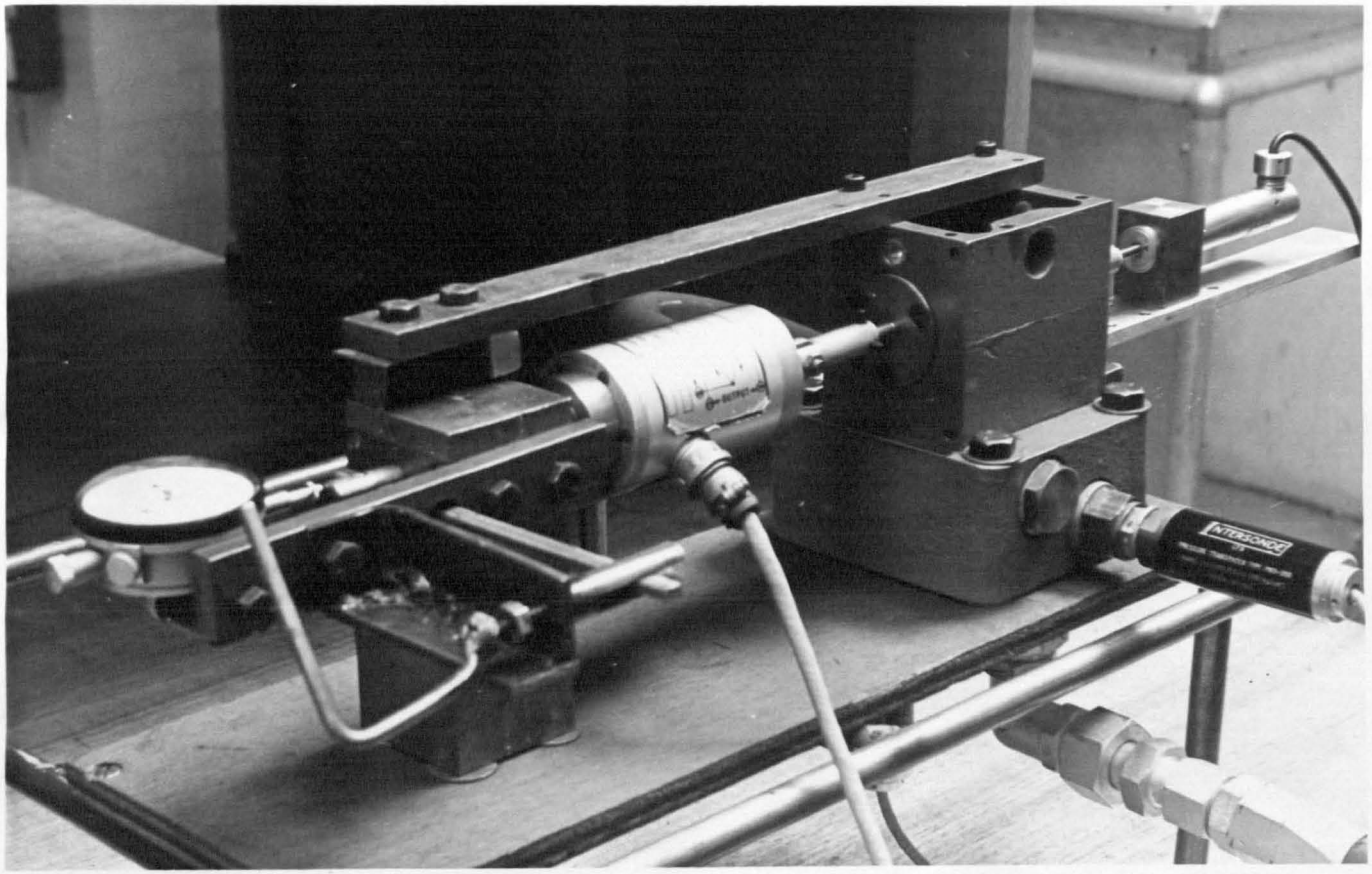

: Photograph of apparatus

Fig. 3.12

the temperatures of the oil at the inlet and outlet were measured by means of thermocouples[44].

The accuracy and suitability of the load and displacement transducers have been discussed in section 2.3.1. The pressure transducers were calibrated on a dead weight tester[45]. The flow meter and the thermocouples were calibrated by means of a bell jar and stop watch and by a mercury-in-glass thermometer respectively.

The schematic diagrams of the equipment to carry out tests on the simple orifice are shown in Figs. 3.13 and 3.14. For the first test a sharp edged orifice was inserted in the bottom of a water tank as in Fig. 3.13, and the water was allowed to discharge freely. The second part of the test was conducted with the discharging water being restricted by a tap as in Fig. 3.14. The pressure of the water, immediately after the orifice and just before the tap was measured by vertical, plastic tubes at these points.

3.2.2 Experimental Results

The object of the tests on the valve orifice was to find the values of $C_v C_c$ from equation 3.19 and $\frac{\cos\theta}{C_c}$ from equation 3.10.

The apparatus was capable of measuring f, q and p_1. However, A_o is the area of the orifice which is a function of x, the width of the orifice opening. To be able to measure x it is necessary to determine the position of the spool when x is zero.

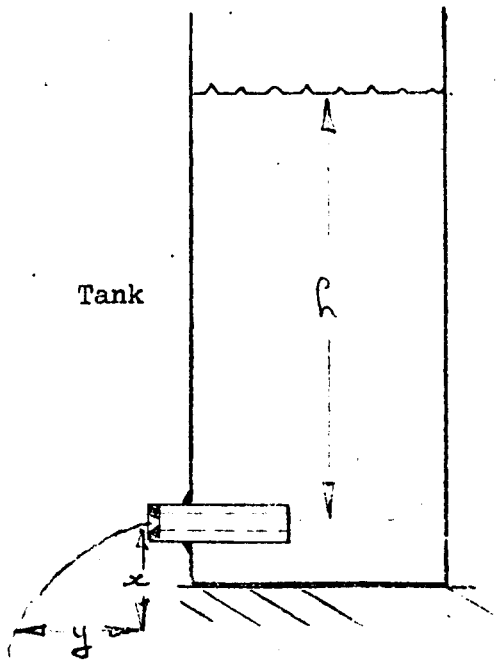

Orifice discharging to atmosphere

Fig. 3.13

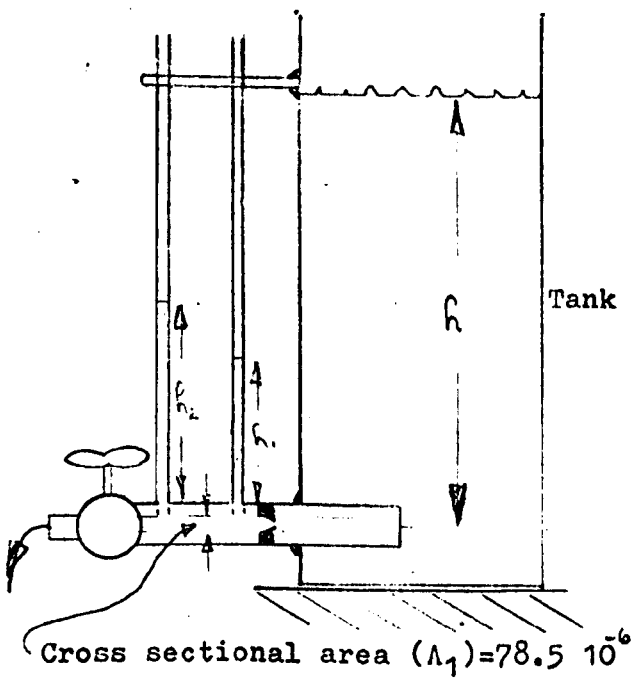

Cross sectional area (A_1)=78.5 10^{-6} m

Orifice discharging into a restrictio

Fig. 3.14

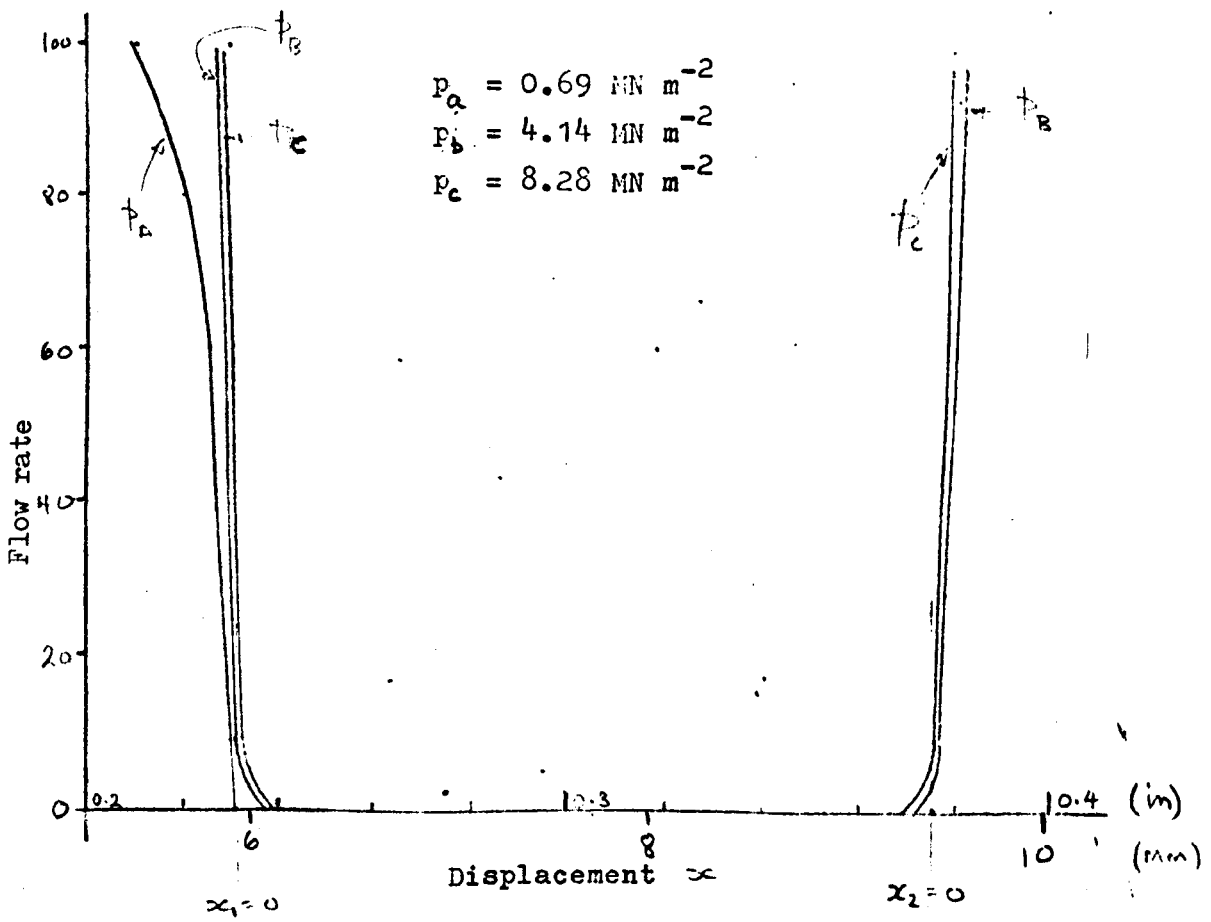

Graph for finding the spool's position

Fig. 3.15

It should be noted that this point is not the point of zero flow, because there is leakage across the spool surface. To find this position the flow rate against displacement for various constant values of supply pressure was plotted. From equation 3.19 it can be seen that for the case when the leakage is negligible compared with the main flow the curve of q/x should be a straight line passing through the x axis at the required reference point. A set of these results are shown in Fig. 3.15.

To find the required constants the spool was displaced by a given amount and the input pressure was varied noting the values of this pressure, flow rate and force on the spool. From these results q^2 against p and q^2 against f were plotted, as shown in Fig. 3.16 and 3.17 respectively. For all these tests the temperature of the oil was kept at approximately 35°C. From equation 3.19, noting that ρ = 858 kg m^{-3} and the diameter of the spool is 1.59 10^{-2} m.

$$C_v C_c = \left[\frac{q^2 \, 17.1 \, 10^4}{p_1 \, x^2} \right]^{1/2} \qquad (3.56)$$

Consider the test with x at 0.038 mm (or 0.0015 in.) from Fig. 3.16, the slope is 3.9 10^{-15} m^7 N^{-1} s^{-2}, therefore from equation 3.56

$$C_v C_c = 0.68$$

The other values obtained from this graph are given in Table 3.1

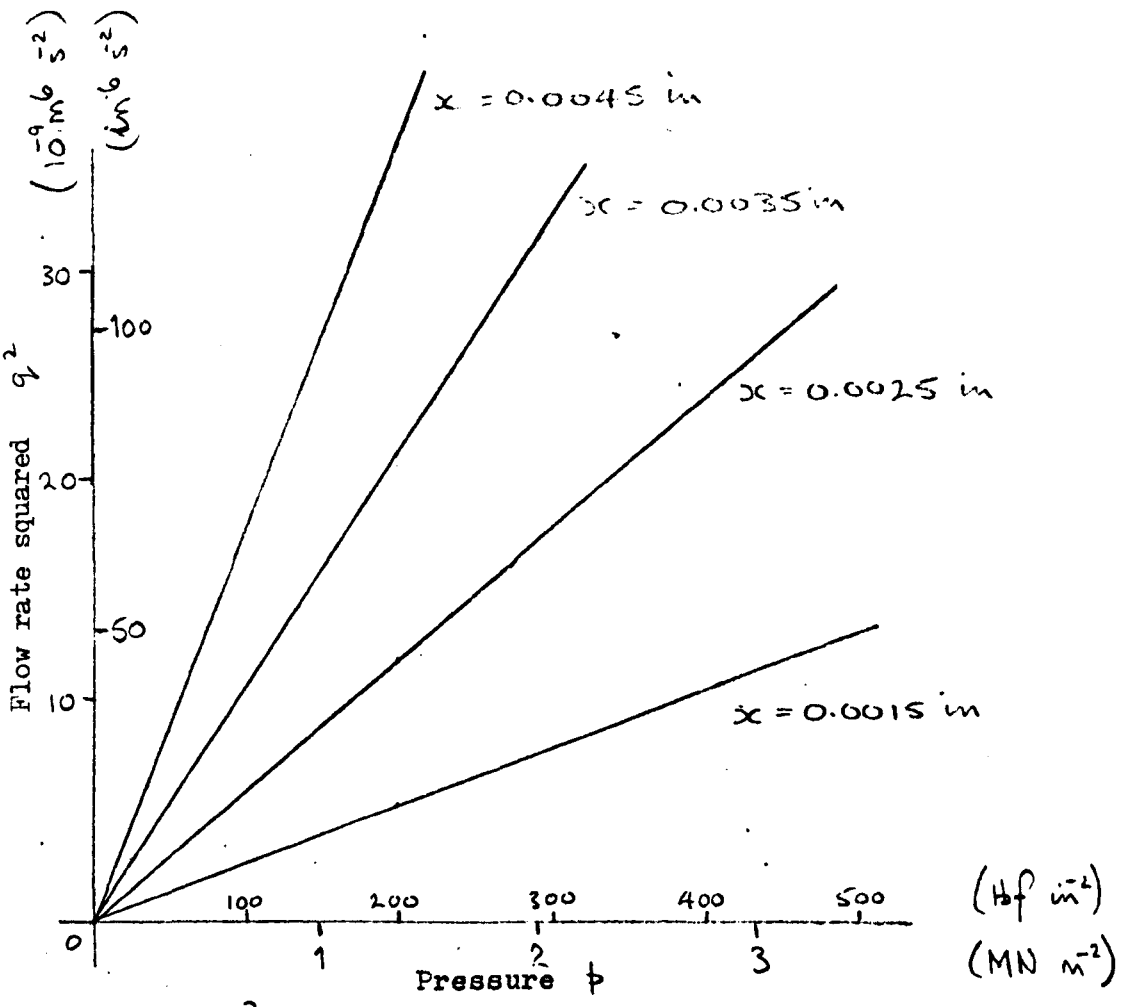

q^2/p curve due to fluid flow in opening 1

Fig. 3.16

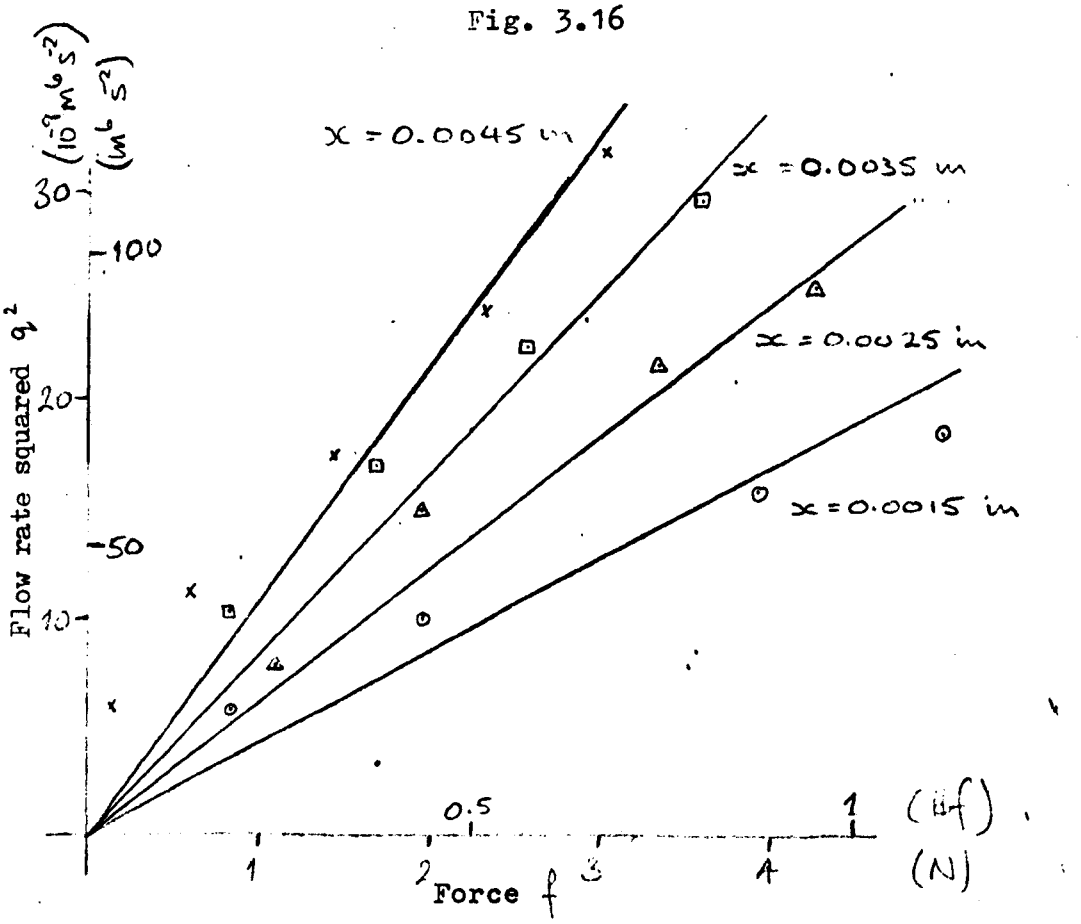

q^2/f curve due to fluid flow in opening 1

Fig. 3.17

	x mm	C_c C_v	$\frac{\cos\theta}{C_c}$
From experiments conducted at Enfield College.	0.038	0.68	0.514
	0.063	0.61	0.604
	0.089	0.59	0.570
	0.114	0.59	0.523
From experiments conducted at Pratt Hydraulics Ltd.	0.191	0.61	
	0.254	0.61	See note*
	0.317	0.58	
Average values		0.60	0.57

*Note: Due to the non-linearities in these tests the results are not quoted here, and will be discussed in section 3.3. The theoretical lines drawn on the grath in Figure 3.19 assume a value of 0.57 for $\cos\theta/C_c$.

Table 3.1

y m	h m	q 10^{-6} m^3s^{-1}	C_v	C	C_c	Other dimensions
0.380	0.510	28.0	0.94	0.72	0.77	
0.420	0.600	30.7	0.95	0.72	0.76	
0.455	0.700	33.0	0.95	0.71	0.75	x= 0.083 m
0.488	0.800	35.7	0.95	0.72	0.76	A_o=0.132 10^{-4} m^2
			0.95	0.72	0.76	Average value
0.347	0.431	14.6	0.94	0.73	0.78	Other dimensions
0.382	0.502	16.0	0.95	0.76	0.79	
0.430	0.601	17.5	0.99	0.75	0.75	x= 0.083 m
0.469	0.719	19.5	0.96	0.75	0.78	A_o=0.73 10^{-5} m^2
			0.96	0.75	0.78	Average value

Table 3.2

From equation 3.10,

$$\frac{\cos\theta}{C_c} = \left(\frac{\rho^2}{f}\right)^{-1} \frac{x}{17100}$$

Thus for x = 0.038 mm from graph in Fig. 3.17 the slope is $4.32\ 10^{-9}\ m^6\ N^{-1}\ s^{-2}$

$$\frac{\cos\theta}{C_c} = 0.514$$

The other values obtained from this graph are given in Table 3.1. The range of pressure and flow rate obtainable in the Control Laboratory at Enfield College was limited well below the valves capacity. Results for the valve's full range were obtained by conducting similar tests at Pratt Hydraulics Limited. Graphs for q^2 against p and q^2 against f for tests at Pratts are given in Fig. 3.18 and 3.19 respectively. The value of the constants found from these results are given in Table 3.1.

The following experiments were conducted on the simple orifice. For the first test the water was allowed to discharge through the orifice into the atmosphere. For various heights of water in the tank the flow rate and the dimensions x and y were measured as in Fig. 3.13. This test was conducted for two sizes of orifice and hence Cv and C_D and thus Cc were calculated.

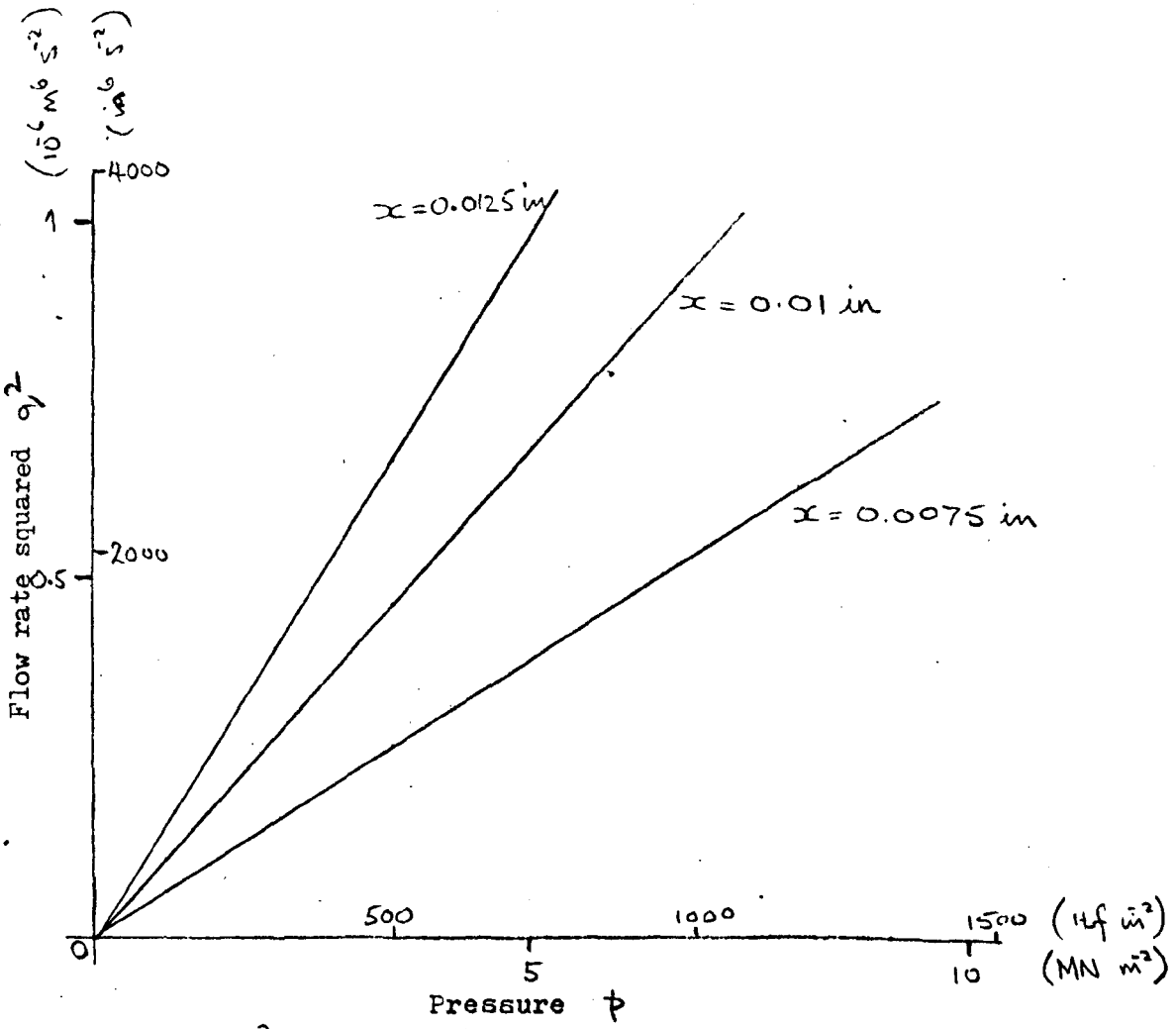

q^2/p curve due to fluid flow in opening 1

Fig. 3.18

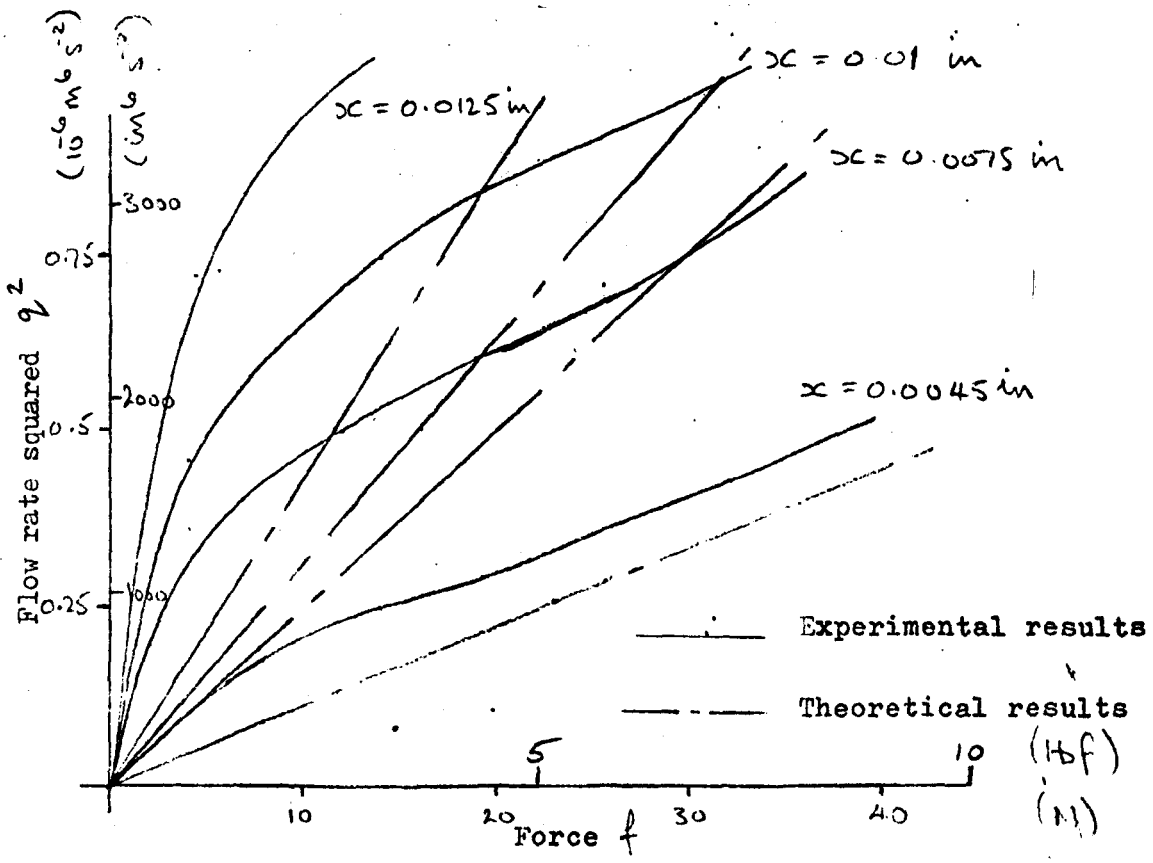

q^2/f curve due to fluid in opening 1

Fig. 3.19

From reference 40

$$C_v = \sqrt{\frac{y^2}{4 \times h}} \tag{3.57}$$

$$C_D = \frac{q}{A\sqrt{2gh}} \tag{3.58}$$

$$C_c = \frac{C_D}{C_v} \tag{3.59}$$

Using the equations and the data included in Table 3.2 the values of Cv, C_D and Cc have been calculated and given in Table 3.2.

For the second test the equipment was modified to enable the outflow of water to be restricted. The pressure just after the orifice and just before the restriction was measured by means of a plastic tube inserted into the pipe as shown in Fig. 3.14.

In this experiment the flow rate and the two pressures (h_1 and h_2) were noted for various values of height of water. These results, with the results found in Test 1, were used to verify equations 3.31 and 3.38.

Equation 3.31 becomes

$$\frac{h - h_1}{q^2} = \frac{1}{2g}\left(\frac{1}{(A_o C_D)^2} - \frac{1}{A_1^2}\right) \tag{3.61}$$

For orifice of area $13.2\ 10^{-6}\ m^2$,

$$\frac{h-h_1}{q^2} = \frac{1}{2(9.8)}\left[\frac{1}{(13.2\ 0.72\ 10^{-6})^2} - \frac{1}{(78.5\ 10^{-6})^2}\right]$$

$$= 5.55\ 10^8 \quad s^2\ m^{-5}$$

For orifice of area $7.3\ 10^{-6}\ m^2$,

$$\frac{h-h_1}{q^2} = 1.69\ 10^9 \quad s^2\ m^{-5}$$

Simarly equation 3.38 becomes,

$$\frac{h-h_2}{q^2} = \frac{1+(C_D A_0/A_1)^2(1-2A_1/C_c A_0)}{2g(C_D A_0)^2} \qquad (3.62)$$

Hence for orifice of area $13.2\ 10^{-6}\ m^2$,

$$\frac{h-h_2}{q^2} = 4.45\ 10^8 \quad s^2\ m^{-5}$$

and for orifice of area $7.2\ 10^{-6}\ m^2$,

$$\frac{h-h_2}{q^2} = 1.47\ 10^9 \quad s^2\ m^{-5}$$

These theoretical results are shown with the experimental results in Fig. 3.20.

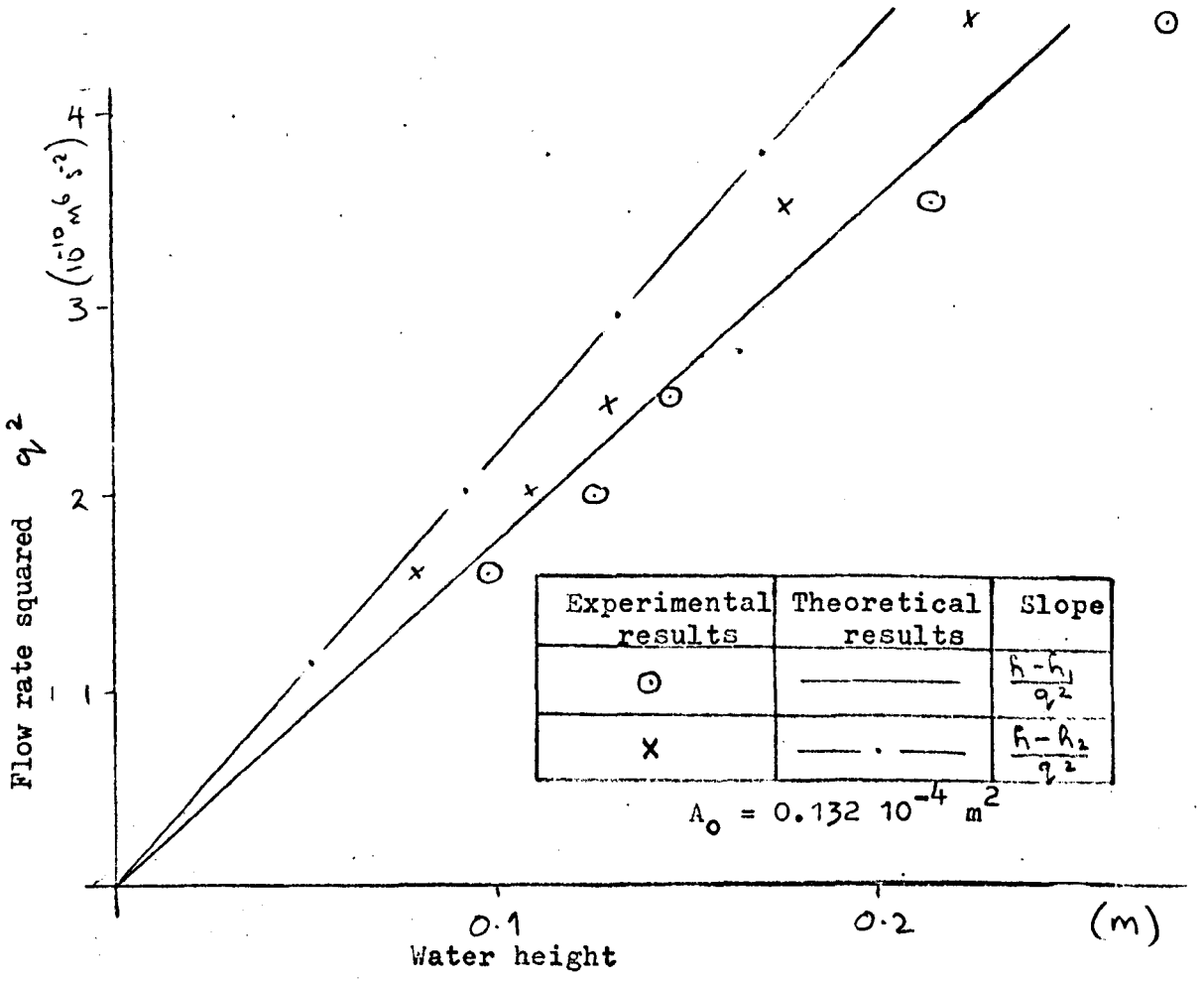

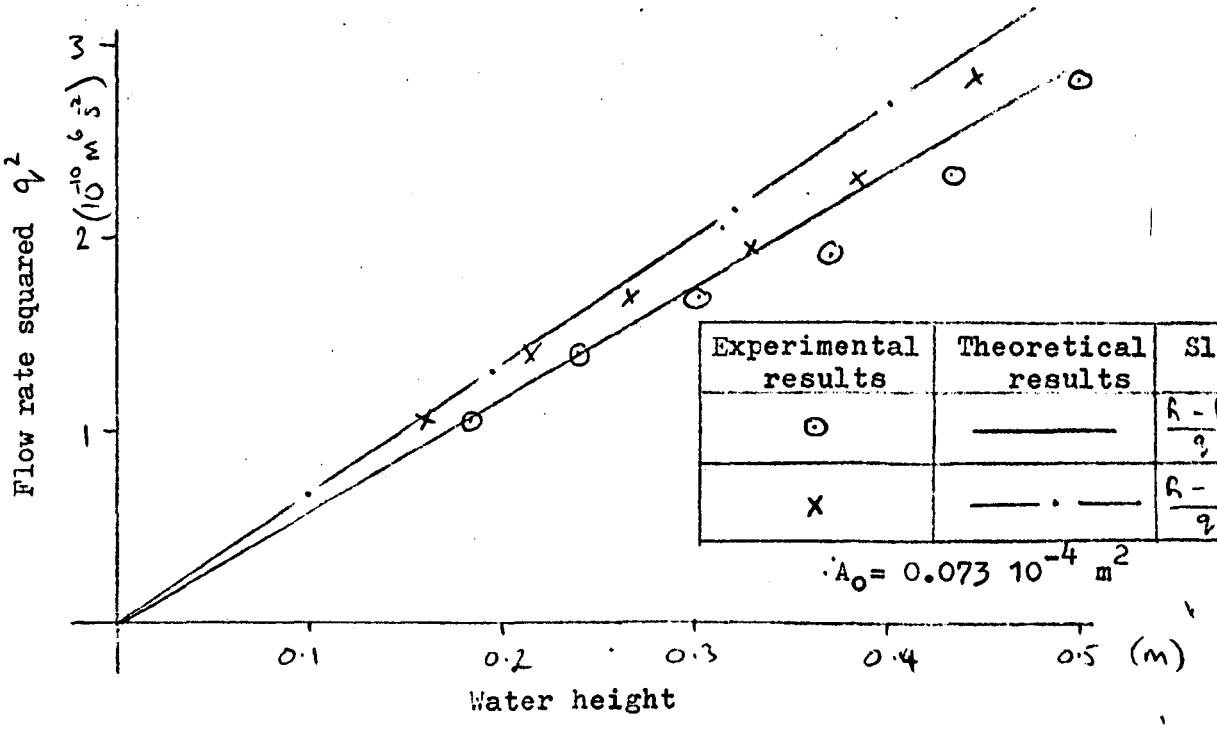

Orifice tests results

Fig. 3.20

3.3 Conclusions

Considering the tests conducted on the valve at Enfield the results (Figs. 3.16 and 3.17) are in good agreement with the theory and with the results in other published work on this subject[14,17].

It should be noted that these results are for relatively small orifice Openings. For the tests conducted at Pratt's the results, (Fig. 3.19), when considering flow rate against force on spool, show significant disagreement with the theory. By considering both Figs. 3.17 and 3.19 it can be seen that all the experimental curves are of similar shape and this differs from the theoretical results. The amount of discrepancy increases with increase in orifice width opening. The theoretical results are plotted from equation 3.10 and by considering this equation it is thought that cos θ may not be a constant, as assumed. Reference 13 experimentally investigates the value of this angle for variation in the orifice dimensions, and it shows that the flow downstream of the orifice can, under certain conditions, attach itself to either the valve body or to the spool, thus making cos θ equal to 0 cr 1 respectively. The tests were conducted on a two dimensional model of the valves orifice and only low pressures were considered (p_{max} = 0.14 10^{-7} N m^{-2}). Thus this reference does show that cos θ can vary. From considering the results obtained, Fig. 3.17 and 3.19, it is therefore suggested that cos θ can vary and is not only dependant on the dimensions of the orifice but is also affected by the flow rate and the pressure drop across the valve.

The orifice test results (Fig. 3.20) although not in perfect agreement, do tend to support the theoretical approach when considering the case of an orifice discharging in a pipe with a pressure greater than atmospheric. The purpose of these tests were to show that the values of C_v, Cc and $\cos\theta$ (if applicable) would be found for an orifice in a valve (see section 3.1.3). The individual values of these constants are required when it is intended to consider a valve as part of a hydraulic system in which the valve directs the fluid flow to a motor. For this case the network representation of the hydraulic part of the valve is as shown in Fig. 3.10, and to calculate the numerical value of the hydraulic resistance, shown in this figure, the above mentioned constants are required.

4. Complete System

In this chapter the work of the previous two chapters is combined to obtain the overall network representation of the complete system. From which a set of independant network equations can be systematically obtained. These equations are simulated on an analogue computer[46] and the dynamic behaviour of the system is studied. The theoretical results are presented along with experimental results.

4.1 Theory

The system, as considered in this work, is complete when one of the solenoids is attached to the valve and the valve's orifice discharges to tank, generally as arranged in Fig. 4.3. In theory this means that the three networks in Figs. 2.6, 3.2, and 3.6 are joined resulting in the network of the solenoid valve system depicted in Fig. 4.1.

Fig. 4.1 (a) represents the electrical elements of the solenoid where,

- e_s - voltage source
- R_e - resistance of the coil
- N^2P - self inductance of the coil
- e - induced voltage due to changes in the magnetic circuit

Fig. 4.1 (b) represents all the mechanical elements of the valve where,

- f_e - force generated by the solenoid (force source)
- M - mass of all moving parts including the solenoid armature

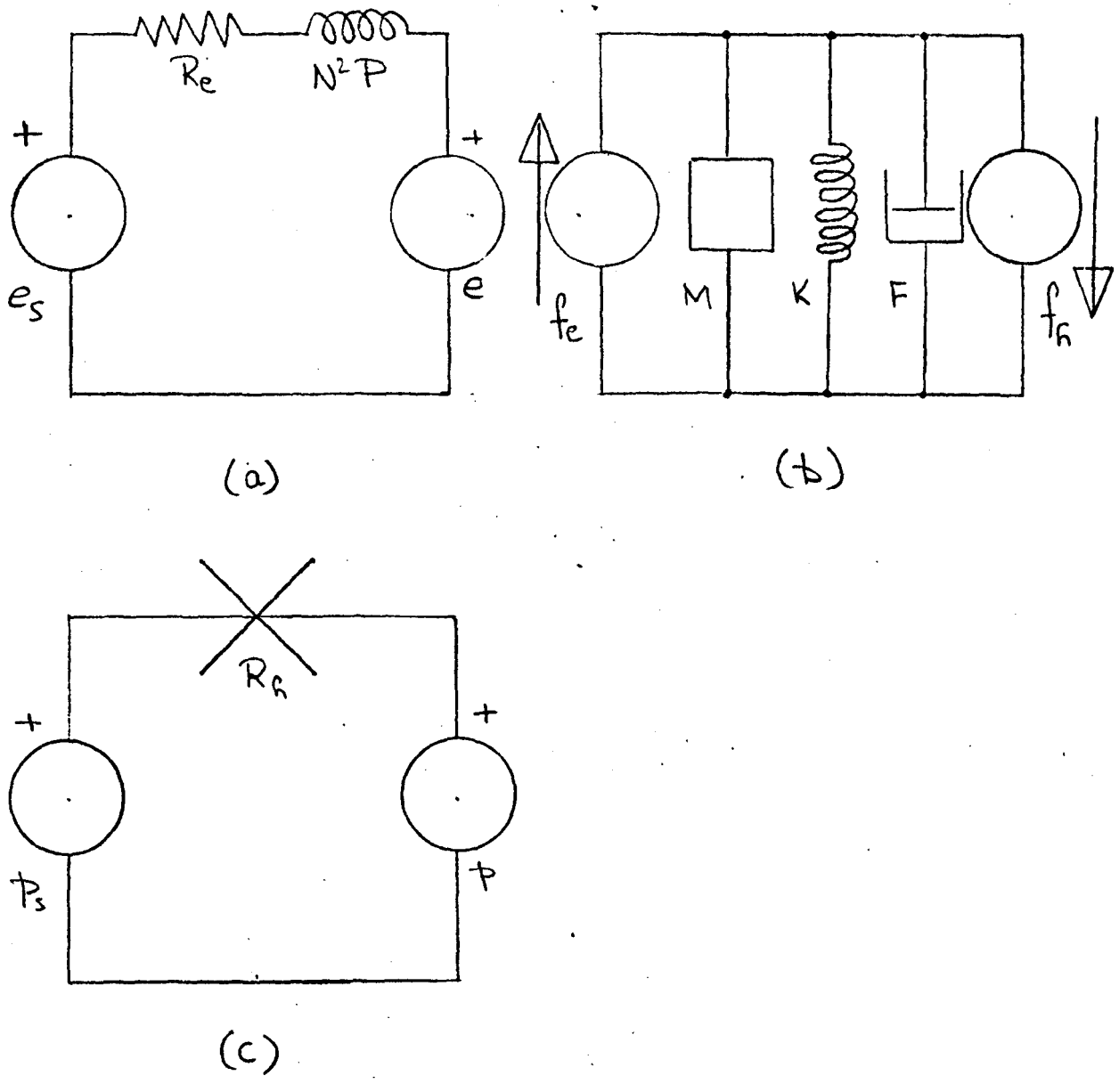

Network of solenoid, hydraulic valve system

Fig. 4.1

K - spring constant

F - viscous friction coefficient between spool and value body

f_h - force acting on the spool due to fluid flow

Fig. 4.1 (c) represents the hydraulic elements of the valve where,

p_s - pressure source

R_h - hydraulic resistance (which is non-linear)

p - ideal pressure drop across the orifice

From topological considerations the set of independant equations can be derived. Where from Fig. 4.1 (a) and (c) the mesh equation 4.1 and 4.3 respectively can be written and from Fig. 4.1 (b) the node equation 4.2 can be written.

$$PN^2 \frac{di}{dt} = e_s - R_e i - N^2 \frac{dz}{dt} i \frac{dP}{dz} \qquad (4.1)$$

$$M \frac{d}{dt}\left(\frac{dz}{dt}\right) = \frac{N^2 i^2}{2} \frac{dP}{dz} - F \frac{dz}{dt} - K_y - \frac{\rho \cos\theta}{\pi D} q^2 - L_1 \rho \frac{dq}{dt} \qquad (4.2)$$

$$p_s = \frac{\rho(1-C_v^2)}{2(C_v C_c A_o)^2} q^2 + \frac{\rho}{C_c^2 A_o^2 2} q^2 \qquad (4.3)$$

Substituting numerical values into equations 4.1, 4.2 and 4.3 and re-arranging where necessary

$$P \frac{di}{dt} = \frac{e_s}{2.58\ 10^6} - \frac{i\ 62}{2.58\ 10^6} - i \frac{dP}{dz} \dot{z} \qquad (4.4)$$

$$\frac{d\dot{z}}{dt} = \frac{f_s}{0.208} - \frac{1.32}{0.208}\frac{dz}{dt} - \frac{10900}{0.208}(z + 1.98\ 10^{-3})$$

$$- \frac{10460}{0.208\,x}q^2 - \frac{6.13}{0.208}\frac{dq}{dt} \qquad (4.5)$$

$$q = 1.49\ 10^{-3} \times p_s^{1/2} \qquad (4.6)$$

where $x = (z - 1.88\ 10^{-3})$

Differentiating equation 4.6 assuming that p_s is constant

$$\frac{dq}{dt} = 1.49\ 10^{-3}\frac{dx}{dt}p_s^{1/2} \qquad (4.7)$$

The terms in equation 4.5 containing either x, q or dq/dt will be zero when $z < 1.88\ 10^{-3}$ m.

4.2 Computing

For analogue computing equations 4.4, 4.5 and 4.6 need to be amplitude and time scaled.

Substituting equations 4.7 and 4.6 into 4.5 and letting the maximum value of the supply pressure p_s be $2.07\ 10^7$ N m^{-2} and to be able to obtain values different from the maximum let $p_s = 2.07\ 10^7\ C$ N m^{-2} where the value of C can vary between 0 and 1.

$$\frac{d\dot{z}}{dt} = \frac{f}{0.208} - 6.35\dot{z} - 52500(z + 1.98\times10^{-3})$$

$$- 2.3\ 10^6 C(z - 1.88\ 10^{-3}) - 197\ C^{1/2}\dot{z} \qquad (4.8)$$

The maximum values of the variables have been estimated from experimental data and these are

$$f = 1000 \text{ N} \qquad \dot{z} = 10 \text{ m s}^{-1}$$

$$z = 0.3\ 10^{-2} \text{ m} \qquad \ddot{z} = 2000 \text{ m s}^{-2}$$

Scaling equation 4.8.

$$\left(\frac{\ddot{z}}{2000}\right) = \left(\frac{f}{1000}\right)2.4 - \left(\frac{\dot{z}}{10}\right)0.0317 - 0.079\left[0.66+\left(\frac{z}{3\ 10^{-3}}\right)\right]$$

$$-3.45K\left[\left(\frac{z}{3\ 10^{-3}}\right) - 0.626\right] - 0.98C^{1/2}\left(\frac{\dot{z}}{10}\right) \qquad (4.9)$$

but,

$$\frac{d}{dt}\left(\frac{\dot{z}}{10}\right) = \left(\frac{\ddot{z}}{2000}\right)200$$

$$\frac{d}{dt}\left(\frac{z}{3\ 10^{-3}}\right) = \left(\frac{\dot{z}}{10}\right)3333$$

Therefore, introduce time scale factor $t = \tau/1000$

$$\left.\begin{aligned}\frac{d}{d\tau}\left(\frac{\dot{z}}{10}\right) &= \left(\frac{\ddot{z}}{2000}\right)0.2 \\ \frac{d}{d\tau}\left(\frac{z}{3\ 10^{-3}}\right) &= \left(\frac{\dot{z}}{10}\right)3.33\end{aligned}\right\} \qquad (4.10)$$

The maximum values of the variables in equation 4.4 which have been estimated from digital computing and experimental work are,

$$\frac{dP}{dz} = 25\ 10^{-4}\ H\ m^{-1} \qquad e = 500v$$

$$i = 5A \qquad \dot{i} = 2000\ A\ s^{-1} \qquad P = 1.5\ 10^{-6}\ H$$

Scaling equation 4.4.

$$\left(\frac{P}{1.5\ 10^{-6}}\right)\left(\frac{\dot{i}}{2000}\right) = \left(\frac{e}{500}\right)0.0648 - \left(\frac{i}{5}\right)0.04 - \left(\frac{i}{5}\right)\left(\frac{dP/dz}{25\ 10^{-4}}\right)\left(\frac{\dot{z}}{10}\right)417 \quad (4.11)$$

and

$$\frac{d}{d\tau}\left(\frac{i}{5}\right) = \left(\frac{\dot{i}}{2000}\right)0.4 \quad (4.12)$$

$\left(\frac{e_s}{500}\right)$ is a sinusoidally varying voltage and its generation is shown in Fig. 2.25. The supply pressure, is assumed constant throughout the experimental work and is thus represented by a constant voltage.

Thus from considering equations 4.9, 4.10, 4.11 and 4.12 and Fig. 2.25 the analogue programme is as shown in Fig. 4.2. It should be noted that there is a slight alteration in the generation of the e_s circuit as shown in Fig. 2.25 to that in Fig. 4.2. The new circuit enables the voltage to be switched on at any point of the waveform during the cycle.

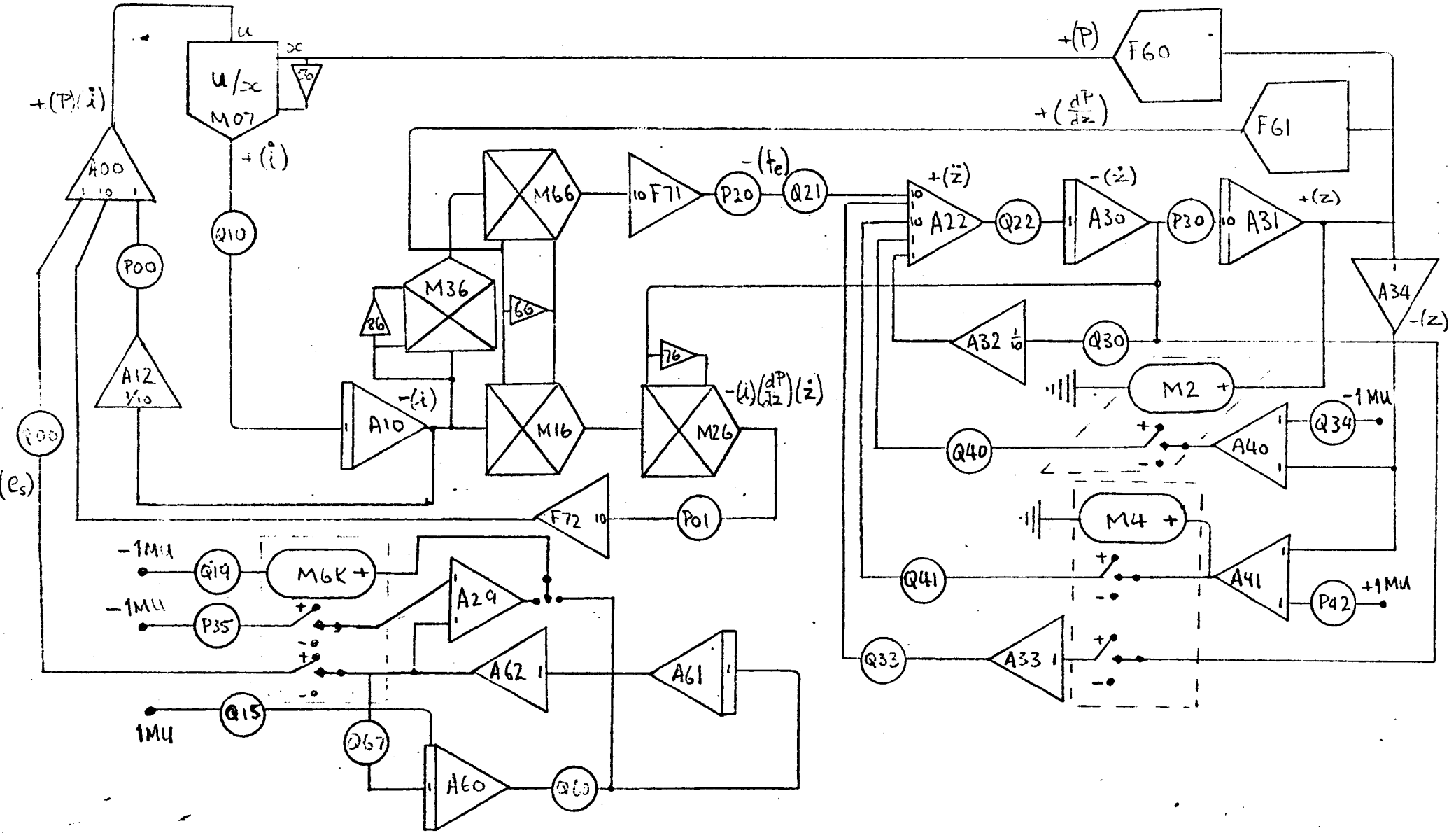

Analogue computer programme circuit diagram for solenoid, hydraulic valve system

Fig. 4.2

It was then possible to simulate the dynamic behaviour of the valve for the case when the voltage is supplied to one solenoid. The variables, e_s, i, z, f_e, di/dt, dz/dt and d^2z/dt^2 being recorded on a chart recorder. The tests were conducted for various values of supply pressure, supply voltage and at different switch on points on the supply voltage cycle, as mentioned above. A sample of these results is shown in Fig. 4.5 (1), and it should be noted that for cases (a) and (b) the valve fails to function.

4.3 Experimental Work

As shown above the dynamic behaviour of the value system is described by equation 4.1 and 4.2 containing two independant variables; the current through the inductor and the velocity (or displacement) of the spool. To study the validity of these equations experimentally it is necessary to monitor these two variables together with the input variables.

4.3.1 Description of apparatus

For the following tests the valve was assembled complete except for the removal of one solenoid as shown in Fig. 4.3 and 4.4, it was replaced by a displacement transducer, and the electrical and hydraulic supplies were connected to the appropriate terminals. An ammeter was placed in series with the electrical supply to monitor the current on a U.V. recorder[47] via suitable arranged resistors. The U.V. recorder was also used to record the supply voltage, and the displacement of the spool

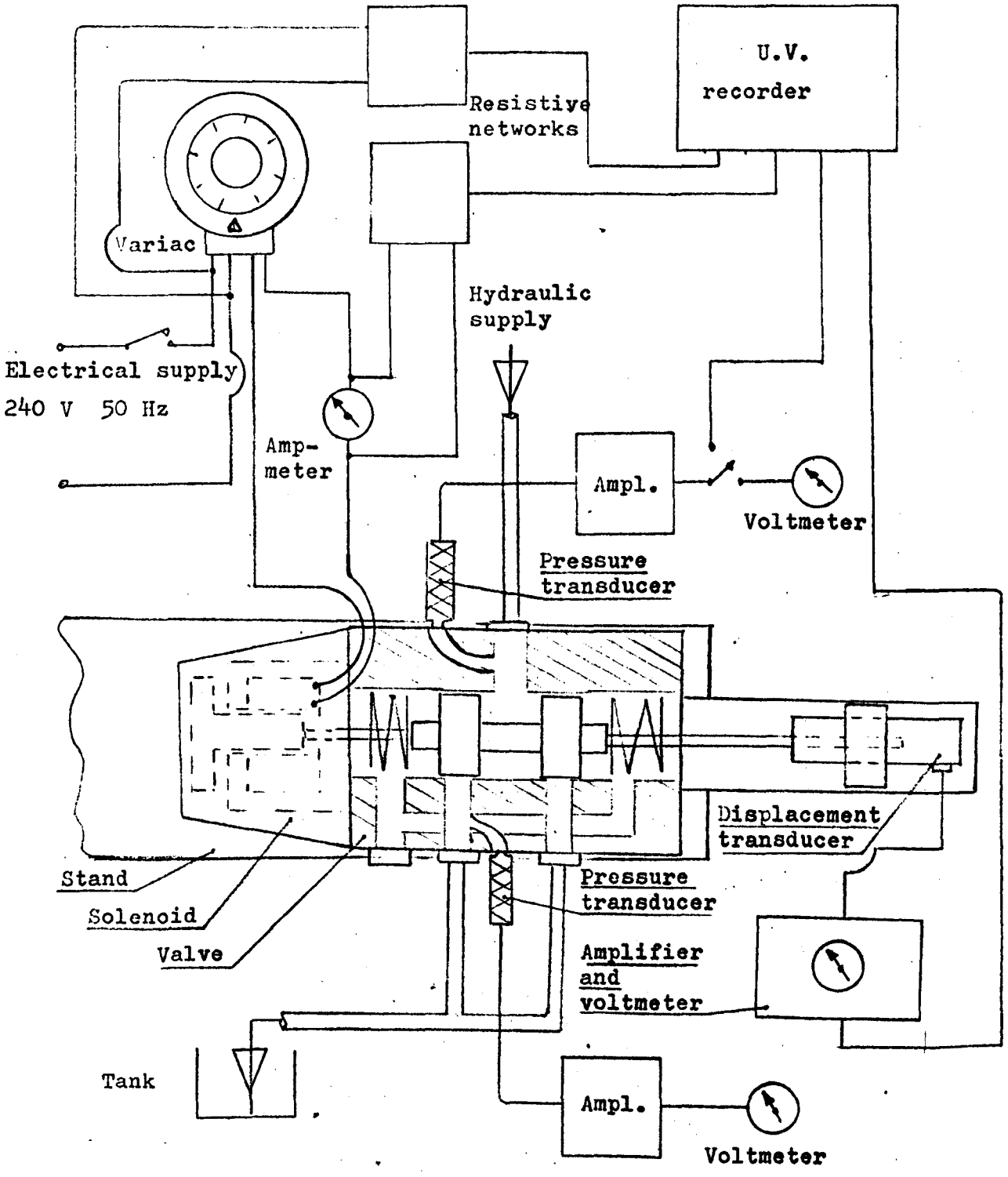

Schematic diagram of experimental apparatus

Fig. 4.3

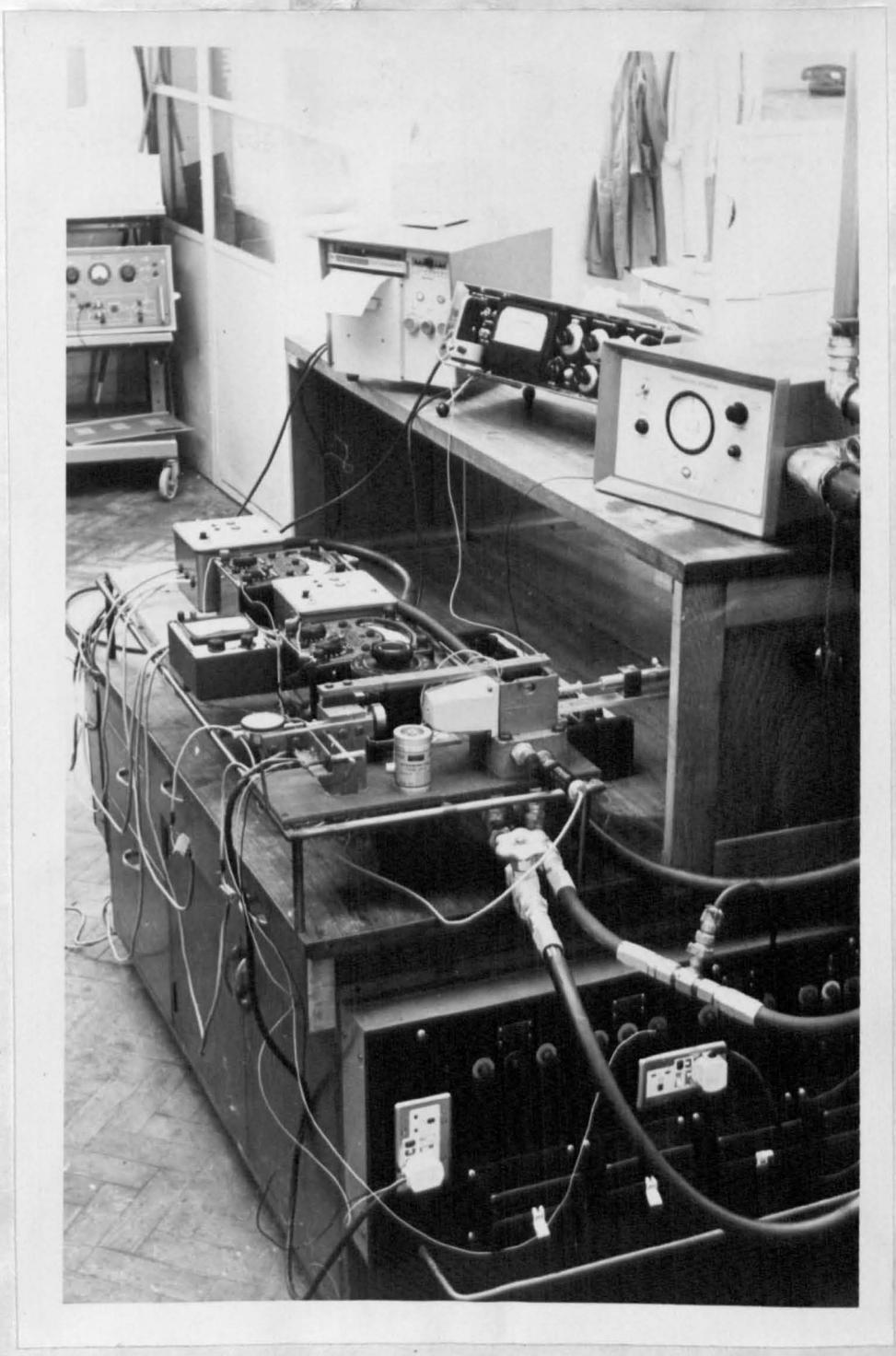

Photograph of apparatus

Fig. 4.4

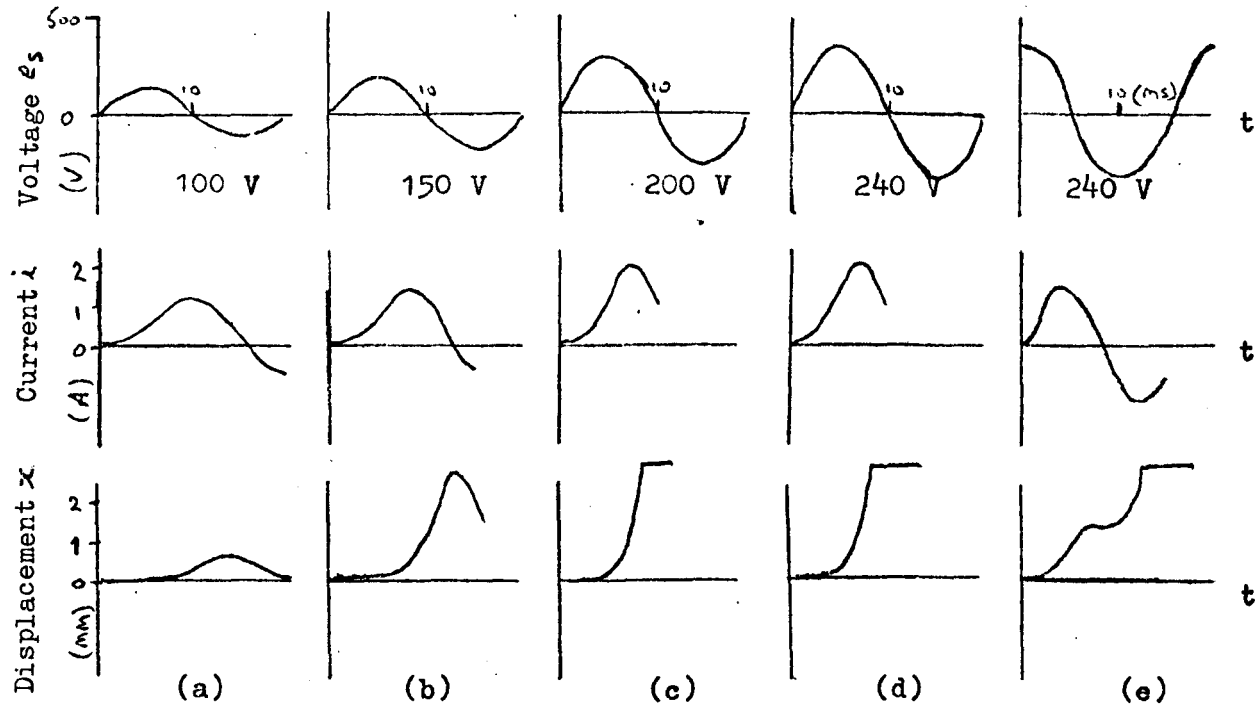

(1) Theoretical results for p_s = 1000 lbf in^{-2} (6.9 10^6 N m^{-2})

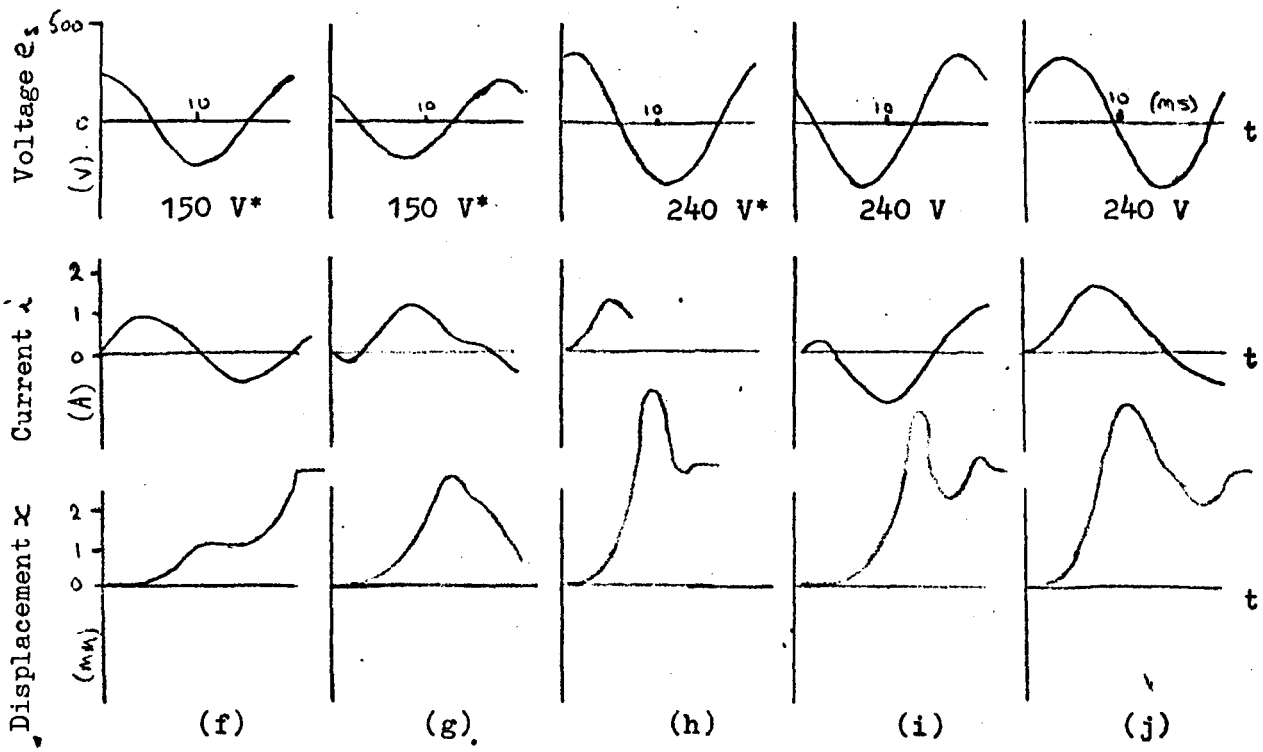

* these rsults were obtained at Pratt Hydraulics Ltd.

(2) Experimental results for p_s = 1000 lbf in^{-2}(6.9 10^6 N m^{-2})

Theoretical and experimental results

Fig. 4.5

via resistors and by means of an inductive-type displacement transducer[30,33] respectively. The pressure of the hydraulic supply was monitored by a pressure transducer[42] which was either connected to a voltmeter or the U.V. recorder.

4.3.2 Experimental Results

With the valve in the off position, i.e., the solenoid disconnected from the electrical supply, the pressure of the hydraulic supply was set at a given value. Then the electrical supply to the solenoid was switched on. The input variable e_s and the variables i and z were recorded on the U.V. recorder. p_s was also monitored but this signal appeared to contain a large amount of noise and tended to obscure the other signals as indicated by the results, therefore this signal was not recorded in the majority of the tests.

The above tests were conducted for various values of input pressures p_s and input voltage e_s. Tests were also conducted to observe the effect of switching the input voltage on at various points on its waveform.

The results are given in Fig. 4.5 (2), and it should be noted that for case (g) the valve fails to function.

4.4 Conclusions

With reference to Figs. 4.6 and 4.7, there is a significant variation in the time the spool takes to reach is maximum position depending on what position of the voltage waveform the supply is initially switched across the solenoid. Also, it is

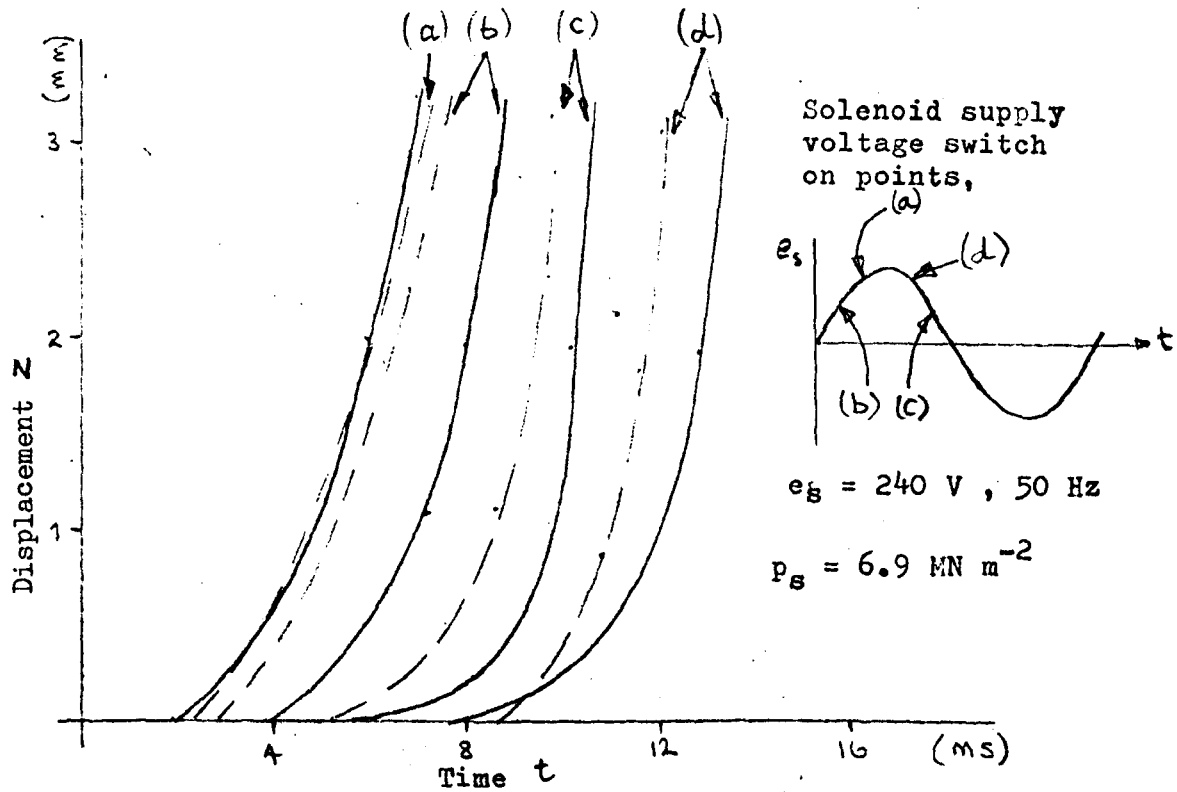

Displacement curve

Fig. 4.6

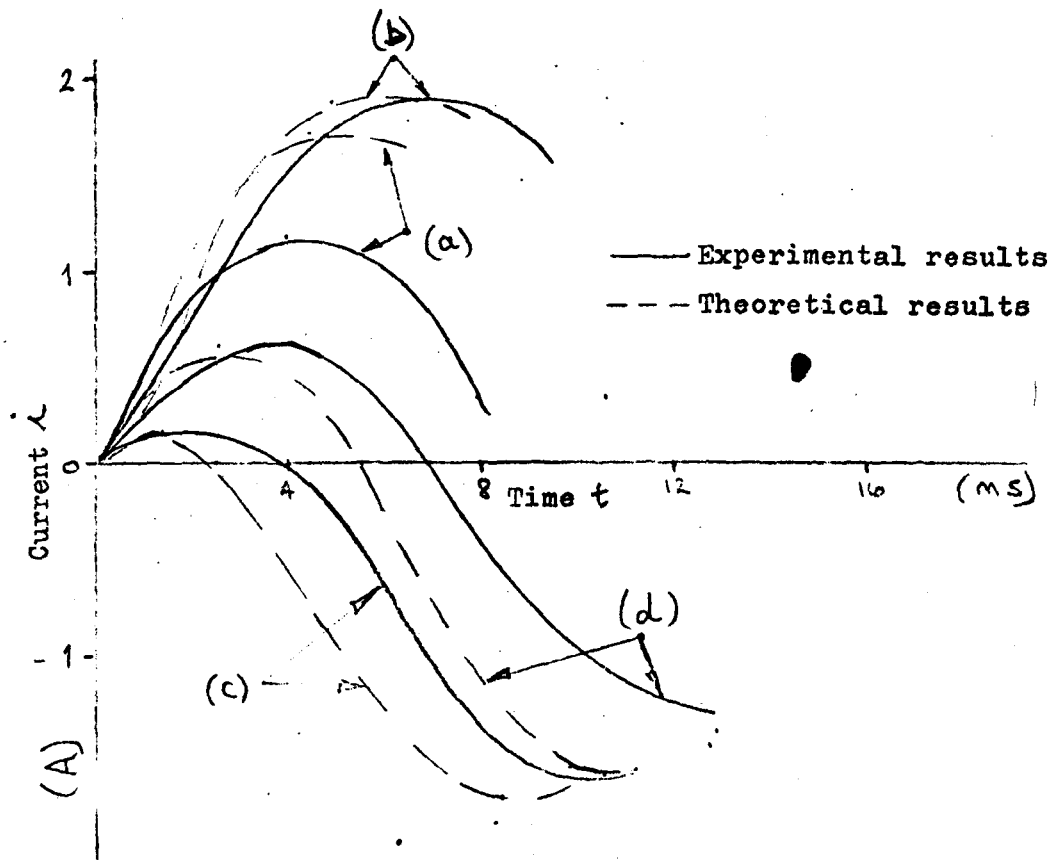

Current curve

Fig. 4.7

noted that if the amplitude of the voltage applied to the solenoid is varied then both experimental and theoretical results show a supply voltage below which the solenoid will not operate, which is about 150 V.

The discrepancy between the theoretical and experimental results is thought to be due to four main factors:

(i) there is an uncertainty in the theoretical value of the viscous friction coefficient

(ii) there is an uncertainty in the theoretical value of the force due to fluid flow

(iii) the hydraulic supply is assumed to act as a constant pressure source

(iv) there is an uncertainty in determination of the force generated by the solenoid.

Considering these four factors:

(i) The theoretical value of the viscous friction coefficient is calculated assuming that there is a constant and uniform gap between the spool and the valve body. In practise the spool will probably be off centre[17,35] and its relative position is likely to vary during the operation of the valve. Also, as previously mentioned in section 3.1.1 there will be friction due to contact between the O-ring and striker pin. It is therefore thought that the viscous friction coefficient will not be a constant and its values tend to be higher than the theoretical value used.

(ii) The graph of the square of the flow rate against force on spool (Fig. 3.19) shows a marked variation between the theoretical and experimental results, as discussed in Chapter 3.3. The graph indicates that at a given flow rate the actual force on the spool is lower than the theoretical value.

(iii) Since a constant pressure source was assumed the flow-rate will be proportional to the width of the orifice opening, this will give rise to large theoretical flow rates, which in turn imply larger theoretical forces on the spool. In Chapter 5 an alternative analogue computer programme is presented which over-comes this problem.

(iv) Further to Fig. 4.7 the theoretical curves of current lag behind the experimental curves, and since the force is proportional to the square of the current (equation 2.20), which in turn govern the displacement curve, this lag in current curves will cause a lag in the displacement curves. A possible reason for this discrepancy is due to the accuracy in estimating the permeance and rate of change of permeance with respect to displacement curves.

The overall effect of these factors could account for the most of the difference between the theoretical and experimental results.

The major effect on discrepancy appears to be due to factor (iv). This is deduced by comparing the spacing of the current curves (Fig. 4.7) with those of the displacement curves (Fig. 4.6). This indicates that if the theoretical and experimental current curves were to be the same, then the corresponding displacement curves would be very close together.

As stated in Chapter 1.1 there are a number of problems affecting the design of a new valve, and to achieve optimum design and performance it is first necessary to have a thorough understanding of the operation, steady state and dynamic characteristics, of the complete system. In the previous chapters the complete valve has been analysed and the theory applied to valve VDS 34[22]. To facilitate the experimental work the hydraulic part of the valve was restricted to the operation of one opening (Fig. 4.3) i.e., there was no hydraulic load. The experimental results for both steady state and dynamic tests support the theoretical calculations.

As stated in Chapter 1.2 it is believed that in previous work concerning valves, either only that part of the valve is considered which comes under one of the well defined engineering disciplines or, if the complete system is analysed, certain characteristics are assumed to be linear and consequently only small displacements of the spool are considered. In the present work neither of these restrictions have been imposed.

5. Design Considerations

The object of this chapter is to suggest:

(i) improvements in the mathematical model

(ii) procedures by which the design of the valve type VDS 34 and solenoid type 18-7202 can be improved.

5.1 Non-ideal Pressure Source

In Chapter 4 the theoretical results were obtained assuming the hydraulic supply to act as an ideal pressure source and by comparison with the experimental results and from theoretical considerations it was concluded that a non-ideal pressure source should be considered. It is therefore intended to consider what effect a non-ideal pressure source will have on the force acting on the spool due to the steady state flow, and thus to determine the necessary alterations in the analogue computer programme used to study the complete system depicted in Fig. 4.2.

Let the valve be supplied by a positive displacement pump[27] whose pressure is controlled by a relief valve.

It will be assumed that the pressure will remain constant whilst there is flow through the relief valve and that there is no leakage across the pump. Therefore the source characteristics will be as given in Fig. 5.1 in which the pressure is determined by the set compression of a spring in the relief valve.

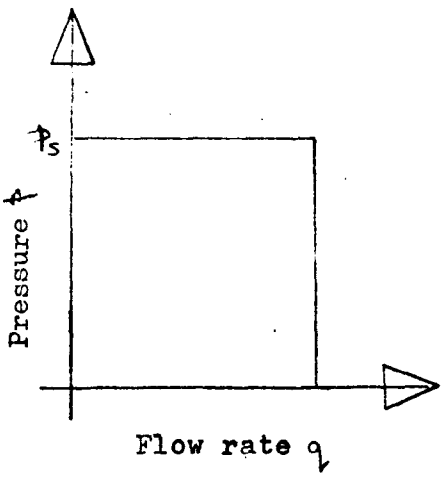

Hydraulic source characteristic

Fig. 5.1

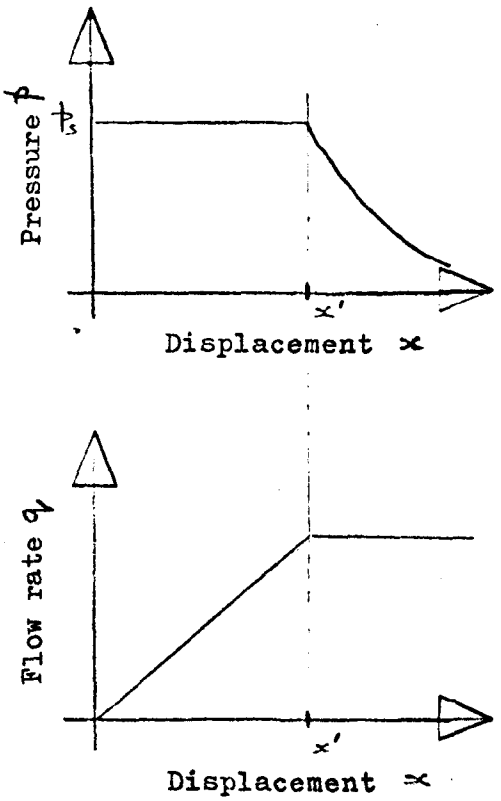

Hydraulic source characteristics as a function of spool displacement

Fig. 5.2

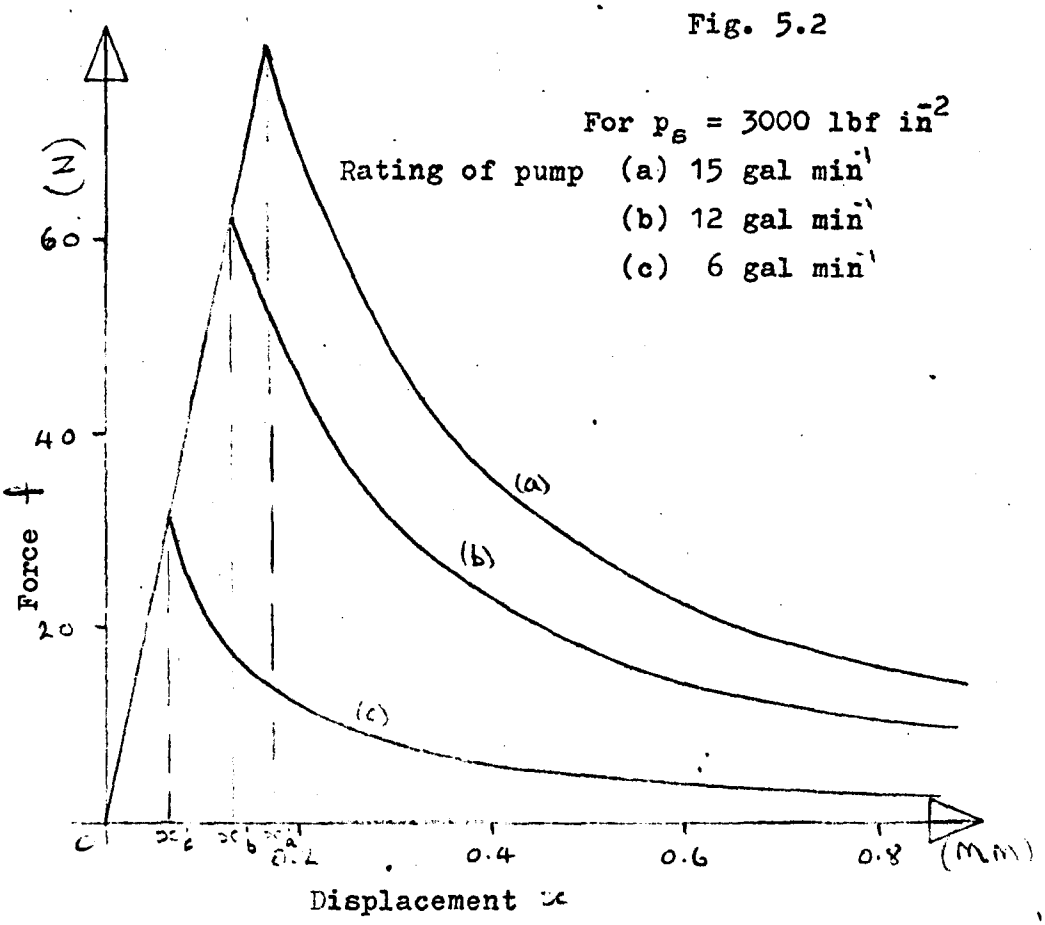

Force due to steady state fluid flow as a function of valve displacement

Fig. 5.3

The hydraulic load of this source is the valve discharging to tank. For the valve from equation 3.53

$$q = 1.49 \quad 10^{-3} \times p_1^{1/2} \qquad (m^3 s^{-1}) \qquad (5.1)$$

Therefore, considering Fig. 5.1 and equation 5.1 the source variables (p_1, q) can be expressed in terms of the load variable x, as in Fig. 5.2 where x^1 is the opening of the valve at which all fluid from the pump passes through the valve.

A graph of force due to steady state fluid flow acting on the spool against displacement of spool when considering this type of hydraulic source can now be plotted. A series of curves as in Fig. 5.3 can be drawn for different rating of pumps by considering equations 5.1 and 3.46.

Let the maximum flow rate be 15 gal/min. ($1.1\ 35\ 10^{-3}$ $m^3\ s^{-1}$) and the nominal supply, pressure (p_s) is 3000 lbf $in.^{-2}$ ($2.07\ 10^7 Nm^{-2}$). Therefore, the value of x^1 in Fig. 5.2 can be found from equation 5.1

$x^1 = 0.167$ mm

For values of x below 0.167 mm the force is given by equation 3.46 and 5.1,

$$f = x\ 480000 \qquad (N) \qquad (5.2)$$

and for value of x greater than 0.167 mm the force is from equation 3.46.

$$f = \frac{0.0135}{x} \qquad (N) \qquad (5.3)$$

The curves of f against x are given in Fig. 5.3 for sources of nominal supply pressure of 3000 lbf $in.^{-2}$ and various values of pump ratings. It can be seen from this graph that there are peak forces over a small range of spool position. It is therefore important in the design of the valve that this peak force be considered.

5.2 Non-ideal pressure source in the analogue computer programme

Letting the maximum flow rate be 15 gal. min^{-1} ($1.135\ 10^{-3}\ m^3\ s^{-1}$) and the maximum pressure be 3000 lbf in^{-2} ($2.07\ 10^7\ N\ m^{-2}$) and to enable different ratings of flow source, from zero to the maximum ratings given above, to be simulated on the analogue computer, then,

$$q = K_q\ 1.135\ 10^{-3} \quad (m^3\ s^{-1}) \tag{5.4}$$

$$p = K_p\ 2.07\ 10^7 \quad (N\ m^{-2}) \tag{5.5}$$

where Kq and Kp are coefficients which can take on values from 0 to 1.

Substituting into equation 5.1

$$x' = 0.167\ 10^{-3}\ \frac{K_q}{K_p^{1/2}} \tag{5.6}$$

Therefore for values of $x < x^1$, equation 5.1 becomes

$$q = 6.2 \times (K_p)^{1/2} \tag{5.7}$$

and for values of $x > x^1$, equation 5.1 becomes

$$q = K_q \; 1.135 \; 10^{-3} \tag{5.8}$$

The non-ideal source affects equation 4.5 which now has to be considered valid in two regions of operation.

When $x < x^1$ then equation 5.7 is substituted into the last two terms of equation 4.5, which gives

$$- \frac{10460\,(6.8)^2 \times K_p}{0.208} - \frac{6.13\; K_p^{1/2}\; 6.8}{0.208} \frac{dx}{dt} \tag{5.9}$$

When $x > x^1$ equation 5.8 is substituted into the last two terms of equation 4.5, which gives

$$- \frac{10460\,(K_q\; 1.135\; 10^{-3})^2}{0.208\; x} \tag{5.10}$$

Noting that $x = (z - 1.88\; 10^{-3})$ equation 4.5 becomes,

for $x < x^1$

$$\frac{dz}{dt} = \frac{f}{0.208} - 6.35z - 52500(z + 1.98\,10^{-3}) \ldots$$

$$-2.3K_p 10^6 (z - 1.88\,10^{-3}) - 197(K_p)^{1/2} z \tag{5.11}$$

and for $x > x^1$

$$\frac{dz}{dt} = \frac{f}{0.208} - 6.35z - 52500(z - 1.98\,10^{-3})$$

$$- \frac{0.065\,K_q^2}{z - 1.98\;10^{-3}} \tag{5.12}$$

and writing x^1 in terms of z^1, equation 5.6

$$z' = x' + 1.88\ 10^{-3} = 0.167\ 10^{-3}\left(\frac{K_q}{K_p^{1/2}}\right) + 1.88\ 10^{-3} \qquad (5.13)$$

Equation 5.11 is identical to 4.8 when

$z < (0.167\ 10^{-3}\ \frac{K_q}{K_p^{1/2}} + 1.88\ 10^{-3})$ therefore the analogue computer programme will be the same as that given in Fig. 4.2. However, when $z > (0.167\ 10^{-3}\ \frac{K_q}{K_p^{1/2}} + 1.88\ 10^{-3})$ equation 5.12 has to be used giving a different programme. The new scaled equation representing equation 5.12 is,

$$\left(\frac{\ddot{z}}{2000}\right) = \left(\frac{f}{1000}\right)2.4 - \left(\frac{\dot{z}}{.10}\right)0.0317 - 0.079\left[0.66 + \left(\frac{z}{3\ 10^{-3}}\right)\right] - \frac{0.011\ K_q^2}{\left[\left(\frac{z}{3\ 10^{-3}}\right) - 0.626\right]} \qquad (5.14)$$

Scaling equation 5.13 gives,

$$z' = 0.0557\left(\frac{K_q}{K_p^{1/2}}\right) + 0.626 \qquad (5.15)$$

The scaled version of equation 5.11 is given in equation 4.9 where K = Kp.

Thus, the modified part of analogue computer programme to simulate equations 5.14, 5.15 and 4.9 is given in Fig. 5.4.

Attempts were made to use the modified analogue computer programme but at the time a suitable computer was not available.

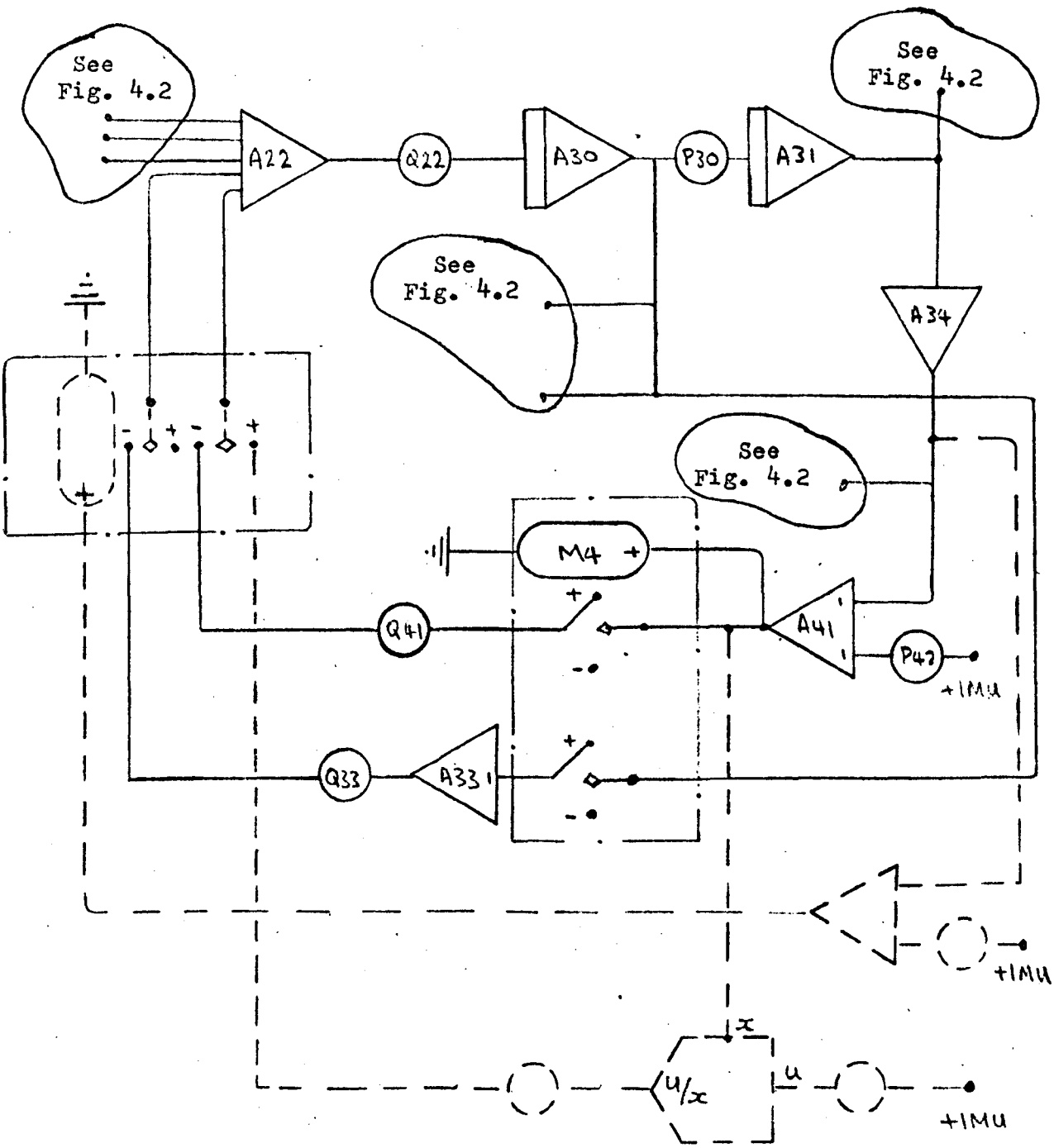

Part of analogue computer programme redrawn from Fig. 4.2 with alterations shown dotted

Fig. 5.4

5.3 Design procedure using Computers

A summary of the criteria for improving the design of the valve, as discussed in section 1.1, is that the valve should control the maximum possible hydraulic power, but it should maintain approximately its external physical size and that the electrical power input be a minimum. An additional criterion is that the valve should operate in the minimum possible time.

A possible method of design is to alter the various parameters of the valve system separately noting the effect of the alteration by means of the computer programmes given, thus determine whether the alteration improves the design of the valve, as defined above, or not. However, since the solenoid parameters can only be altered individually on the digital computer and the valve parameters on the analogue computer this method of design has to be carried out in two stages. In general, the valve will be able to control the maximum amount of hydraulic power in the fastest time if at any particular displacement the force from the solenoid is a maximum, noting that the mass of the armature will affect the time of operation. Thus the force displacement curve can be used as a criterion of "goodness" of the solenoid. This characteristic for any particular solenoid can be obtained by the theoretical approach used in Chapter 2. It would therefore be useful to start off with an existing solenoid and then to alter its parameters (e.g., dimensions, number of turns etc.) by a small amount and re-calculate its new force/displacement characteristics to compare with the original characteristics. This process could be repeated a large number

of times until a maximum curve is obtained. This approach would require vast amounts of calculation which could only be done on a digital computer. To achieve this the same basic programme as given in Fig. 2.18 could be used except that all the dimensions of the solenoid and the number of turns of coil would be given symbols and the permeance of the flux paths would be calculated in terms of these symbols, then a separate data card would be added to the programme. To enable the assignment of symbols to the relative dimensions of a solenoid Fig. 2.15 is re-drawn giving Fig. 5.5

Further to Fig. 5.5

Equation 2.33 becomes

$$P_5 = P_1 = 0.52 \mu l_4 \qquad (5.16)$$

equation 2.35 becomes

(assume g remains < 1.5 t)

$$P_2 = \frac{2\mu l_4}{\pi} \log_e \left(1 + \frac{l_1}{z}\right) \qquad (5.17)$$

equation 2.35 becomes

$$P_6 = \frac{2\mu l_4}{\pi} \log_e \left[1 + \frac{t}{z + l_6 - l_2}\right]$$

where $\frac{l_4 - l_3}{2} = \frac{2\pi (t + z + l_6 - l_2)}{4}$

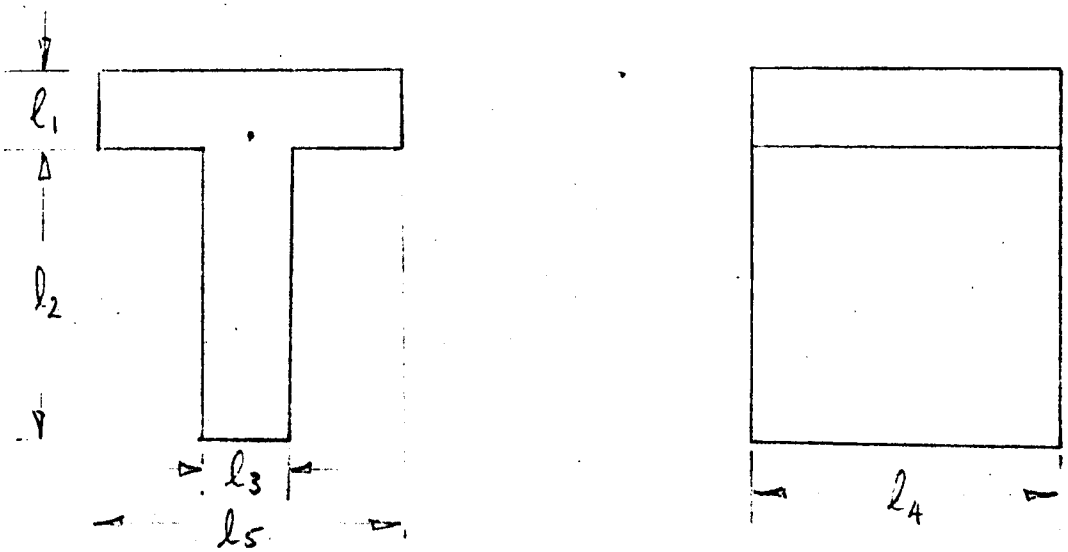

(a) Armature

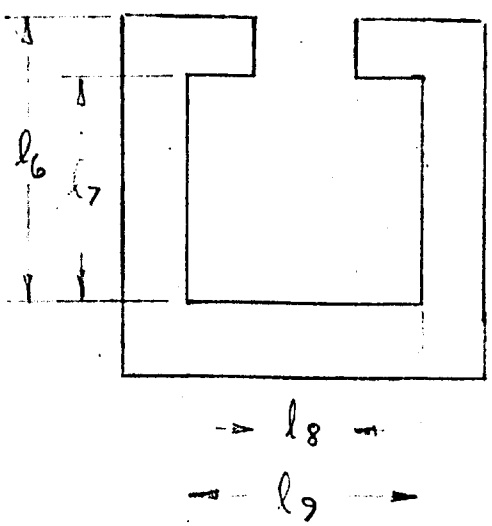

(b) Yoke

Part of solenoid

Fig. 5.5

$$\therefore t = \frac{l_9 - l_3}{\pi} - z + l_6 - l_2$$

$$\therefore P_6 = \frac{2\mu l_4}{\pi} \log_e \left[1 + \frac{-(z + l_6 - l_2) + (l_9 - l_3)/\pi}{z + l_6 - l_2} \right] \quad (5.18)$$

equation 2.36 becomes

$$P_4 = \frac{\mu l_4 (l_6 - l_7)}{0.5 (l_8 - l_3)} \quad (5.19)$$

equation 2.37 becomes

$$P_3 = \frac{\mu l_4 (l_5 - l_3)}{z} \quad (5.20)$$

$$P_7 = \frac{\mu l_3 l_4}{z + l_6 - l_2} \quad (5.21)$$

equation 2.38 becomes

$$P_8 = \frac{\mu [l_7 - (l_9 - l_3)/\pi]^2 l_4}{2 (l_9 - l_3) l_7} \quad (5.22)$$

Therefore, equation 2.70 becomes

$$P_A = 2 \left[\frac{l_4 (l_6 - l_7)}{0.5 (l_8 - l_3)} + \frac{l_4 (l_5 - l_3)}{z} + \frac{2 l_4}{\pi} \log_e \left(1 - \frac{l_1}{z}\right) + 0.52 l_4 \right] \quad (5.23)$$

$$P_B = 2\left[0.52\,l_4 + \frac{2l_4}{\pi}\log_e\left(1 + \frac{l_2 - l_6 - z + (l_9 - l_3)/\pi}{z + l_6 - l_2}\right)\right.$$
$$\left. + \frac{(l_7 - (l_9 - l_3)/\pi)^2 l_4}{2(l_9 - l_3)\,l_7} - \frac{l_3\,l_4\,0.5}{z + l_6 - l_2}\right] \qquad (5.24)$$

$$P_T = 0.638\ 10^{-7}\ \frac{P_A\,P_B}{P_A + P_B} \qquad (5.25)$$

Thus equation 5.23 and 5.24, when written in Fortran IV can replace the expression for A and B in the computer programme given in Fig. 2.18.,and by differentiating these two equations (with respect to displacement) the new expressions for E and D can be found. The programme will now compute the force/displacement characteristic for any given physical size of solenoid. An additional programme could be added to enable the dimensions of the solenoid to be altered by increments and to compare the resultant force curves automatically.

Using these results or the existing characteristics of the solenoid type 18-7202 the modified analogue computer programme can be used to investigate the effect of the following changes.

(a) to vary the spring stiffness, potentiometer Q40 and Q34 are varied

(b) to vary the amount of initial compression of the spring (i.e., when the spool is central), potentiometer Q34 is varied

(c) to represent a non-linear spring, potentiometer Q40 is replaced by a function generator

(d) to vary the amount of travel of the spool before the orifice starts to open, potentiometer Q34 and P42 are varied

(e) to vary the radial dimension of the spool, potentiometers Q33 and Q41 are varied

(f) to investigate the action of the valve when the solenoid is de-energised and the spool returning to its original position, initial condition can be applied to the z integrator (A31).

To carry out a similar investigation when the valve is operating through both Openings there will be additional forces due to flow and rate of change of flow forces, the formulae for calculating these forces are given (equation 3.47 and 3.49) and can be included in the analogue computer programme.

The following simple considerations can be deduced from this work.

Further to Fig. 3.1, the orifice area is equal to the circumference of the spool times the axial distance (x) between the spools surface S_s and the valve body surface S_p. Thus the same orifice area, at the fully open position, can be obtained by increasing the diameter of the spool and decreasing the distance x. The effect of decreasing x would be to bring the armature of the solenoid closer to its fully home position during the period the flow forces are acting on the spool,

thus the force available from the solenoid will be greater. In addition, the peak flow force, as shown in Fig. 5.3, would occur at a point closer to the force axis which again means that there will be a higher force available from the solenoid to overcome this force. If the diameter of the spool was to be increased by a factor of two then for the same area the orifice opening distance (x) is halved and the increase in force available from the solenoid at the point when the orifice just starts to open will be increased by approximately 45% (see Fig. 2.30). The limit by which the spool diameter can be increased will be determined by consideration of the possible increase in leakage between the spool and valve body, possible increase in the chances of hydraulic lock occurring, and manufacturing techniques; however, these factors have not been considered in this work.

The force/displacement curve for the solenoid in the case when the solenoid is operating the valve can vary depending on the transient behaviour of the current and the armature displacement. Examples of this characteristic, obtained from the computer results, are shown in Fig. 5.6. Because of the large variation in the curves shown in Fig. 5.6 it is not thought useful to design a non-linear spring solely based on the force/displacement curve determined for the steady state current condition when the armature is stationary.

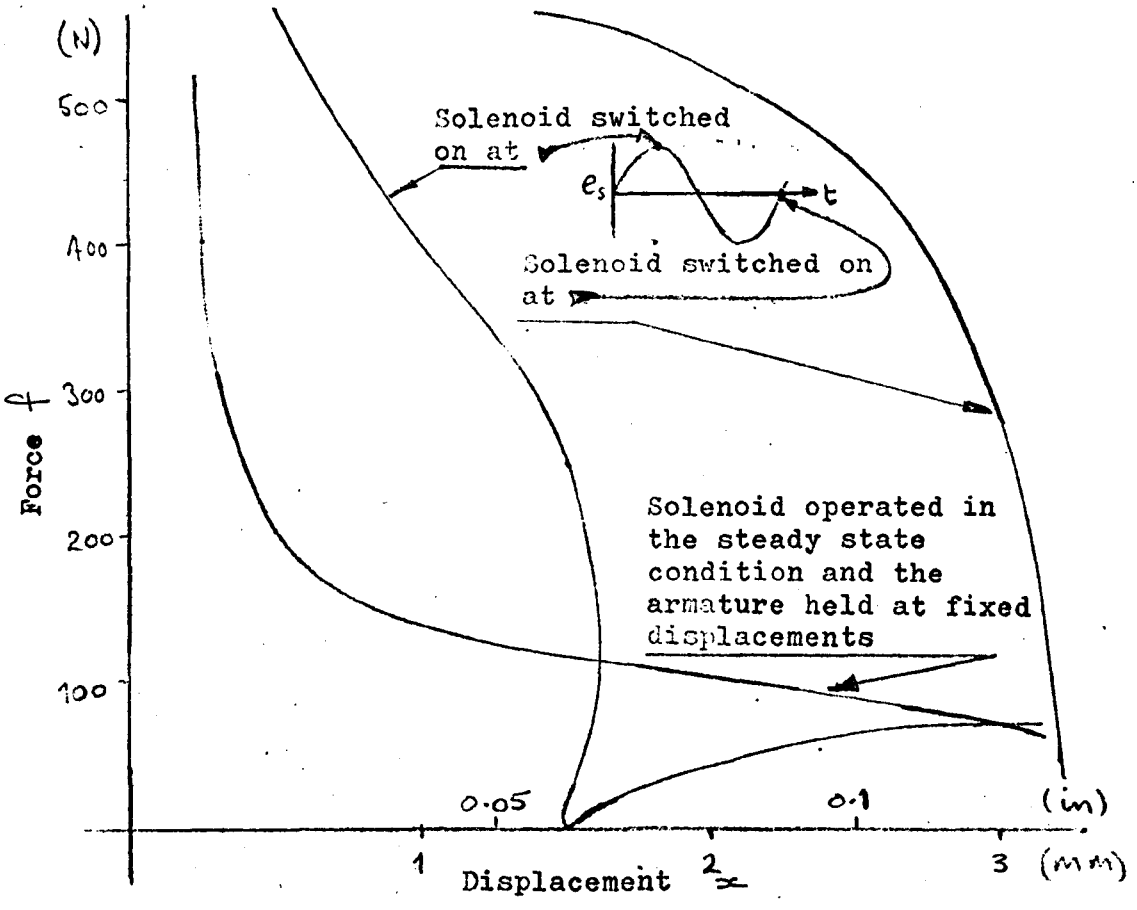

Force / displacement charateristics for solenoid type 18-7202

Fig. 5.6

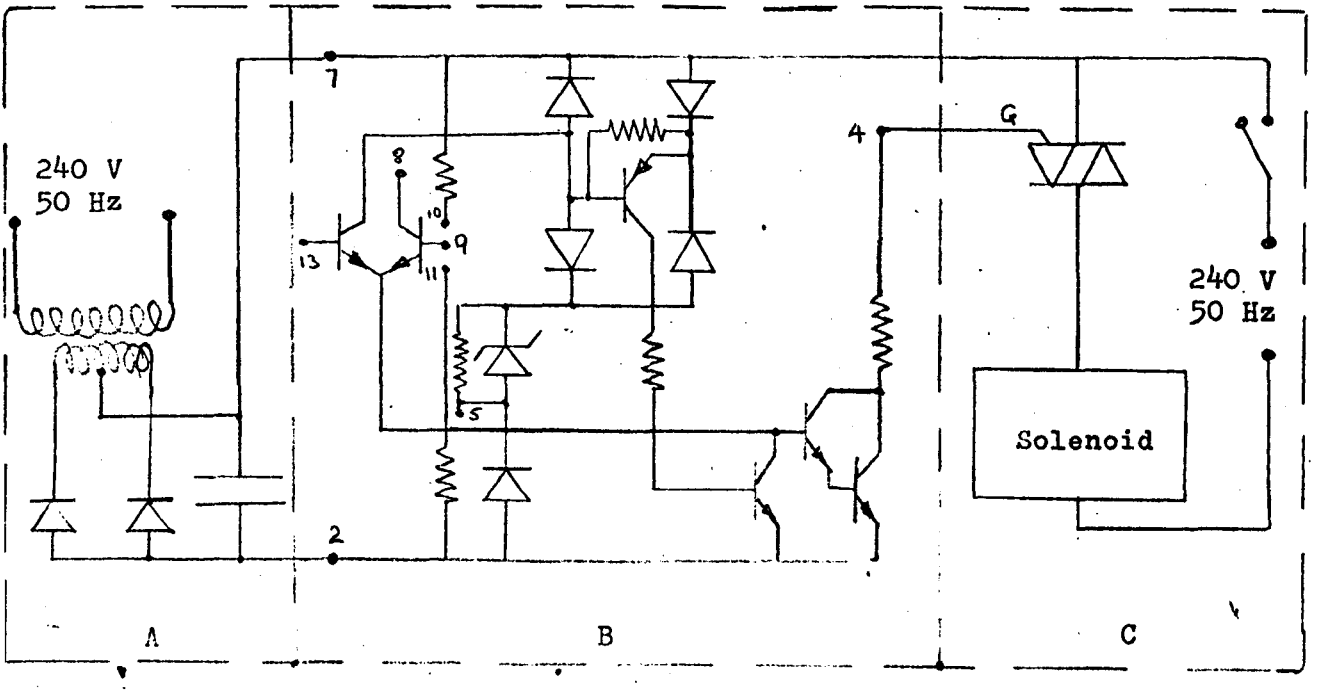

Electrical circuit for switching on the solenoid when the supply voltage is at zero

Fig. 5.7

5.4 Stationary position in the spool displacement curve

Further to Fig. 4.5 (e), (f) it is seen that the spool can stop and even move backwards, this occurs when the solenoid is switched on when the supply voltage is at its peak. The spool's motion is momentarily halted approximately in the region of the orifice starting to open. It is not thought that this will have any detrimental effect in the majority of applications of the valve. However, should it be decided to eliminate this effect in any particular application a circuit is given in Fig. 5.7 which ensures that the voltage is always supplied when the supply voltage is at zero.

Further to Fig. 5.7, the circuit given in section A has a mains voltage input and provides a low power d.c. output which is the supply for circuit B. Circuit B is an integrated circuit[48] where terminals 5, 8, 9, 10, 11, 13 are not used in this application. The function of this circuit is to ensure that the triac in circuit C is only fired when the mains supply voltage is passing through zero. The triac is a semi-conductor switch which enables the a.c. mains to be switched on or off depending on the voltage supplied to its gate terminal, (indicated by G on Fig. 5.7). The cost of the complete circuit is approximately £7.

6. Discussion and conclusions

Considering the proposed programme of work for this thesis given in the application form submitted to the C.N.A.A. it can be seen that the theoretical and experimental work has been covered within certain boundaries and assumptions.

The precise nature of these boundaries and assumptions have been defined in the relevant chapters of this work and the consequence of some of these assumptions are discussed later. From considering the proposed design criteria it can be concluded that the ultimate aim of this work was to design a valve which had the same overall size as the existing valve (or smaller), but was capable of controlling higher hydraulic power with solenoids that needed less electrical power input, all at an economical price. This has not been fully accomplished. However, it is thought that Chapter 5 does provide the tools by which an improved design of the valve could be attempted.

References 17, 18, were consulted extensively throughout this work, and in particular the application of the theory given in reference 18 for the calculation of the permeance of the flux paths in the solenoid was found to give good results. The writer would therefore like to express his gratitude to the authors of these references whose work has greatly aided the understanding of the valve system.

The problem has also been used as an example in the application of systems analysis, and shows the advantage of obtaining individual networks of each sub-system and by joining these networks together a network of the complete system is formed; the governing equations for the complete system can be found from this network. This shows that network analysis yields a uniform method of solving problems which include a number of sub-systems, whether these sub-systems be from the same engineering discipline or not.

It is thought that future work on this subject could be divided into two main divisions, these being,

1. To accept in principle the network representation of the valve system given in this thesis as being adequate to represent the valve and to investigate further the operation of the valve. In particular the performance of the valve when the supply voltage to the solenoid is switched off and the spool is moving back to its equilibrium position under the action of the springs. Thus to use the computer programmes given in Chapter 5 (or modified programmes), to aid the design of a new valve to meet a set of specification. It should be noted that alterations in the numerical values of certain parameters in the network are necessary to represent the valve when there is fluid flow through both of its openings. The necessary information for finding the new values can be found in Chapters 3 and 5. To study the operation of the valve when it supplies a hydraulic load it is necessary to replace the network given in Fig. 4.1 (c) with the combination of the network given in Fig. 3.10 and a network that will represent the hydraulic load. This latter network would have to be derived for the particular load.

2. To consider various aspects of the valve which either have been shown to need further consideration or has not been investigated in this work:- Further to Fig. 3.19 and References 13, 15, there is a good indication that the angle of flow through the orifice is not a constant, as assumed in this thesis. From the experimental results given in Fig. 3.19 this angle appears to be a function of the flow rate and the orifice axial gap width. The effect of this discrepancy is to reduce the force on the spool due to steady state fluid flow.

Further to Fig. 4.5 the experimental results show that the spools motion is often oscillatory before settling in the fully-open position. This part of the dynamic operation of the spool cannot be studied theoretically with the existing analogue computer programmes given in this thesis because the amplifiers reach the limit of their operation. Therefore to study the spools complete dynamic behaviour it would be necessary to consider the permeance of the iron path in the solenoid and then to produce a modified and re-scaled analogue computer programme.

Some aspects of the valve which have not been considered in this thesis are

(a) hydraulic lock between spool and valve,

(b) friction due to '0' rings,

(c) the effect of hysteresis and eddy currents in the solenoid,

(d) when the valve is connected in certain systems and the spool is in the central position the pressure at the tank ports can be high. Thus there will be a force acting on the ends of the striker pins pushing against the solenoid,

(e) further to Fig. 1.1, if the flow of fluid is as indicated, there is a pressure drop along the fluid path between the two tank ports, this pressure difference between the fluid acting on the two ends of the spool thus giving an additional force acting on the spool.

References

1. Seely, S. "Dynamic System Analysis". Reinhold Publishing Corporation, 1964.

2. Korn, J. and Evans, F.J. "Application of network theory and the principle of duality to transducers". Instrument Practice, Vol. 24, No.2. February 1970.

3. Korn, J. and Simpson, K. "Theory and experiments for teaching measurement". Instrument Practice, October 1970 to July 1971.

4. Reza, F.M. and Seely, S. "Modern network analysis" McGraw-Hill 1959.

5. O'n Roe, P.H. "Network and Systems" Addison Wesley Pub. Co. 1966.

6. McCloy, D. "Discharge characteristics of servo valve orifices" Fluid Power International Conference, 1968.

7. Williams, H. "Effect of oil momentum forces on the performance of electro-hydraulic servomechanisms". Pro.I.Mech.E. Automatic Control. January 1960.

8. Harpur, M.A. "Some design considerations of hydraulic servos of jack type". Proc.I.Mech.E., Conference on Hydraulic Servomechanism, 1953

9. Hadekel, R. "Hydraulic Servos". Proc.I.Mech.E., Conference on Hydraulic Servomechanism, 1953

10. Conway, H.G. and Collinson, F.G. "An introduction to hydraulic servomechanism theory". Proc.I.Mech.E., Conference on Hydraulic Servomechanism, 1953

11. Noton, G.J. and Turnbill, D.E. "Some factors influencing the stability of piston-type control valves. Proc.I.Mech.E., Vol. 172, No. 40, 1958

12. Lorenz and Stringer, J.D. "Oil hydraulics spool valve operating times" Proc.I.Mech.E. 1966, Vol. 181, part 1, No. 4.

13. McCloy, D. and Beck, A. "Flow hysteresis in spool valves" First Fluid Power Symposium, January 1969.

14. Shearer, J.L. "Resistance characteristics of control-valve orifices" Proc.I.Mech.E. Automatic Control January 1960.

15. MacLellan, G.D.S., Mitchell, A.E. and Turnbull, D.E. "Flow characteristics of piston-type control valves" Proc.I.Mech.E. Automatic Control January 1960.

16. Raymond, R.E. "Electrohydraulic analogies, Systems Approach" Hydraulics and Pneumatics, March, April and June 1961.

17. Blackburn, J.F., Reethof, G. and Shearer, J.L. "Fluid Power Control" M.I.T. Press 1960.

18. Rotor, H.C. "Electromagnetic devices" Wiley, 1945.

19. Nasar, S.A. "Electromagnetic energy conversion devices and systems" Prentice Hall

20. Fitzgerald, A.E. and Kingsley, C. Jnr. "Electric machinery" McGraw-Hill, 1961.

21. Kron, G. "Equivalent circuits of electric machinery" Dover.

22. Anon. Pratt Precision Hydraulics Limited, Technical Data for solenoid operated directional control valve Type VDS 34.

23. Anon. Expert Limited. Specification notes for solenoid Type 18-7202.

24. Anon. Magnet-Schultz. Specification sheets for a.c. solenoids

25. Vince, J.A. "Fortran for students" Computer Centre, Enfield College, 1968.

26. Langill, A.W. Jnr. "Automatic control systems engineering" Prentice Hall, 1965.

27. Korn, J. and Others. "Hydraulic transmission systems" International Textbock Co. Limited, 1969.

28. Korn, J. and Simpson, K. "Application of signal flow graphs" Bulletin of Mechanical Engineering Education. Vol. 9, 1970.

29. Anon. Ether Engineering Limited Catalogue: Industrial transducers.

30. Anon. Sangamo Controls Limited. Specification sheet for inductive displacement transducer.

31. Anon. Hewlett Packard Limited. Instruction Manual for Model 175A.

32. Anon. Intersonde Limited. Technical instruction note reference TIN501.

33. Anon. Boulton Paul Electronics. Instruction Manual for transducer meter Type C.52.

34. Haberman, C.M. "Vibration Analysis". Charles E. Merrill Pub. Co. 1968.

35. Guillon, M. "Hydraulic servosystem analysis and design" Butterworth Ltd., 1969.

36. Pefley, R.K. and Murray, R.I. "Thermofluid mechanics" McGraw-Hill, 1966.

37. Swanson, W.M. "Fluid Mechanics" Rinehart and Winston, 1970.

38. Pao, R.H. "Fluid Mechanics" Wiley, 1966.

39. Welty, J.R., Wicks, C.E. and Wilson, R.E. "Fundamentals of momentum heat and mass transfer", Wiley, 1969.

40. Duncan, W.J., Thom, A.S. and Young, A.D. "The mechanics of Fluids" Edward Arnold, 1960.

41. Anon. Shell International Petroleum Co. Limited. Catalogue: Technical Data on Shell Tellus Oils.

42. Anon. Intersonde Limited. Data sheet for pressure transducer Type PR15-350.

43. Anon. Meter-Flow Limited. Operating Manual for frequency to d.c. converter Type M707.

44. Anon. Comark Electronics Limited. Instrument Handbook for Thermocouple multimeter Type 160C.

45. Anon. Budenberg Gauge Co. Limited. Catalogue: Operating and Maintenance Instructions.

46. Electronic Associates Inc. Analogue computer used at I.C.I. Limited.

47. Anon. Honeywell Limited. Technical Manual for Visicorder Oscillograph Model 1706.

48. Galloway, J.H., General Electric: Application sheet for the Integrated Circuit PA424.

Appendix

Between the 11th November 1968, and the 1st April 1969, the writer attended a course on a part-time basis at the City University, Department of Automation Engineering. This was a full-time postgraduate course in automation engineering leading to a Degree of Master of Science. The subject matter studied was :-

(a) Systems Theory and Design (Dynamics analysis and Models)

(b) Control Theory (Linear and non-linear)

(c) Computing (use of Fortran Computer language)